THE EXPRESSION OF THE TRANSCRIPTION FACTOR *BROAD* AND RNA-BINDING FACTORS IN THE MIDGUT OF THE MOSQUITO *AEDES AEGYPTI* DURING METAMORPHOSIS

Kathryn Ray

A dissertation submitted to the Graduate Faculty in molecular, cellular, and developmental biology in partial fulfillment of the requirements for the degree of Doctor of Philosophy

The City University of New York

2013

This manuscript has been read and accepted for the Graduate Faculty in Biology in satisfaction of the dissertation requirement for the degree of Doctor of Philosophy.

May 1 2013

Chair of Examining Committee
Dr. James T. Nishiura, Brooklyn College

September 16, 2013

Executive Officer
Dr. Laurel A. Eckhardt

Dr. Peter N. Lipke, Brooklyn College

Dr. Barbara Studamire, Brooklyn College

Dr. Diana P. Bratu, Hunter College

Dr. Edward B. Dubrovsky, Fordham University

Supervising Committee

THE CITY UNIVERSITY OF NEW YORK

ABSTRACT

Expression of the transcription factor *broad* and RNA binding factors in the midgut of the mosquito *Aedes aegypti* during metamorphosis

by Kathryn Ray

Thesis supervisor: James T. Nishiura, Associate Professor, Brooklyn College, CUNY

Transcription factors, microRNAs and RNA binding factors frequently interact to coordinate gene expression during development. The transcription factor *BROAD* (*BR*) is a global regulator of insect gene transcription and governs the timing of the commitment to pupate. I determined *BR* expression in the *Ae. aegypti* midgut by qPCR, and correlated its expression with that of nine miRNAs and three RNA-binding factors. During midgut metamorphosis the expression of these factors was dynamic and reproducible.

To better understand the changes in expression patterns, I evaluated the effects of hormone analogs on expression. Using this approach I uncovered concurrent up-regulation of *BR*, *miR-34* and *miR-14* in the pupal midgut when treated with methoprene, and found that RH2485 accelerated expression of *BR, BRAT*, and microRNAs *let-7*, and *miR-125*. Treatment with each hormone analog resulted in a change in *BR* expression.

Finally, I evaluated the effect of nutrients on expression levels. Surprisingly, though most transcripts were down-regulated during starvation, the expression of *BR* did not decrease, while microRNAs *miR-34* and *miR-14* were elevated. This may identify a novel role for *miR-34* during starvation in an invertebrate, and raises the possibility that *miR-34* and *miR-14* are part of a starvation-induced stress response in the mosquito midgut.

In summary, this expression analysis suggests that microRNA regulation plays an important role during midgut metamorphosis, and reveals a new layer of regulatory complexity in the control of development in *Ae. aegypti*.

Acknowledgments

Most importantly, appreciation and sincere thanks to Dr. James T. Nishiura for giving me the opportunity to work in your lab. I am fortunate to have you as a mentor. I am grateful for your generosity and truly respect your scientific insight.

To my committee members, Dr. Barbara Studamire, Dr. Peter Lipke, Dr. Diana Bratu, and Dr. Shaneen Singh, for your helpful direction throughout the course of this work. Many thanks to Dr. Edward Dubrovsky for consenting to be the outside examiner.

To my friends, associates, and teachers in the biology departments of Brooklyn and Hunter Colleges: it has been a great pleasure to work and learn with you. Thanks to Dr. Martin Schreibman and Dr. Paul Forlano for welcoming me into your labs and teaching me histology, and to Dr. Catherine McEntee for helpful editing.

Finally, to my family: Lenny, Lowell, and Lily.

TABLE OF CONTENTS

LIST OF TABLES page

LIST OF FIGURES

CHAPTER 1 page

CHAPTER 2 page

CHAPTER 3 **page**

LIST OF ABBREVIATIONS

organisms

Aaeg-, Ae. aegypti	*Aedes aegypti*
C. cinquefasciatus	*Culex cincuefasciatus*
C. elegans	*Caenohabditis elegans*
Dme-, *Dmel.*	*Drosophila melanogaster*
T. castaneum	*Tribolium castaneum*

genes, mutants, and gene products, complexes

BR	BROAD
BRZ1, Z2, Z3, Z4	*BR* zinc finger isoforms 1,2,3, and 4
npr	*nonpupariating lethal mutation - dmeBR* mutation
BRAT	Brain Tumor
CYP18a1	cytochrome p18a
DPP	*decapentaplegic*
DIB, PHM	*disembodied, phantom*
EcR	Ecdysone receptor
EGFR	epidermal growth factor receptor
FISC	F*ushiTarazu*-F1 Interacting Steroid-receptor Coactivator
FMRP	Fragile-X Mental Retardation Protein
hnRNP-K	heterogeneous ribonucleoprotein-K
ILP	insulin-like peptide
JHE	Juvenile Hormone esterase
Kr-H	Kruppel Homolog 1
MET	Methoprene tolerant
miRISC	microRNA-Induced Silencing Comple
AGO1	argonaute 1
GW182	glycine-tryptophan repeat 182
NOT1	part of CCR/Not1 deadenylase complex
P13K	phosphatidylinositol 3-kinase
RPS7	ribosomal protein S7
RBP8	encodes small common subunit of 3 RNA polymerases
RNA Pol II	RNA polymerase II
VN	Vein
USP	Ultraspiracle

RNA transcript, protein motifs and domains

mRNA	messenger RNA
BTB	broad, tramtrack, bric-a-brac
Trim-NHL	tripartite motif and *Ncl*, *Ht2a*, and *Lin-41*domain
KH domain	K homology RNA-binding domain (identified in hnRNP-K)
RGG box	arginine-glycine-glycine motif
bHLH-PAS domain	basic helix-loop-helix, Per-Arnt-Sims DNA-binding domain
C2H2	cysteine, histidine zinc finger
LXXLL	leucine-X-X-leucine-ucine (nuclear receptor binding motif)
DBD, LBD	DNA-binding domain, ligand-binding domain
UTR	un-translated region
poly-A tail	polyadenylated tail

A-U rich	adenylate-uridylate-rich nucleotide region
nt	nucleotide

molecular biology techniques, solvents, technical terms, physical laws

c(T)	cycle threshold
DAPI	4',6 diamidino 2-phenylindole blue fluorescent nuclear stain
DMSO	di-methyl sulfoxide solvent
ED_{50}	effective $dose_{50}$
EtOH	ethanol
$-\Delta G$	negative delta G – change in free energy
miRNA	microRiboNucleicAcid
qPCR	quantitative polymerase chain reaction
RACE	rapid amplification of cDNA ends
RNAi	RNA interference

hormones and hormone analogs

A1, A2, A3	sampled adult stages: day 1, day 2, and day 3
JH	Juvenile Hormone
JHA	Juvenile hormone analog
meth	methoprene
PTTH	prothoracicotropic hormone
RH2485	methoxyfenozide

mosquito phenotypes, cell and tissue physiology

DAG, TAG	diacylglycerides triacylglycerides
EC	enterocytes
EE	enteroendocrine cells
P bodies	processing bodies
P0, P1, P2	sampled pupal stages: at pupation, day 1, and day 2
PRT	pigmented respiratory trumpets
RT	respiratory trumpets

Project overview

The purpose of this project is to determine the levels of *BROAD* (*BR)* expression in the midgut of the mosquito *Ae. aegypti* and to correlate *BR* expression with that of RNA-binding factors that might modulate *BR* transcript abundance to coordinate the timing of midgut metamorphosis.

Chapter 1 describes midgut metamorphosis, provides a review of *BR* expression patterns and regulation in other insects, identifies potential regulatory factors (microRNAs and RNA binding factors) that might affect *BR* mRNA expression levels, and analyzes their expression levels in parallel with *BR* expression in order to establish a baseline of expression patterns in the developing midgut.

Chapter 2 analyzes the effects of ecdysone and juvenile hormone agonists on the expression of *BR* and potential *BR* regulatory factors. Hormones control developmental progression in the midgut, and alter the expression patterns of *BR* and of microRNAs (miRNAs). Possible interrelationships emerge as expression patterns change in response to treatment with hormone agonists.

Chapter 3 shows the results of experiments designed to determine the effect of starvation and nutrient restriction on *BR* and RNA-binding-factor expression in the midgut.

Public health significance

The mosquito *Ae. aegypti* is the vector for Dengue fever. Dengue fever is the most rapidly spreading viral disease in the world. Prevention and control of Dengue depends on vector control methods. In the adult female mosquito, midgut epithelial cells form the first barrier to the Dengue virus. A better understanding of the factors that regulate mosquito midgut development

may suggest novel control measures to prevent virus entry through midgut epithelial cells, and so, prevent vector ability to transmit the Dengue virus to humans.

Additionally, it is clear that miRNAs participate in many biological processes, yet little is known about the hormonal regulation of miRNA expression, or the roles they play in mosquito development. This study offers insight into hormonal and metabolic regulation of ancient and evolutionarily-conserved miRNAs and suggests novel biological functions for these miRNAs in the context of a dynamic developing system.

CHAPTER 1

The expression of *BROAD (BR)* and RNA binding factors in the midgut of the mosquito *Aedes aegypti (Aaeg)*

BACKGROUND

Role of *BROAD* in insect development

Winged insects undergo morphological changes in the transition from immature to adult form. Hemimetabolous insects undergo a partial metamorphosis in which progression from nymph to adult does not involve a pupal stage. The hemimetabolous adult often has wings and is reproductive but its appearance resembles the nymph. In contrast, holometabolous insects have a complete metamorphosis, and pass through four life stages: egg, larva, pupa, and adult. Holometabolan adult morphology is completely different from that of the larva. The expression pattern of *BR* homologs differ in holometabolous and hemimetabolous insects, as does the pace of their developmental timing [1, 2].

The gene *BR* encodes an insect transcription factor widely studied for its role in insect development. Certain genes are considered important because they control pivotal developmental programs in response to multiple signaling pathways. *BR* may be such a gene.

In *Drosophila melanogaster (D. melanogaster), BR* expression is restricted to the late third instar, at the end of larval development, when an ecdysone pulse initiates a cascade of transcription factor signaling and the onset of metamorphosis [3-7]. Evidence that *BR* is required for the initiation of metamorphosis in *D. melanogaster* comes from the analysis of *BR* mutants that develop normally as larvae, but are unable to undergo metamorphosis, and die as larvae [8]. The expression of *BR* has become known as the molecular marker of the commitment to pupate [9, 10].

The abundance of an mRNA transcript during development is determined not only by the rate at which it is synthesized, but also by the rate at which it is degraded [11]. Transcribed gene products might be translated into protein, or be degraded, or be sequestered and protected [12]. Control of the abundance of an mRNA transcript at the level of translation allows a rapid response to environmental change, because it doesn't involve mRNA synthesis, processing, or transport [13].

Post-transcriptional regulation of mRNA by microRNAs (miRNAs)

miRNAs are short, non-coding RNAs that imperfectly bind an mRNA target to regulate gene expression post-transcriptionally [14-17]. miRNAs base-pair to partially complementary targets in the 3' untranslated regions (3' UTR) of the target mRNA [12, 18].

miRNAs were first discovered in the nematode *C. elegans* as heterochronic mutants with developmental timing defects [14, 17, 19]. Heterochronic genes encode factors that control developmental timing, and heterochronic mutants have either precocious or delayed development [20]. Characterization of the heterochronic pathway in *C. elegans* offered, by analogy, a new basis for understanding the regulation of developmental timing in insects at the molecular level [21]. *D. melanogaster* homologs of *C. elegans* heterochronic miRNAs include *miR-125 (lin-4), let-7* and another ancient miRNA, *miR-34*. During metamorphosis in *D. melanogaster*, increased ecdysone concentrations elevate *let-7* and *miR-125* expression, but reduce *miR-34* expression [22-25]. *D. melanogaster* mutants unable to synthesize ecdysone have higher levels of *miR-34*, and lower levels of *miR-125* and *miR-100* [25].

miRNAs, hormonal regulation, and *BR*

Three lines of evidence connect the insect developmental timing gene *BR* to these heterochronic miRNAs during metamorphosis. First, the *D. melanogaster* mutant gene *nonpupariating,* (*npr*)

encodes a defective BR protein. Homozygotes don't undergo metamorphosis, and die as larvae [8, 10]. Thus, BR is required for metamorphosis. BR elevates *let-7* and *miR-125* expression, and reduces *miR-34* expression, because in *D. melanogaster npr* mutants, *let-7* and *miR-125* levels are lower and *miR-34* is higher [25]. Second, when ecdysone is added to *D. melanogaster* S2 cells, *miR-125* and *miR-100* are induced, but adding the juvenile hormone analog methoprene to S2 cells increases *miR-34* levels, and decreases *miR-125* and *miR-100*. It is well established that ecdysone induces *BR* expression [3, 5-7, 26, 27]. Third, it was shown that RNA interference (RNAi) against the *BR* common region (targeting all four *BR* isoforms - Figure 1.2) down-regulates *miR-125* and *let-7* expression in *D. melanogaster* [25].

Possible feedback loops between *br* and miRNAs

Often, both transcription factors and miRNAs are differentially expressed during development. Both can widely impact gene expression, and they may form reciprocal regulatory loops [28, 29].

Translational control of mRNA levels: the importance of the 5' UTR and the 3' UTR

Translational control can result from interactions between RNA-binding proteins and the 5' and 3' untranslated region (UTR) of an mRNA transcript. Regulatory elements found in the 5' and the 3' untranslated regions permit RNA-binding by factors that can mediate multiple aspects of mRNA processing, including cytoplasmic localization, translational efficiency, and mRNA stability [12, 30, 31]. In particular, the 3' UTR is critical for mRNA translational control [32], and the length of the poly-A tail affects translation efficiency. Long poly-A tails correlate with translation, while short poly-A tails correlate with translational repression [32].

miRNAs bind the 3'UTR of their target genes

miRNAs associate with the **miR**NA **i**nduced **s**ilencing **c**omplex (miRISC), which is composed of Argonaute (AGO1) and its binding partner GW182 [33]. This miRNA-RISC complex

recognizes and binds target mRNAs through imperfect sequence complementarity between the miRNA and the target mRNA 3' untranslated region (3'UTR) [34]. miRISC controls gene expression by affecting the translational efficiency or the stability of target mRNA [33] (Figure 1.1). One miRNA might bind many mRNAs, and several miRNAs may target a single mRNA transcript [35].

FIGURE 1.1 miRNA-induced silencing complex (miRISC) components

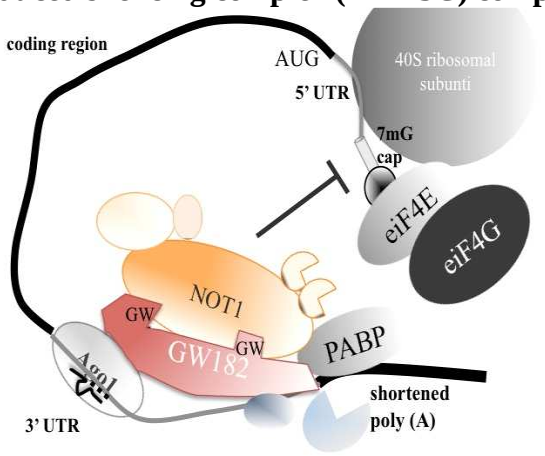

Figure 1.1 Inhibition of translation by mRISC components AGO1, GW182, and the de-adenylase scaffold NOT1 binding to the target mRNA 3'UTR to confer post-transcriptional gene repression. (after Hafner 2011 [36])

***In silico* analysis of *BR* secondary structure and possible miRNA binding sites**

To evaluate the possibility of miRNA or RNA-binding factor interaction with *BR*, I began with an analysis of *BR* mRNA isoform 3'UTRs.

Genomic organization of *Ae. aegypti Broad* - isoforms resulting from alternative splicing

The N-terminal BTB (Broad, Tramtrack, Bric-*a*-*brac*) domain facilitates dimer- or multimerization [37]. A central common region is predicted to be intrinsically unstructured. There are four sequenced *BR* isoforms in *Ae. aegypti*, which differ in their terminal exon due to alternative splicing. Each variable terminal exon encodes a unique pair of C2H2 sequence-specific DNA-binding zinc fingers. In the encoded proteins, conserved cysteine and histidine

residues coordinate a zinc ion that enables the domain to fold and fit into the groove of the double helix, allowing cis-regulatory, sequence-specific binding [38]. Each isoform has different DNA binding affinities and may target different regions in the genome.

FIGURE 1.2 *BR* isoforms in *Ae. aegypti* genome (Vectorbase)

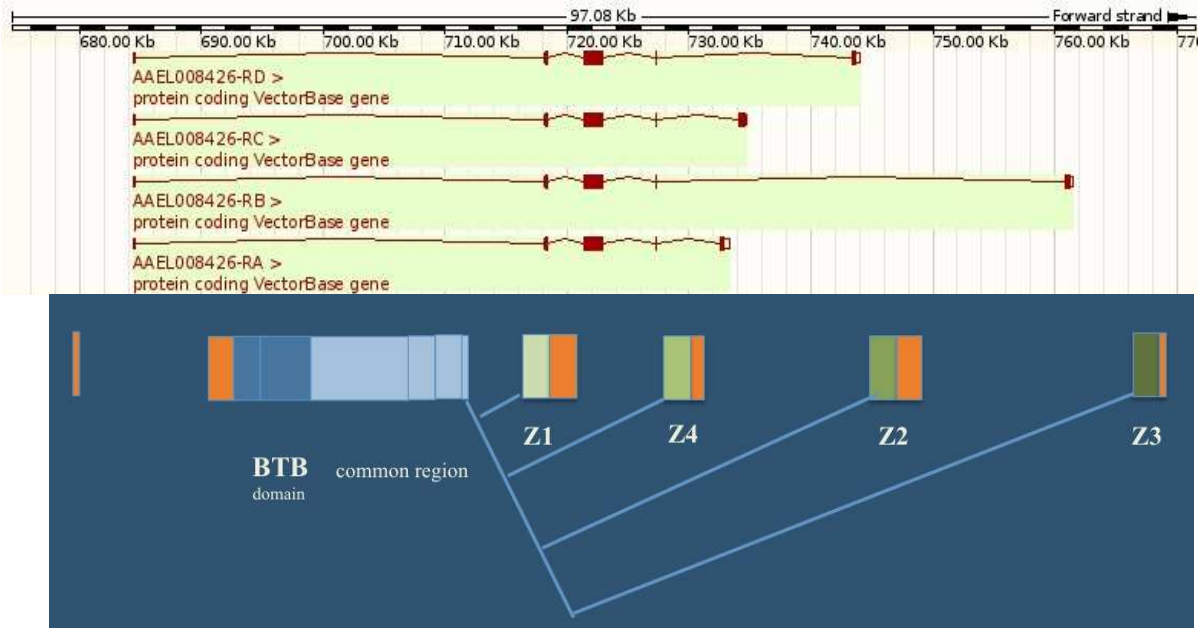

Figure 1.2*BR* locus in *Ae. aegypti* genome showing alternate splicing of the terminal exon 5' and 3' UTR-**orange**, BTB domain-**dark blue**, common region-**lt. blue**, zinc fingers-**green** We cloned the first exon in our lab in 2003 (Genbank AY528664).

Table 1.1 3'UTR length and total transcript length for each isoform

***br* isoform**	**locus length**	**cDNA (nt)**	**3'UTR**	**protein (aa)**
br Z1	50.31	2371	510	561
br Z2	59.65	2201	424	607
br Z3	77.08	2139	**201**	609
br Z4	48.95	2228	**134**	542

Table 1.1 Comparison of *BR* isoforms: distance spanned in the *BR* locus, cDNA length, and 3'UTR length. *BR*Z3 has the most distal exon, and spans 77.08 kb 5' UTR - 3'UTR. Note the **shorter lengths of Z3 and Z4 3'UTRs** compared to Z1 and Z2 3'UTRs.

A comparison of the 3'UTR lengths of isoforms Z3 and Z4 with Z1 and Z2 shows that the Z4 and Z3 isoform 3'UTRs are much shorter (Table 1.1, Figure 1.3 B).

Predicted secondary structure of *BR* isoform mRNA

Folding analyses done on MFOLD [39] offer insight into the potential RNA structures of *BR* messenger RNA. These folding approximations show two-dimensional representations of RNA

transcript secondary structure, and are based on thermodynamics and the estimated free energies of the structures. But predicted structures are only approximations, and the number of potential structures increases greatly with the RNA sequence length. Analysis of predicted potential secondary structures can suggest inherent folding characteristics and energetic binding constraints within individual *BR* mRNA isoforms. This may help estimate the likelihood of possible interactions with RNA-binding proteins in translational regulation of *BR* mRNAs. Transcribed RNAs may switch amoung different structure-states *in vivo* because of sub-cellular conditions, such as local pH changes, or RNA binding-factor interactions [39]. In the folding analyses shown, the secondary structures are depicted in a circle, with the 5' end depicted adjacent to the 3'end. In Figure 1.3, which shows a representative prediction for each of the four *BR* isoforms, the 5'UTR is red (start) and the 3' UTR is black (end).

In addition to directing the identity of a protein, the mRNA sequence dictates the three dimensional structure of the encoded RNA in the cell. The transcript's folded shape itself may have a regulatory effect on processes such as splicing and translation. In the *BR* transcripts, a central loop was consistently predicted to be unstructured (Figure 1.3A). This loop lies within the common region of the encoded protein, where asparagine (N) repeats are encoded in the nucleodtides (AAC-AAC-AAC…which encodes N-N-N). This large loop occurs near an exon-exon boundary.

Each of the *BR* isoform mRNAs has a different terminal exon and so, folds differently in the 3' UTR, where miRNAs are most likely to bind (Figure 1.3B).

FIGURE 1.3 *BR* isoform mRNA - predicted secondary structure – (MFOLD)

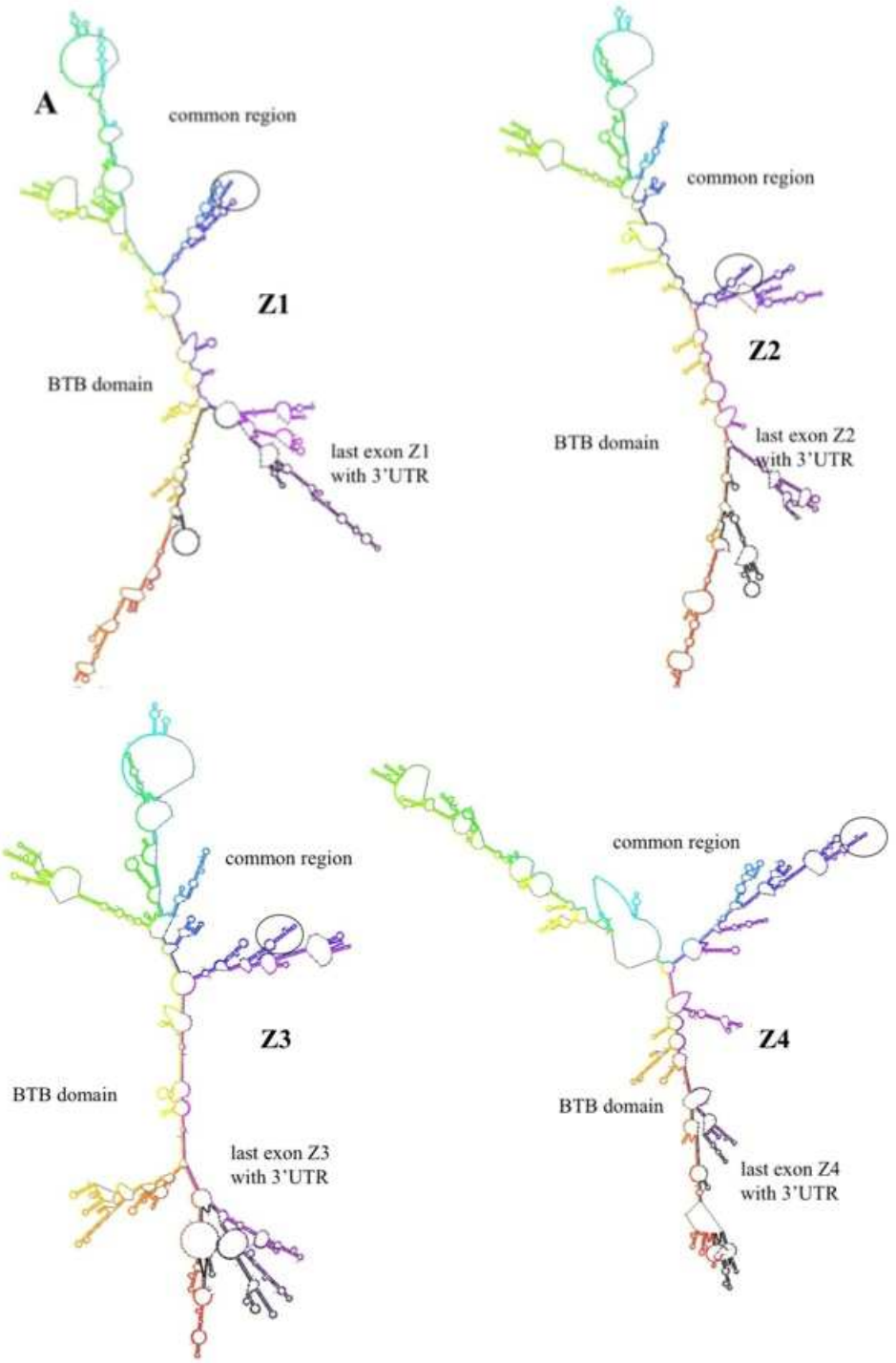

Figure 1.3 A. Folding predictions for each *BR* isoform mRNA transcript [40]. AAC repeats comprise the unfolded central loop (blue) region. A fold that is common to multiple predictions is circled.

5' UTR begins - **Red** 3' UTR ends - **Black**

FIGURE 1.3 *BR* isoforms - last exon only - predicted secondary structure – (MFOLD)

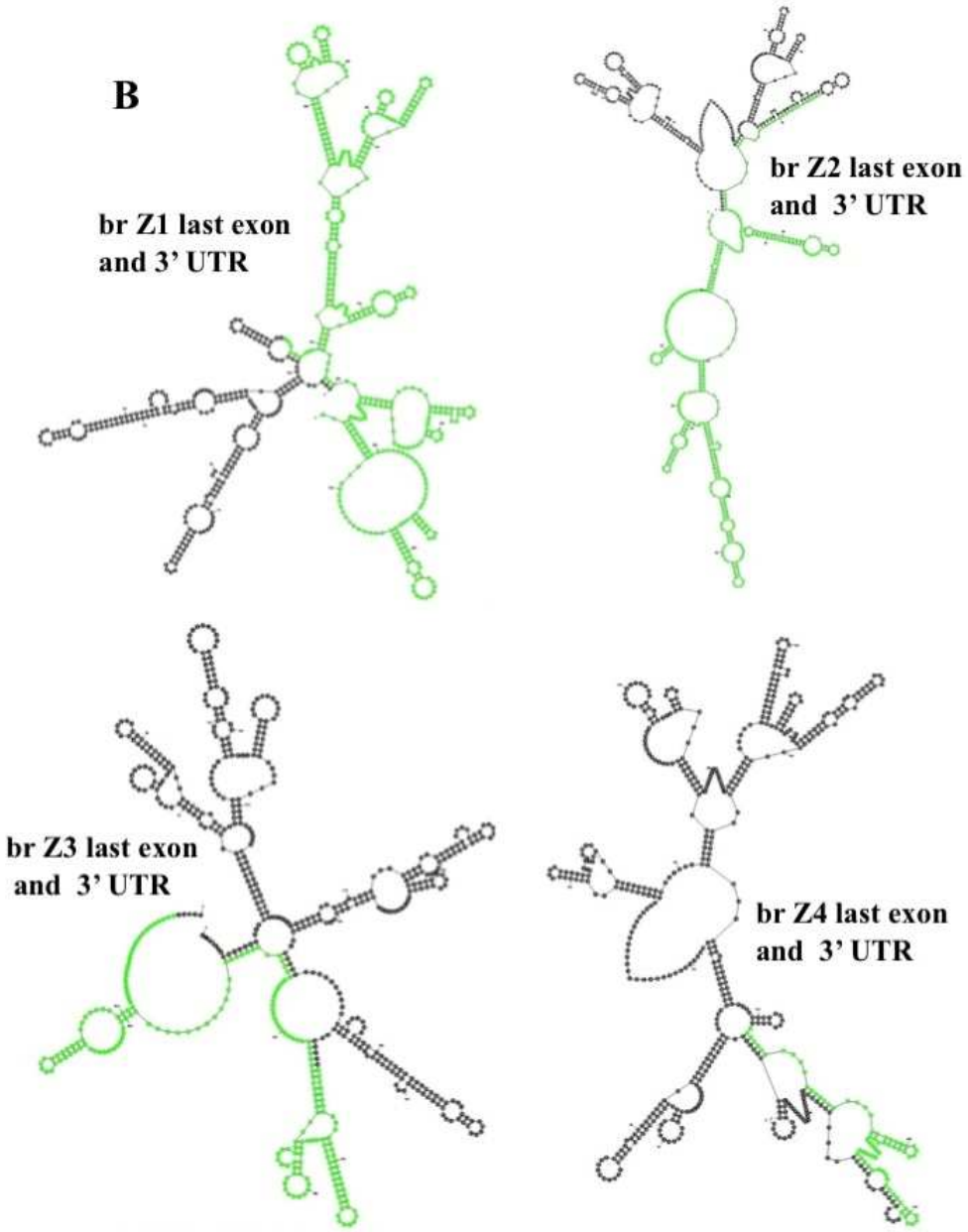

Figure 1.3 B. Folding predictions for the four variable terminal exons. 3'UTRs of Z1 and Z2 are longer than 3'UTRs of Z3 and Z4, and so have more complex secondary structures **Zinc-finger coding region - black. 3' UTR - green**.

Folding of a single RNA strand on the MFOLD web server returns many potential secondary structure folds, so there are high false positive rates, but it is informative to compare different folds to look for regions of stem loop formation, which are stable common structures. The openness and structural context of the target 3' UTR structure is thought to have a strong effect

on target recognition by miRNAs [41]. Figure 1.4A shows regions of stem-loop folding variants in *BRZ*3 3'UTR that are consistenty predicted because of energetic favorability.

FIGURE 1.4 Different folding predictions for *BRZ*3 3' UTR in *Ae. aegypti* (MFOLD)

A

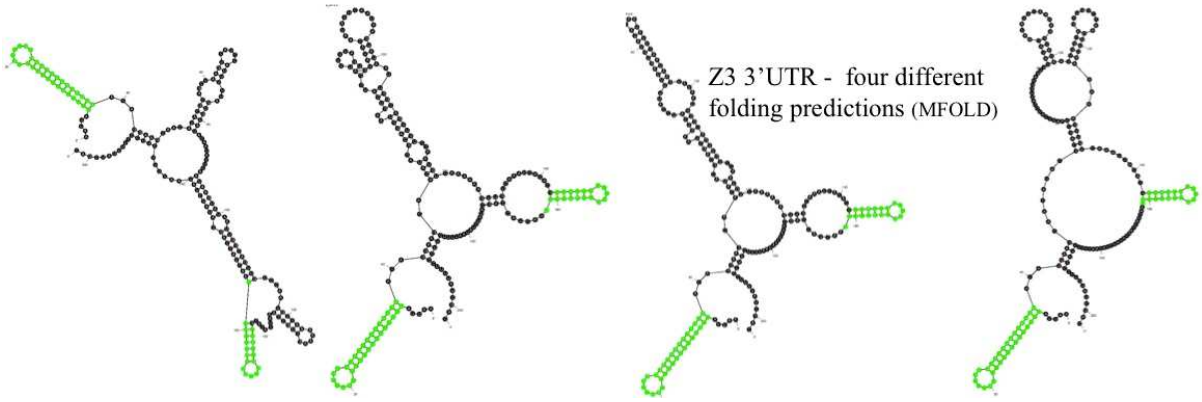

B

Br Z3 3' UTR - *Aedes*
65 A's, 45 C's, 33 G's, 59 U/T's, and 0 N's.

```
  10          20          30          40          50
AAUUAUCUCC UUUUCUCCCA UCCGAGGAGA AAAGAGGAAC AGGAAGCAAC

         60          70          80          90         100
AUACGCAGCU AAGUCAUCCA UUUUUAGUGU AUACAAUAUU CAAUAAGUAU

        110         120         130         140         150
AAUUGGCAGU UGUCCAAUGU CAAAAAAGUU GUCAAAUCAC ACGCGAUCGG

        160         170         180         190         200
CCGGCGAUCG UUAACUACCA GCAUAUCUAU AAUUUUCUUC CCUUUUAUCG

        210         220         230         240         250

AC
```

Figure 1.4 A. ***Ae. aegypti BRZ3:*** **different folding predictions for 3'UTR** with predicted **stem loop secondary structures highlighted in green** (MFOLD)
B. *BRZ*3 3'UTR formatted sequence with **stem loop nucleotides in bold** and miR-34 binding predictions underlined: **MFOLD [39]** miRNA binding prediction: **Microinspector [42].**

***In silico* analysis of possible miRNA binding to *BR* 3'UTRs**

To determine if miRNAs might target *BR* transcripts I did a bioinformatic search for potential miRNA binding interactions with *BR* isoform 3'UTRs.

miRNAs are only partly complementary with their targets, which makes binding prediction uncertain. Most prediction programs consider seed region (nucleotides 2-8 in the 22 nt miRNA)

complementary pairing with the target mRNA 3'UTR. However, 3' base- pairing can compensate for sites with imperfect seed complementarity [43]. Also important is the energetic (-ΔG) favorability of binding, which involves the 'openness' of the target-binding site (free from 3'UTR secondary structures), and evolutionary conservation of the target binding site motif in the 3'UTRs of closely related species [34, 41]. miRNA binding sites are frequently found in local A-U rich regions of the 3'UTR, but usually not within the first 15 nucleotides, or in the center of long 3' UTRs [41].

FIGURE 1.5 *miR-34* binding predictions on *BR* Z3 3'UTR
A

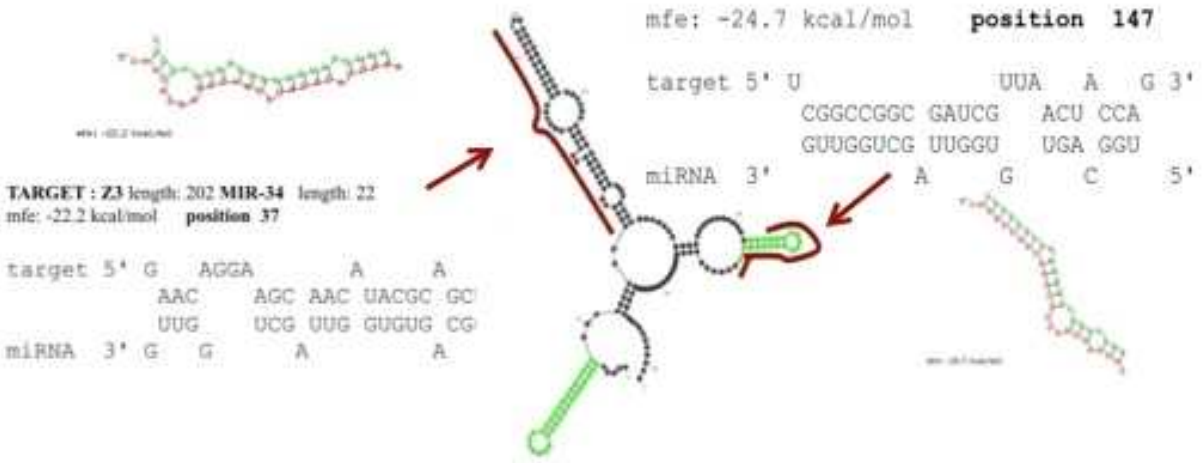

Figure 1.5 An example of 2 possible binding sites on Z3 3'UTR for *miR-34* (red arrows and lines indicate regions of miRNA complementarity (prediction-RNA hybrid: Bielefeld University Bioinformatics Server [44])

FIGURE 1.6 *BR* 3' UTR secondary structure in closely related *C. quinquefasciatus*

A

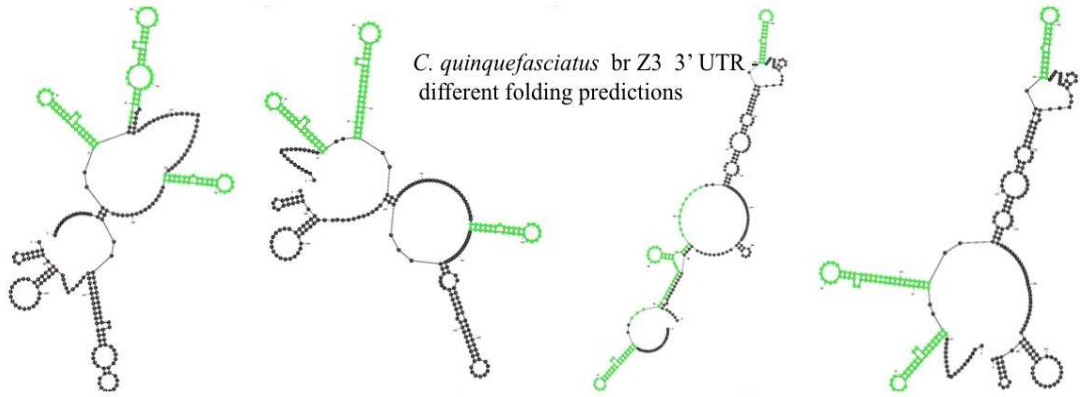

B

6-38, 144-162 highlighted in green above.
br Z3 3'UTR Culex
Linear RNA folding at 5%, window = 7, max folds = 50
113 A's, 85 C's, 58 G's, 100 U/T's and 0 N's.

```
          10          20          30          40          50
 UUUCCCUACA CAGGAUCUCU CGAACAUCUU CUUCGAGUAA GAUCCUUCUC
          60          70          80          90         100
 UUCUGAUCCU GCUCAAGCUA AUACCAGCCA GCUAGCGUCA UCAACAGAUA
         110         120         130         140         150
 GAGAGAAACA AACAAAACAA AAACAAACGC AUAUGCAGCU AAGUCAUCCA
         160         170         180         190         200
 UUUUAGUGUA UACAAUUUUA GCAUAAGUAA CUGGCAGUUU GUCAAUGUCU
         210         220         230         240         250
 AAUAGUUGUC AAGUCUCACA CACAUACAAA CUCACACACA UCAAACACGU
         260         270         280         290         300
 GCGGGAUCGU GAUCCCACGC AAGUGGUCCA CCAGCAUAUC UAUAUGGGUU
         310         320         330         340         350
 UAAUUUCUUG CUUUGGUUUC AUCUUAAGCG GAAUGAGUUG AAAUUAUUCG
         360
 ACACCU
```

Figure 1.6A. *C. cinquefasciatus BRZ3* 3' UTR folding predictions with **stem loop secondary structures highlighted in green** (MFOLD) **B** *BR*Z3 3'UTR formatted sequence with **stem loop nucleotides in bold** and *miR-34* binding prediction underlined (MFOLD- Zuker)

FIGURE 1.7 *miR-34* binding predictions on *BR*Z3 3'UTR in *Culex* and *Ae. aegypti*

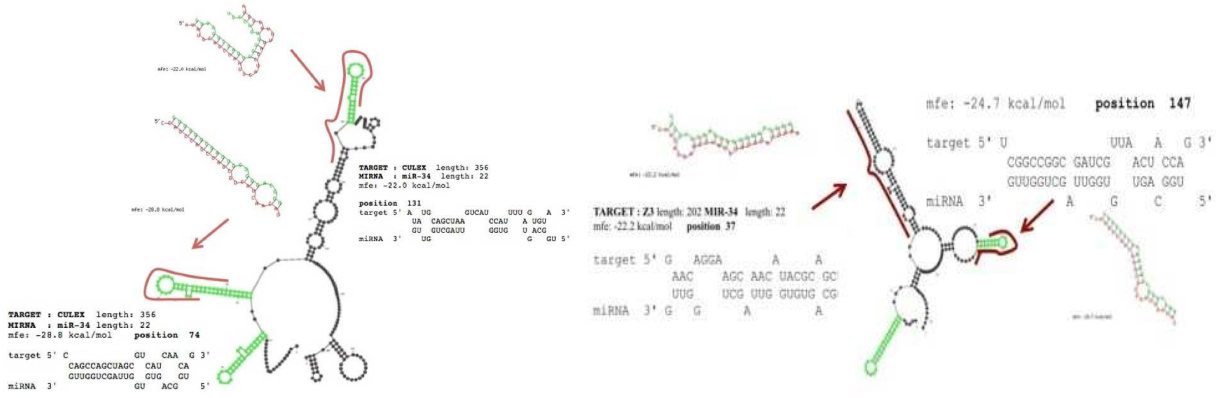

Figure 1.7 Comparison of *miR-34* binding predictions on *Culex* and *Ae. aegypti* 3' UTR

Because *BRZ*3 expression levels were highest in the midgut and showed the steepest drop, I focused primarily on miRNAs predicted to target *BRZ3: miR-34, miR-317, miR-190* and *miR-7* were predicted to bind *Z3* 3'UTR (Microinspector [45], PITA algorithm at Segal lab [46], Targetscan [47], StarMir [48]). These miRNAs are present in the *Ae. aegypti* genome (Broad Institute, MIT), and predicted to fold as hairpin precursor miRNAs (pre-miRNAs) by MFOLD. They all are in miRbase [49]. I cloned *Aae-miR-7, miR-7*, let-7, miR-34,* and *miR-277.*

Table 1.2 miRNA bioinformatic prediction programs used

program	reference	url
microinspector	Rusinov 2005	http://bioinfo.uni-plovdiv.bg/microinspector/
RNA hybrid	Kruger 2006	http://bibiserv.techfak.uni-bielefeld.de/rnahybrid/submission.html
Targetscan (fly)	Lewis 2005, Ruby 2007	http://www.targetscan.org/fly/
Pictar (invertebrates)	Lall 2006	http://pictar.mdc-berlin.de/cgi-bin/new_PicTar_fly.cgi?species=fly
RNA22	Miranda 2006	http://cm.jefferson.edu/rna22v1.0/
pita (Segal lab)	Kertesz 2007	http://genie.weizmann.ac.il/pubs/mir07/mir07_prediction.html
starMir	Ding 2005	http://sfold.wadsworth.org/cgi-bin/starmir.pl

Other RNA binding proteins that may affect *BR* mRNA levels

*BRZ*3 and Z4 have short 3'UTRs, and don't offer many binding possibilities. *BRZ3* and *Z4* transcripts were also the most abundant in the midgut. The presence of a predicted miRNA target sequence alone is a poor indicator of *bona fide* binding and regulation. Competition for binding sites with other RNA-binding co-factors can change local sequence context to either prevent or provide better access for miRNA binding. To determine which miRNAs and RNA-binding proteins might target *BR* 3'UTR, I did a bioinformatic and literature search (Table 1.2). Based on these results, I selected nine miRNAs and three RNA-binding factors for further analysis because they were predicted to bind *BR*, or to interact with *BR* transcripts (Tables 1.3 and 1.4).

Table 1.3 Selected miRNAs and their location in *Ae. aegypti* genome

miRNA	Primary transcript location	Hormonal regulation
miR-317 **miR-277** **miR-34**	*Aedes* supercontig. 1.265 cluster miR-277 and mir-34 are 545 base pairs apart – possibly in the same primary transcript	miR-34 is juvenile-hormone induced and ecdysone repressed in Drosophila (Sempere 2003)
miR-100 **let-7** **miR-125**	*Aedes* supercontig. 1.43 cluster miR-125 and let-7 are 255 base pairs apart – probably in the same primary transcript	miR-125 and let-7 are ecdysone induced in *Drosophila* (Sempere 2003)
miR-7	*Aedes* supercontig 1.359 Located inside the terminal intron of *hnRNP-K* (*rhea* in fly), a deeply conserved position for miR-7 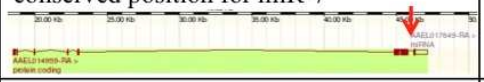	Not known to be hormonally regulated but known to act in Notch and EGFR signaling in *Drosophila* (Lai 2005, Carthew 2005)
miR-190	*Aedes* supercontig 1.195 Located inside the last intron of *talin*, a deeply conserved position for miR-190 	Not known to be hormonally regulated. mir-190 function has not yet been studied in insects.
miR-14	*Aedes* supercontig. 1.249	miR-14 acts in ecdysone signaling and regulation in *Drosophila* (Varghese 2007)

Table 1.4 RNA-binding proteins in this study

RNA- BINDING FACTOR	FUNCTION	RNA BINDING MOTIF/ DOMAINS	REFERENCE
brat	Translational repressor	NHL-RBCC, interacts with Ago1, pumilio	Edwards 2003
lin-28	Inhibits let-7	Cold shock,flexible linker, zinc knuckle	Moss 2007
hnRNP-K	Translational repressor, affects mRNA stability, splicing (harbors miR-7)	HEAT repeat – scaffolding platform	Basquin 2012

Ae. aegypti larval midgut morphology and development

The basic structure of the larval mosquito alimentary canal consists of three main regions, the foregut (pharynx, esophagus, proventriculus or cardia), the midgut (with anterior gastric cecae) and the hindgut (malphigian tubules, ileum, rectum) (Figure 1.8).

The proventriculus acts as a valve to control food passage into the midgut. Cells inside the proventriculous secrete the peritrophic membrane, a chitinous tube that holds ingested food. Nutrients pass though this tube to be digested and absorbed in the midgut. The hindgut and the malphigian tubules reabsorb fluids and balance ions and metabolites [50].

FIGURE 1.8 *Ae. aegypti* larval midgut (from Christophers [51])

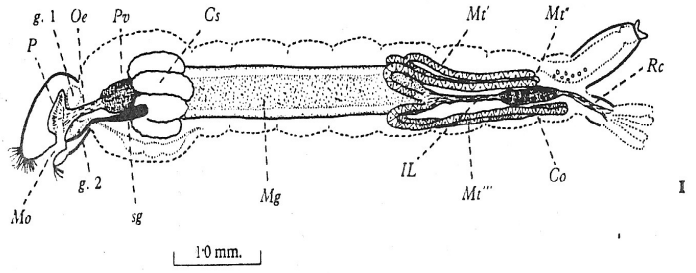

FIGURE 1.8 The larval alimentary canal *Mo* mouth, *P* pharynx, *g-1, g-2* supra- and sub esophageal ganglion, *Oe* oesophagus, *Pv* proventriculus, *sg* salivary gland, *Cs* gastric ceaca, *Mg* midgut, *Mt* Malpighian tubules (dorsolateral and ventrolateral), *Il* ileum, *Co* colon, *Re* rectum

The larval midgut is composed of cells of different sizes and functions. Among these are polyploid enterocytes (EC) of various ploidy levels. These cells have microvilli on their apical side, face into the lumen, and basally attach to the basement membrane, which is surrounded by the visceral muscles. There are also secretory entero-endocrine (EE) cells, and small diploid adult midgut progenitor (stem) cells that lie closest to the basement membrane. The stomatogastric nervous system forms a network of longitudinal peripheral ganglia around the midgut that connects with the brain [52].

FIGURE 1.9 *Ae. aegypti* midgut epithelial cells and visceral muscle network

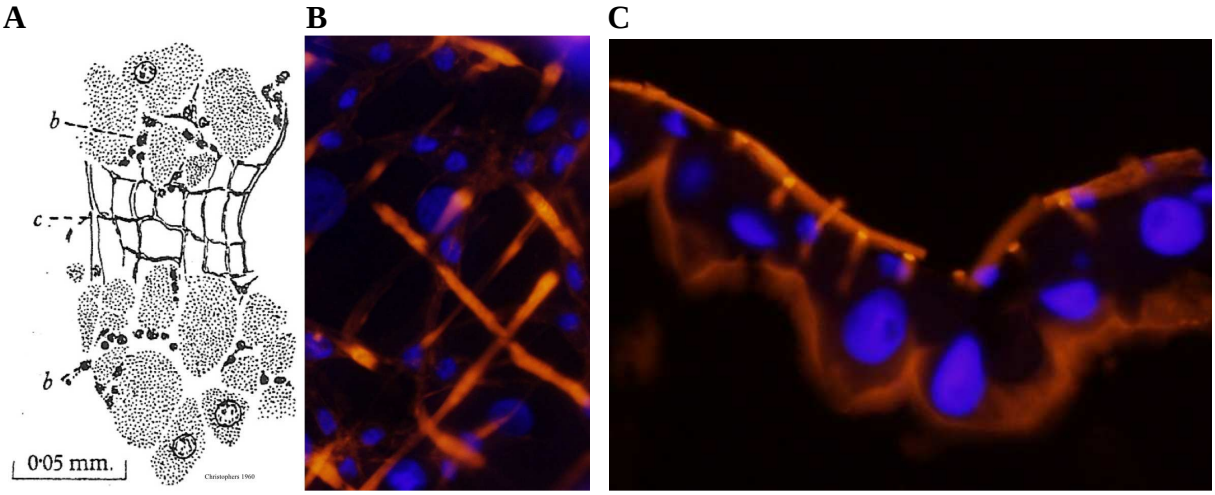

Figure 1.9 A Schematic of midgut tissue shows large larval migut enterocytes and smaller, more basal diploid cells (b), overlying the peripheral muscle [51] **B. Epithelial cell nuclei on the visceral muscle network** that surrounds the midgut. **C.** Cryosection of larval midgut showing **large, polyploid nuclei in enterocytes with actin-rich apical microvilli**, and **small nuclei closest to the muscle network** that surrounds the basement membrane on the basolateral side (top). B and C: DAPI (nuclei) and phalloidin (microvilli and muscle network).

The visceral muscle network that surrounds the basement membrane of the midgut epithelial cells (Figure 1.9) is open to the circulating hemolymph, and undergoes rhythmic peristaltic contractions. The axons of the stomatogastric nervous system enervate the midgut and extend from anterior to posterior. Tracheal attachments supply oxygen to the midgut epithelium via tracheal ducts from air taken in through the respiratory siphon in the tail.

Midgut epithelial cell proliferation

Progenitor stem cells have long been observed in *Ae. aegypti* midgut [51, 53], but stem cells are difficult to identify unambiguously. Lineage analysis is the best way to identify a self-renewing pluripotent cell [54]. *Ae. aegypti* is not amenable to genetic studies, and stem cells have not been identified in the midgut epithelium by mosaic analysis with a repressible cell marker (MARCM). However, in the *D. melanogaster* midgut, MARCM has clearly identified intestinal stem cells. They lie close to the basement membrane, and these stem cells depend on signals from the visceral muscles and trachea to maintain their ability to self-renew [54-57]. The visceral muscles

and the basement membrane form a niche environment from which the morphogens decapentaplegic (DPP, a TGFß ligand) and vein (VN, an EGFR ligand) signal to instruct cells closest to the basement membrane to remain as stem cells [58]. The self-renewing stem cell in the larval midgut maintains progenitor-cell identity as long as it lies closest to the niche [54, 55, 59]. In *D. melanogaster*, *BR* is required for adult midgut progenitor cell differentiation and acts in the EGFR pathway [60].

FIGURE 1.10 Larval enterocytes and diploid adult midgut precursors

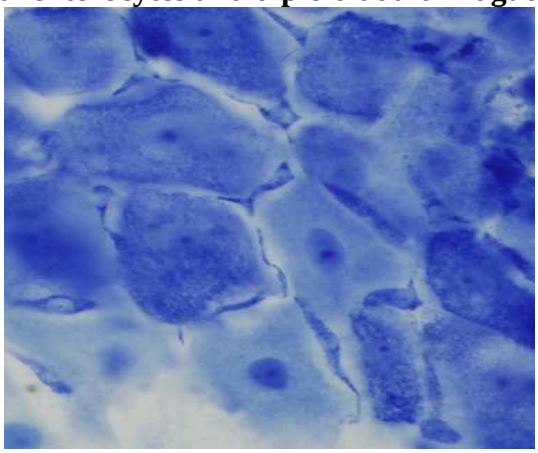

Figure 1.10 Small, potentially undifferentiated adult precursor cells with cytoplasmic extensions surround large larval enterocytes in *Ae. aegypti* midgut, mid-4th instar. (Methylene blue stain)

RESULTS

Morphological description of *Ae. aegypti* midgut developmental changes

The developmental stages described here correspond to the sample times in the expression analyses that follow, and span the course of midgut metamorphosis from late larva to adult.

Larval midgut development: 24-36 hours By 24 hours after the last larval molt, well-fed larvae attain critical weight [9]. At 32 hours the midgut epithelium is composed of large larval enterocytes with nuclei, and some large enterocytes **without** nuclei (Figure 1.11 C), as well as diploid cells with small nuclei. At 32 hours these small cells are often in pairs, as if recently divided. Visceral muscles surrounding the midgut have a lattice-like structure of longitudinal and

crosswise fibers. Phalloidin highlights a ring of intense staining that may correspond to the pyloric ring, thought to have endocrine function [61] (Figure 1.11A, arrow). Methylene blue stain shows diploid cells extending around older, larger larval epithelial cells (Figure 1.11).

FIGURE 1.11 Midgut at ~ 32 hours

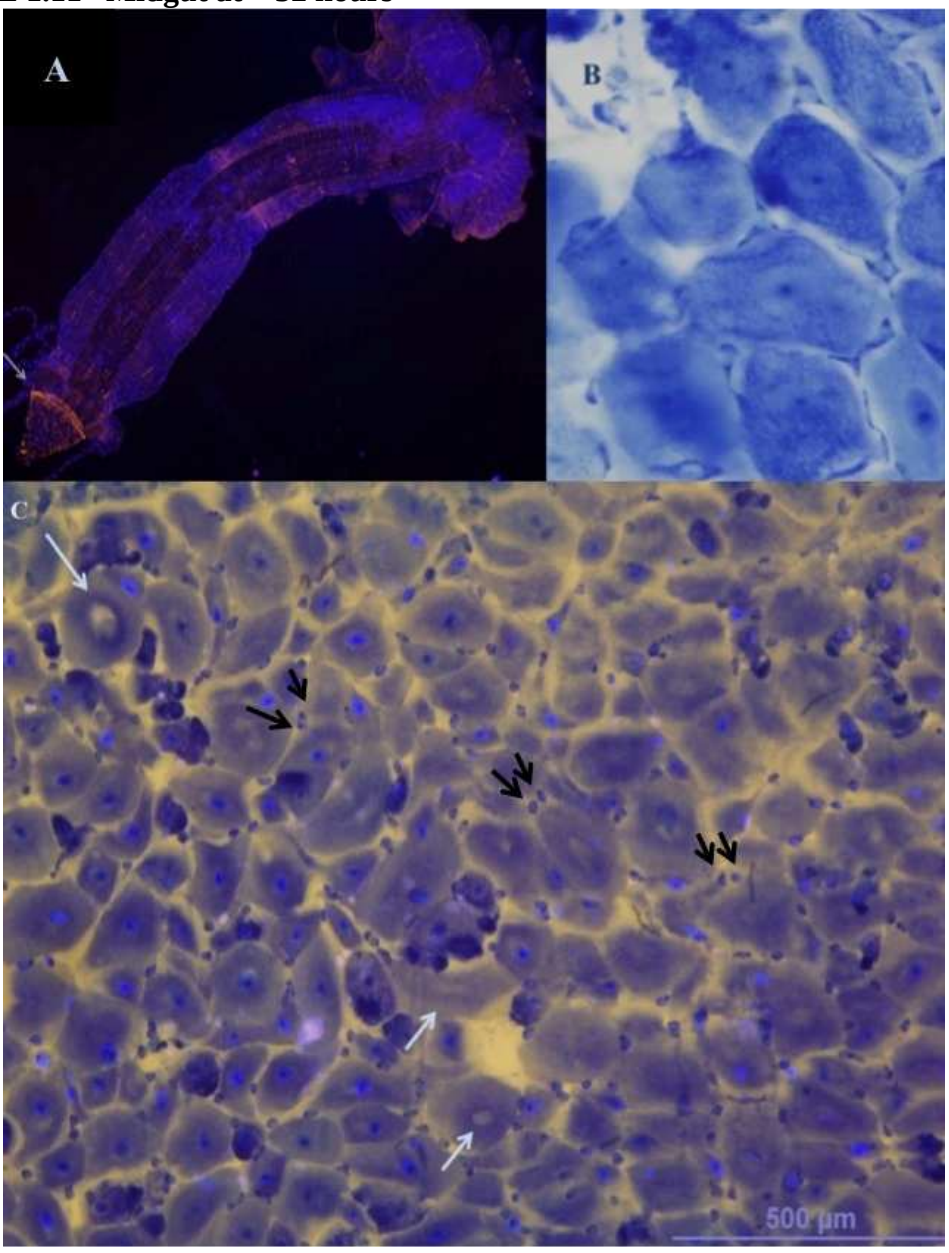

Figure 1.11 A. ~32 hour midgut showing gastric cecae (anterior, right), and malphigian tubules (lower left) **B. Large enterocytes with small cells extending around them at ~36 hr C. Midgut epithelium at 32 hours,** composed of large and intermediate larval **enterocytes, some without nuclei (arrows**), and **small cells, frequently paired** perhaps recently divided (dark arrows). (DAPI, phalloidin and methylene blue staining)

48 hours Around 48 hours the midgut reaches maximum size (determined by measuring midguts in living larvae through transparent cuticles over developmental time) Figure 1.12.

FIGURE 1.12 Larva and midgut at ~48 hours

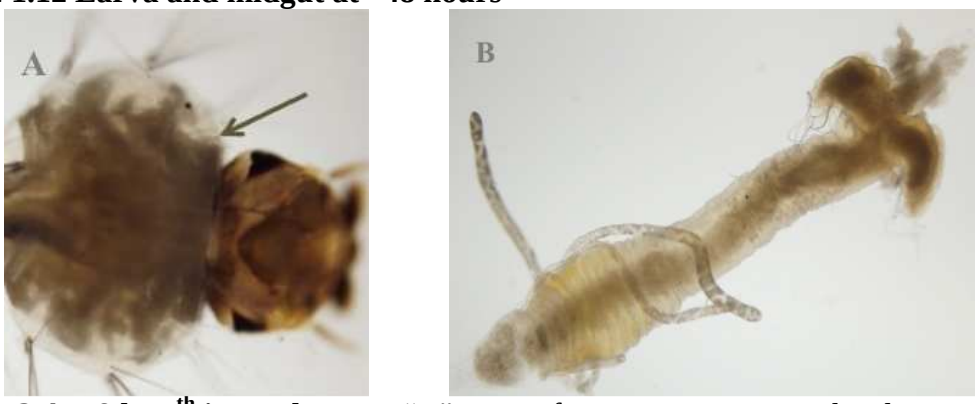

Figure 1.12 A. 48 hr 4th instar larva at "V" stage of respiratory trumpet development (arrow). Imaginal discs beginning to form in larval thorax. **B. ~ 48 hr midgut.** Peritrophic membrane inside midgut. Fat body loosely associated with gastric ceacae (top, right).

Cell proliferation in the midgut occurs mid-4th instar

Cell proliferation in the midgut has been described during midgut metamorphosis [62, 63], and cell division increases, particularly in the posterior midgut, around 48 hrs in the 4th instar.

FIGURE 1.13 Anterior midgut ~ 60 hr

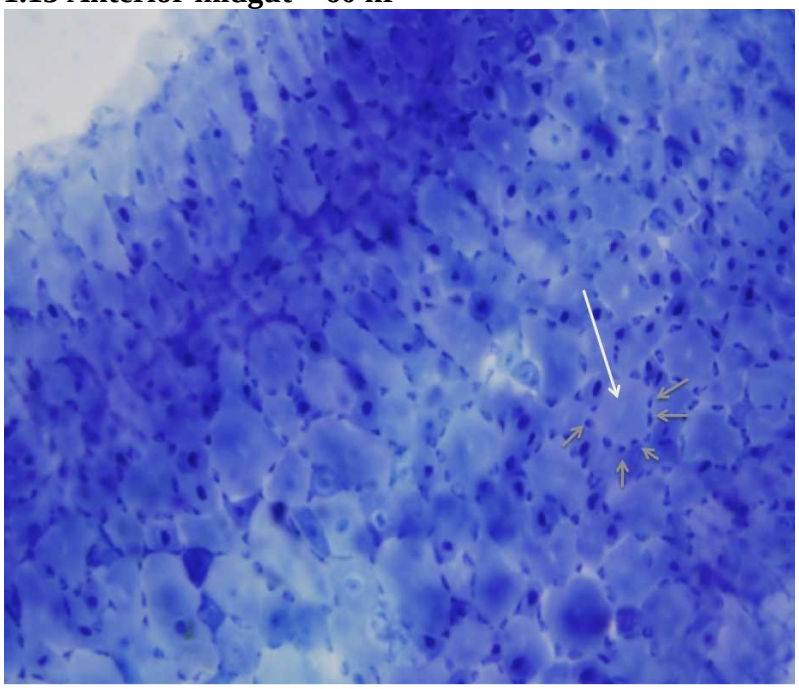

Figure 1.13 Small proliferative cells (gray arrows) surround large larval enterocytes (white arrow)

66 hours Larvae are a range of sizes and developmental states; some have already molted by 66 hours and others are still large and without pigmented respiratory trumpets, such that it is a challenge to confirm their true developmental stage. Perhaps small variations in feeding affected developmental progress, though feeding was controlled. More likely, developmental diversity within a staged cohort comes from differences between males, which are smaller and pupate earlier, and females, which grow larger and pupate later.

Another way to stage larvae, rather than counting hours from the last larval molt, is to look for developmental markers. Towards the end of the 4th instar, pupal respiratory trumpets form and become visible underneath the larval cuticle. Staging by respiratory trumpet and eye development is another way to measure developmental progress in the larva, and to anticipate when they might pupate.

V-stage: Pre-pupal respiratory trumpets form a visible **V** shape underneath the larval cuticle (Figure 1.15A). The midgut is close to maximum size at this stage. Larvae still feed, and fat body accumulates in their thorax and abdomen. Insect fat body is analogous to the liver, and acts as a lipid storage vessel. Fat body reserves are carried over from the larvae to the pupa. (V stage corresponds to ~42 hours after molt).

RT stage (Respiratory **T**rumpets): Under the transparent cuticle of the larval thorax, respiratory trumpets are visible, and the leg imaginal discs grow larger. Clouds of fat body surround the gastric cecae. Even after dissection, gastric cecae continue to contract rhythmically, a reminder of how dynamic the midgut environment is in a living larva. Tracheal branches are attached to the gastric cecae and connect to the midgut at intervals along the length of the midgut epithelium. The peritrophic membrane is intact inside the lumen. The larval midgut has not yet fully contracted. This stage roughly corresponds to ~56 hours after the last larval molt. The

posterior midgut has many diploid cells, while both polyploid and diploid cells are present in the anterior midgut. Sexual dimorphism is apparent at this stage, and the larger females take longer to pupate than the smaller males.

PRT stage: Pigmented **R**espiratory **T**rumpets are visible under the larval cuticle, a sign that the larva will soon pupate (Figure 1.14A). Imaginal leg discs enlarge on both sides of the thorax, and the eyes change as a semi-arc of adult compound ommatidia grows around the 5 larval ocelli. The posterior-central midgut contracts slightly; circular visceral muscle bands pull closer together. The contracted bands of visceral muscles overlie diploid cells arranged in lines parallel to the muscle bands: perhaps the muscles organize the new cells, which seem to lie on top of them. Few polyploid cells remain in the posterior midgut, though large larval enterocytes are still present in the anterior midgut, surrounded by ~8 small diploid cells at this stage (Figure 1.13). Near pupation, the peritrophic membrane detaches (Figure 1.14B, arrow) and the midgut contracts and shortens.

FIGURE 1.14 Larva and larval midgut at Pigmented Respiratory Trumpet (PRT) stage

Figure 1.14 A. PRT-stage larva with pigmented respiratory trumpets (arrow) and developing eyes
B. Larval midgut with peritrophic membrane detached and passing out of the midgut (arrow). Note that gastric cecae are opaque, as if filled (Anterior right, posterior left.)

Figure 1.14 C

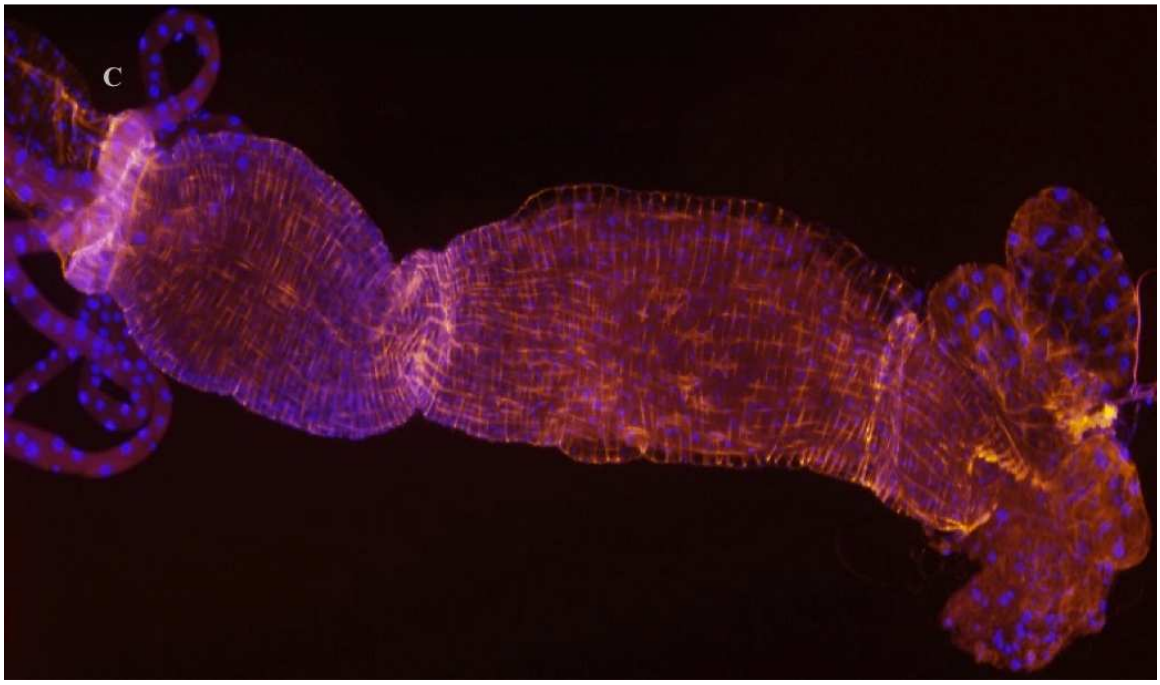

Figure 1.14 C. Same midgut as B, fluorescent image: visceral muscles (phalloidin) and nuclei (DAPI -blue). Note large polyploid nuclei (blue) in gastric cecae (right). Also note contraction just below gastric cecae and in central midgut (posterior-left, anterior-right)

Pupal midgut development

PUPA 0-15 hrs The new pupa have a soft, unpigmented cuticle. The larval headcap is no longer present; the head and the thorax merge into the pupal cephalo-thorax. The adult eyes continue to mature and darken. (**P** stage in upcoming expression analyses.)

FIGURE 1.15 New unpigmented pupa and pupal midgut

Figure 1.15 A. The newly emerged pupal cephalothorax, with developing wing and legs visible though the soft transparent pupal cuticle, and a ventral air bubble (middle).
B. Contracted pupal midgut, with degenerating gastric cecae (anterior, right) and meconium forming inside (beige mass inside midgut).

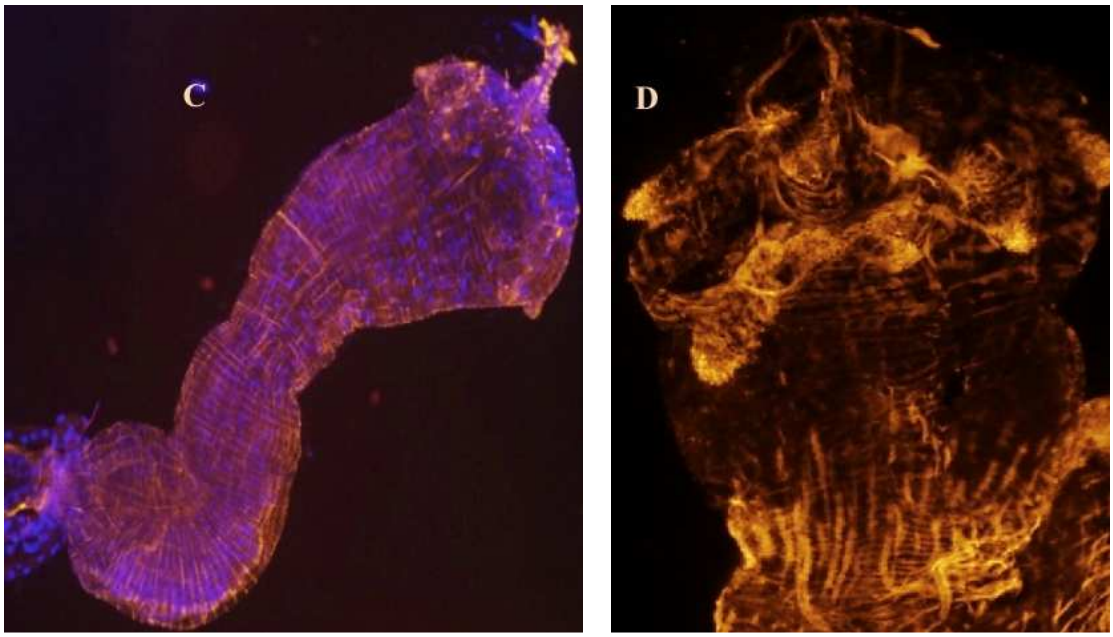

Figure 1.15 C. Same midgut as in B, stained with DAPI and phaloidin. **D.** 4 hr pupal midgut. Visceral muscle network and contracted tips of degenerating gastric cecae (phalloidin).

An air bubble forms in the cephalothorax (Figure 1.15A) that helps orient the pupa at the air surface in relation to the respiratory trumpets [51]. Developing legs and wings are visible under the transparent cuticle. A newly-molted pupa takes in air through the respiratory trumpets in the cephalothorax (Figure 1.15A), instead of through the larval respiratory siphon in the tail; the transition from larva to pupa literally turns it upside down, and the pupa attaches to the water surface by its respiratory trumpets instead of hanging head-down from its siphon. Pupae are sensitive to movement and quickly move down in the water column in response to light and motion. The pupa has no mouth and does not feed, and the pupal midgut is closed to the outside while the adult midgut forms.

Internally, fat body surrounds the gastric cecae, anterior to the midgut. Breakdown of the gastric cecae begins shortly after pupation (Figure 1.16 B-D). In the anterior midgut, obsolete larval enterocytes detach from the basement membrane and slough into the central lumen to form the meconium. This inner mass can be seen inside the pupal midgut (Figure 1.16 B, D). The

gastric cecae shrink. After approximately 15 hrs, the outer cell layer of the midgut is entirely composed of small diploid cells, and the larval cells are clustered in the interior lumen. During the first 15 hrs after pupation the midgut changes dramatically as the larval midgut degenerates. This stage corresponds to **P 3-15** hr in the expression analyses.

FIGURE 1.16 Pupa ~10 hours after pupating

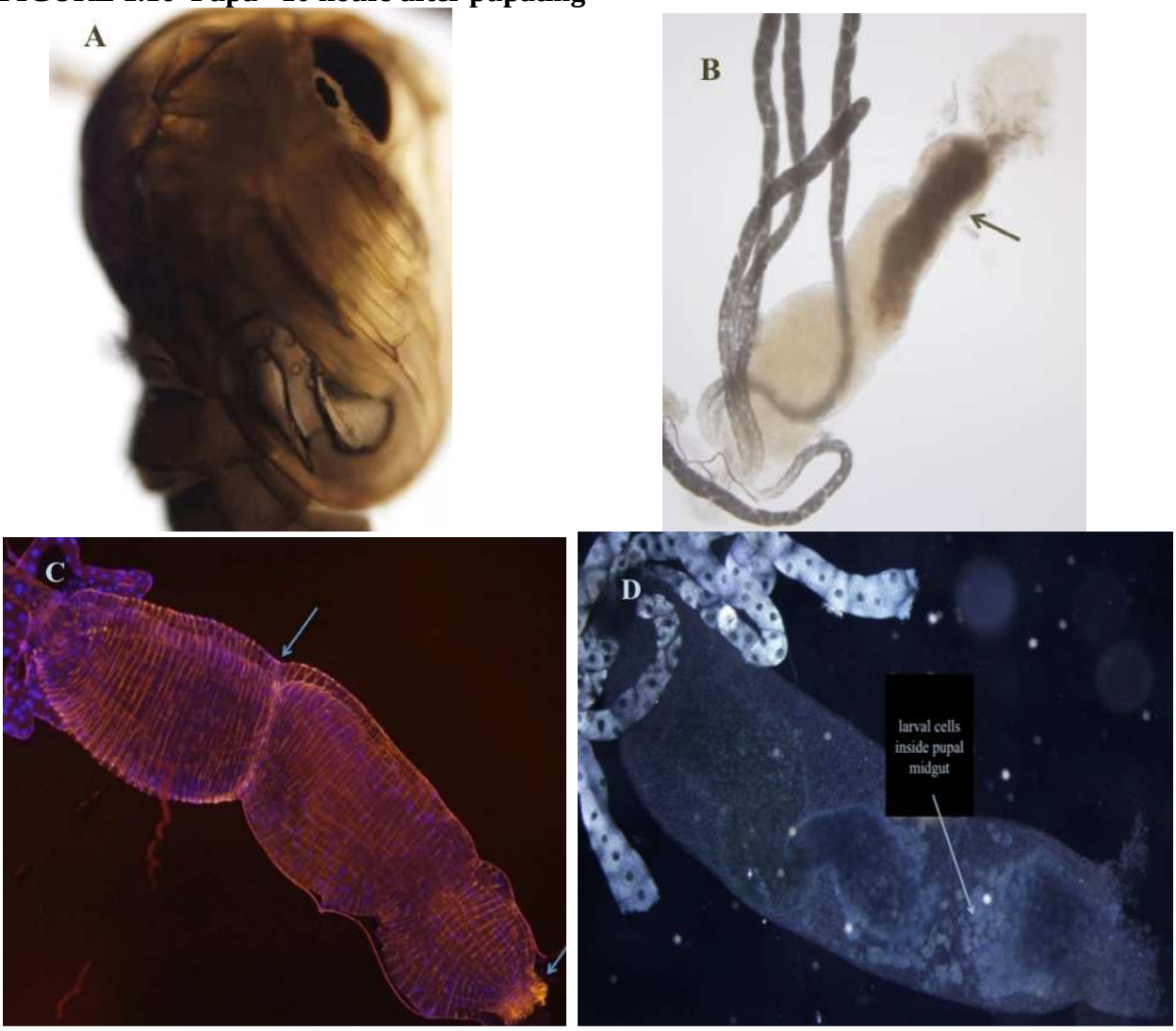

Figure 1.16 Pupa ~10 hours after pupating **A.** Pupa at ~10 hours. The pupal cuticle darkens and hardens. **B.** Detached larval cells formed the internalized meconium (arrow) as the larval midgut degenerated **C.** DAPI and phalloidin stain of midgut showing inner larval cells and a central and an anterior constriction (arrows). The gastric cecae are gone. **D.** Larval enterocytes clumped inside the newly-formed adult midgut composed of much smaller cells. (phase contrast)

PUPA-15 hrs-24 hours: day 1 By 24 hours after the molt the outer midgut cell layer is entirely composed of diploid cells, with a localized dense area of small nuclei at the border of the anterior midgut where three adult structures take shape: two small paired dorsal diverticula and a larger, single oval structure, the ventral diverticulum, or crop (Figures 1.17, 1.19).

FIGURE 1.17 Pupal midgut 24 hours after pupating (Day 1)

Figure 1.17 (day 1) **24 hour pupal midgut** with dorsal (top) and ventral (bottom) diverticulum (crop) forming at anterior (circles, to right). Malphigian tubules are to left (posterior). This stage corresponds to P1 in expression analyses. Phase contrast image.

Inside the midgut detached larval enterocytes are visible and their mass seems to diminish over time. These cells are thought to be absorbed [51], but the mechanism of resorbtion is unknown. It is uncertain if surrounding pre-adult midgut cells are capable of digestion.

PUPA – day 2 The day 2 pupa encloses a pharate adult: adult pigmentation and structures can be seen beneath the pupal cephalothorax (Figure 1.18 A). The difference between a male and a female midgut becomes obvious: the male midgut is shaped like a thin tube, while the female midgut has an urn-like widening in the posterior, which will later hold the blood meal.

FIGURE 1.18 Pupa day 2 (**P2** in expression analyses)

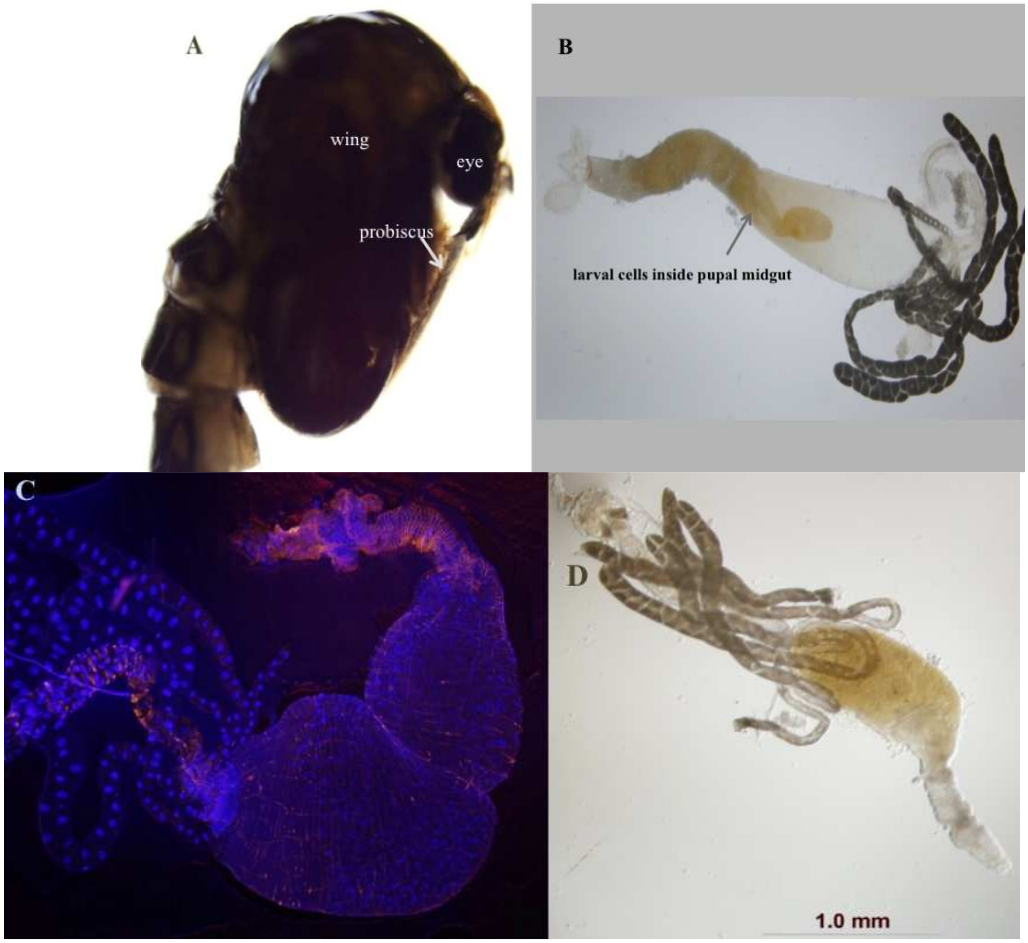

Figure 1.18 Pupa day 2 A. Late pupa: darkly pigmented, eyes fully formed, probiscus wraps around wing inside pupal cephalothorax. Dark markings on dorsal segments show adult pigmentation. **B.** Adult diverticulum forming (right - posterior). Larval cells (meconium) inside midgut. **C.** Late pupal female midgut showing adult anterior structures (phalloidin, DAPI) **D.** Late pupal female midgut with meconium still visible inside, now more diffuse (anterior - right)

NEWLY ECLOSED ADULT

FIGURE 1.19 Adult alimentary canal: mosquito alimentary canal showing the position of the dorsal and ventral diverticulum and the midgut in the adult mosquito [64].

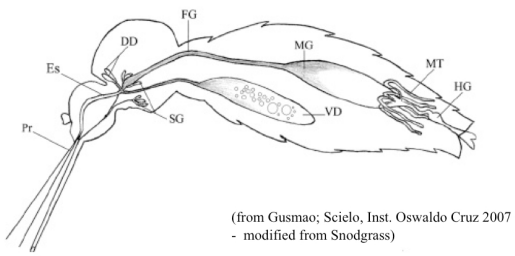

Pr-probiscus, *Es*-esophagous, *DD*-dorsal diverticula, *SG*-salivary gland, *VD*-ventral diverticula (or crop – see C and D), *FG*-foregut, *MG*-midgut, *HG*-hindgut

FIGURE 1.20 Newly emerged adult midgut

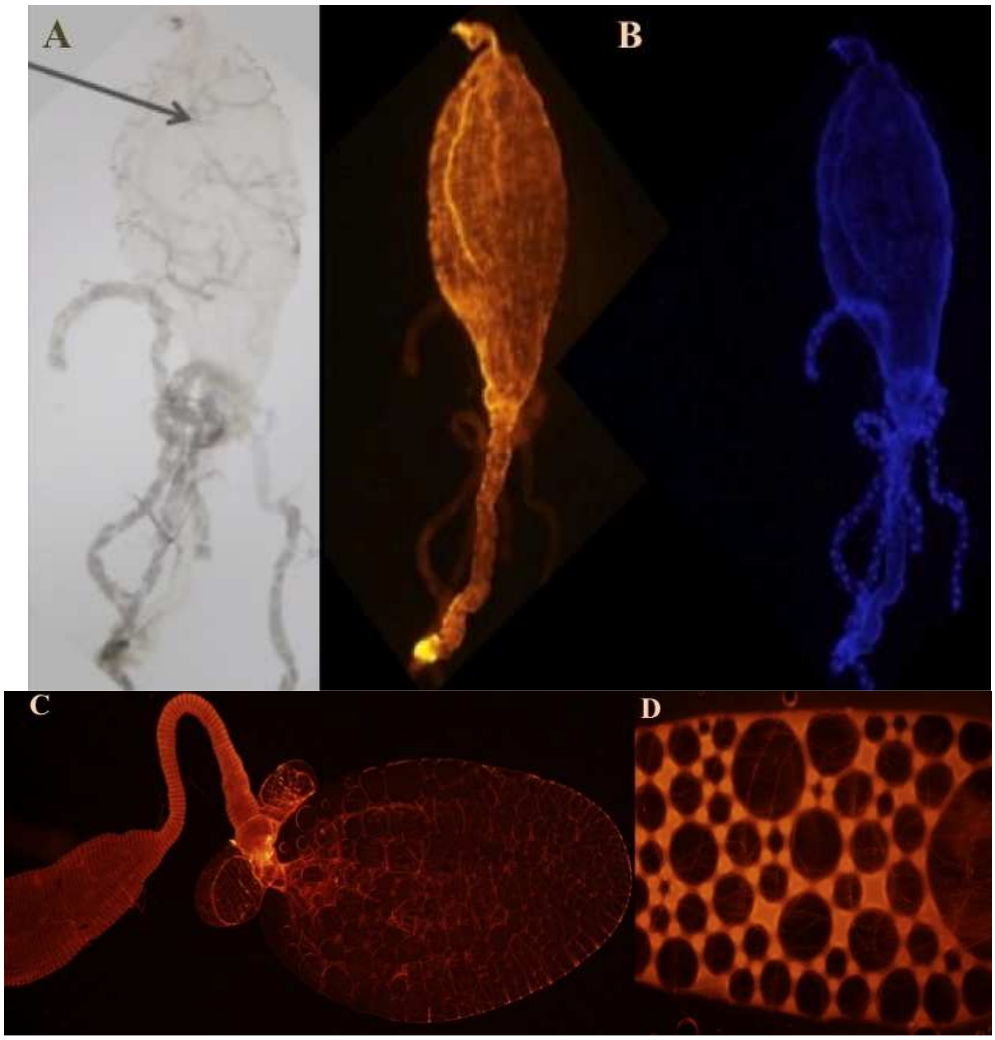

Figure 1.20 Newly emerged adult (A1 in expression analysis)
A, B. Adult female midgut tracheal branches (arrow); same midgut: phalloidin - visceral muscles (orange), DAPI - nuclei (blue). **C. Dorsal and ventral diverticula** (right, anterior) filled with air. **D.** Ventral diverticulum or crop (closer view) folds back under midgut (**vd** – top drawing) holds floral nectar and microorganisms [64].

The period immediately after eclosing from aquatic pupa to winged adult is a critical time of ovarian maturation for the female mosquito [65]. Newly emerged *Ae. aegypti* females require about three days to become competent for vitellogenesis (yolk production) in response to a blood meal [66]. Biosynthesis of juvenile hormone (JH) begins after adult emergence, and increased JH levels indicate readiness to begin reproduction [67]. By day 3 (**A3**) the adult is competent for a blood meal.

This is the stage where the expression analysis ends; thus the span studied follows midgut metamorphosis from the early 4th instar larva to the reproductively mature adult.

Expression pattern of *BR* isoforms in the midgut during metamorphosis

To analyze *BR* transcript levels in the midgut during metamorphosis, I used quantitative PCR (qPCR). Of the four isoforms, *BR*Z3 and Z4 had the highest expression levels in the midgut (Figure 1.21A). At the beginning of the 4th instar *BR*Z3 expression was moderate, then increased around 24 hr and reached a peak around 48 hr. After this peak, *BR* transcript levels dropped precipitously before pupation, and stayed low thereafter (Figure 1.21). This expression pattern was repeatable. In *D. melanogster*, *BR* is transcribed in response to increasing ecdysone titer [68]. In *Ae. aegypti*, ecdysone titers have been determined [69], and the ecdysone level increases first around 20 hours after the molt to 4th (Figure 2.6), when *BR* expression increased.

FIGURE 1.21 *BR* isoform expression in *Ae. aegypti* midgut 4th instar – early adult

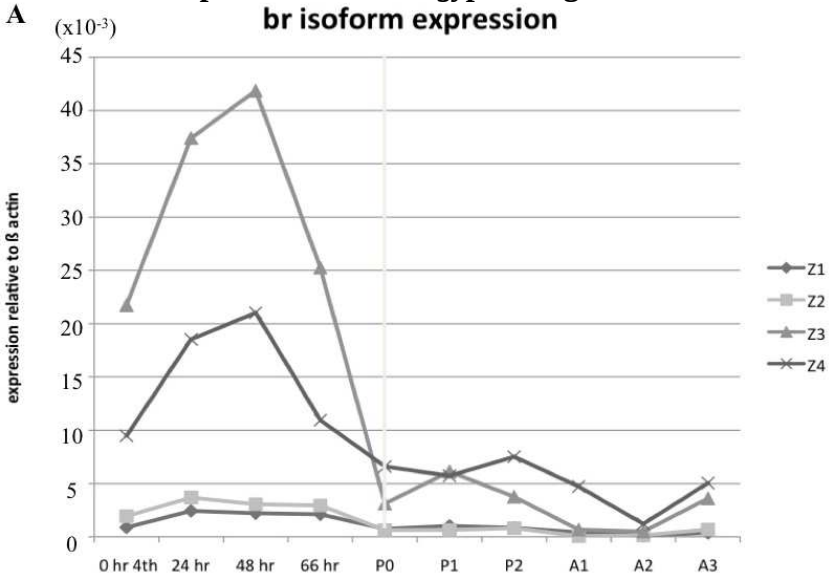

A. *br* isoform expression in *Ae. aegypti* midgut during metamorphosis – relative expression levels of four *BR* isoforms, 4th instar to early adult *BR* expression increased until ~48 hours, then *BR* transcript levels fell sharply and remained low in the pupa and adult. **Z3 was most abundant isoform** in the midgut. **P0** - larva to pupa molt (Figure 1.15), **P1** - pupa day 1 (Figure 1.17) **P2:** pupa day 2 (Figure 1.18), **A1**: adult, day 1 (Figure 1.19) **A2**: day 2 **A3**: day 3

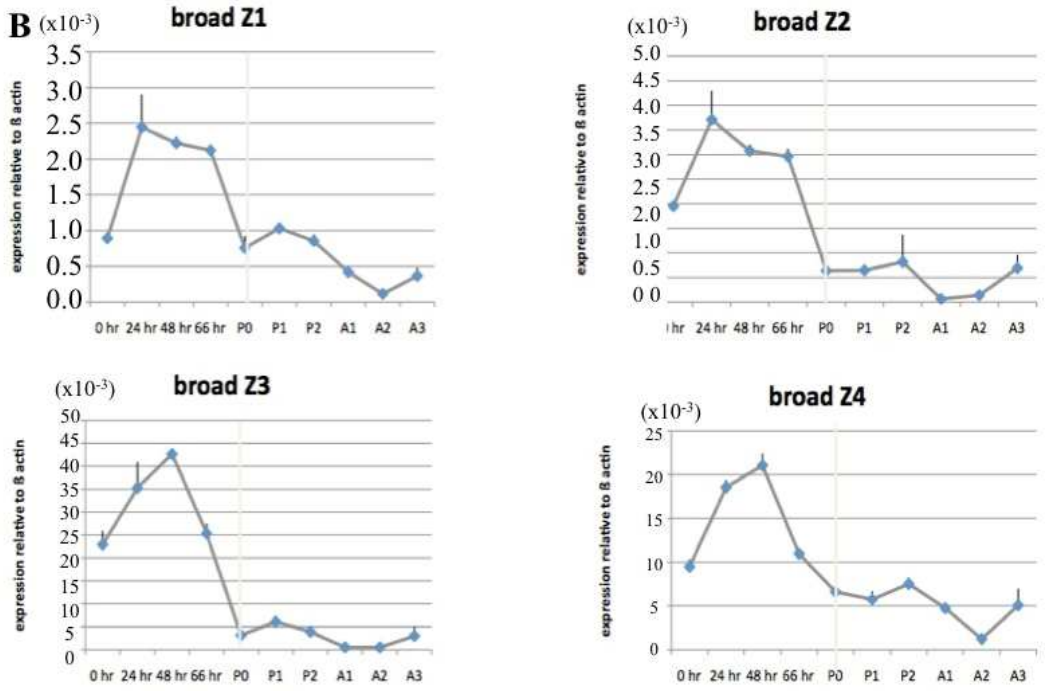

Figure 1.21 B. Expression pattern of each *BR* isoform during midgut metamorphosis
*BR*Z1 had the lowest expression, Z2 peaked at 24 hours, and *BR*Z3 and Z4 expression levels were the highest, and showed the steepest decrease.

Expression of miRNAs during midgut metamorphosis

I hypothesized that changes in *BR* expression levels during metamorphosis might result, in part, from developmental timing mechanisms involving miRNAs. Therefore, by using qPCR, I measured the expression levels of miRNAs predicted to interact with *BR.* These experiments were repeated several times, and results shown here were repeatable.

Genomic organization of *miR-317-2, miR-277* and *miR-34*

Because *miR-34* is ecdysone-responsive in other organisms, the expression of *miR-317, miR-277* and *miR-34* was investigated in *Ae. aegypti*. *miR-34* is deeply conserved in all metazoans [70]. These three miRNAs are located in Supercontig.1.265 in the *Ae. aegypti* genome (Fig 1.22). Clustering of these three miRNAs is evolutionarily conserved in insects (Fig 1.22B). Their genomic proximity suggested they might be coordinately regulated. Another copy of *miR-317* is located in Supercontig. 1.153. In the honeybee, flour beetle, and annelid worm, these 3 miRNAs

are situated inside an intron of the gene *RBP8*, which encodes a subunit of RNA pol II (Figure 1.22).

FIGURE 1.22 *miR-317, miR-277, miR-34* in *Ae. aegypti* genome on Supercontig 1.265 and ***miR-34, miR-277* and *miR-317* proximity in insects and in an Annelid**

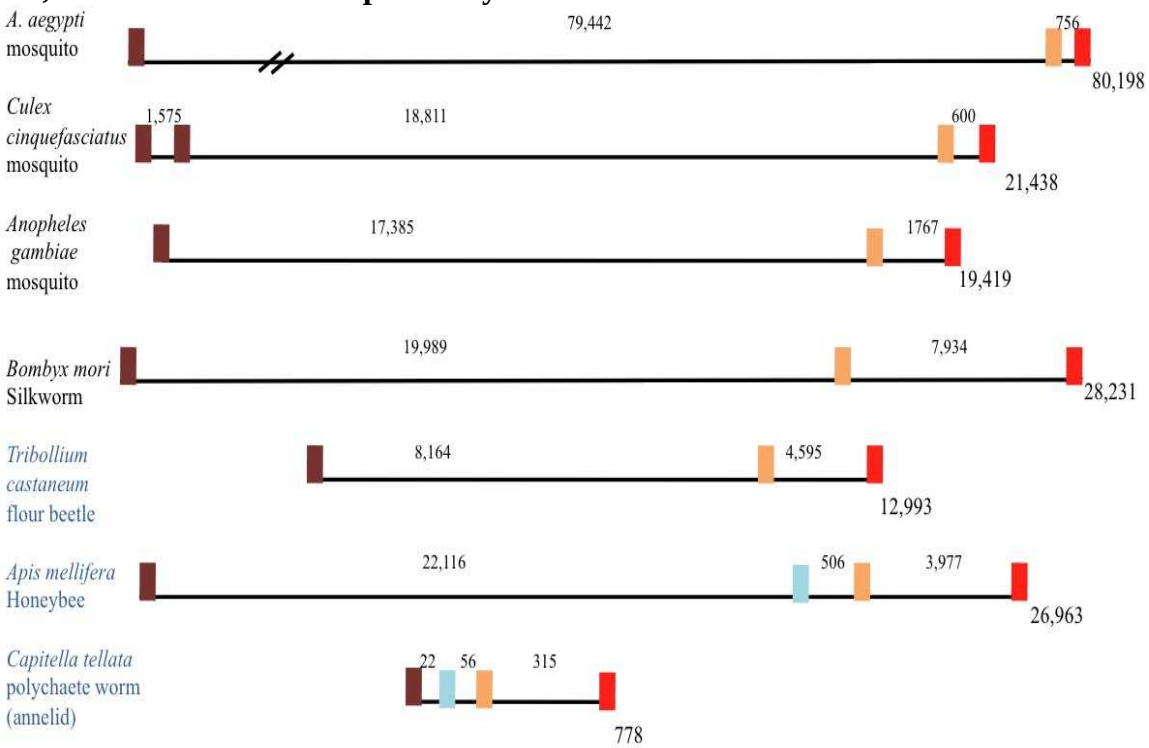

Figure 1.22 As in the honeybee and the flour beetle**,** in *Capitella tellata*, the annelid worm, ***miR-317, miR-277* and *miR-34*** are intronic within *RBP8* [71]. The conserved proximity of these three miRNAs suggests they were grouped together in a common ancestor before the Arthropods separated from the Annelids ~ 600 mya. *RBP8* is a small common subunit of RNA polymerases I, II, and III. This intronic location for *miR-34* has not been previously annotated. Numbers above the lines indicate the number of basepairs between the miRNAs.

miR-317 - **brown** *miR-277* - **yellow** *miR-34* - **red**

Expression of *miR-317, miR-277* and *miR-34* during mosquito midgut metamorphosis.

miR-34 and *miR-317* expression levels were high in 4th instars, decreased in pupae, then increased again in the adults. Their similar expression pattern in the midgut supported the hypothesis that they were co-regulated (Figure 1.23). However, the relative abundance and expression pattern of *miR-277* expression differed from that of *miR-34* and *mir-317; miR-277* was lower in the larvae, increased in the pupa, then decreased in day 3 adults.

FIGURE 1.23 *miR-317, miR-34, miR-277* expression - *Ae. aegypti* midgut 4th instar-adult

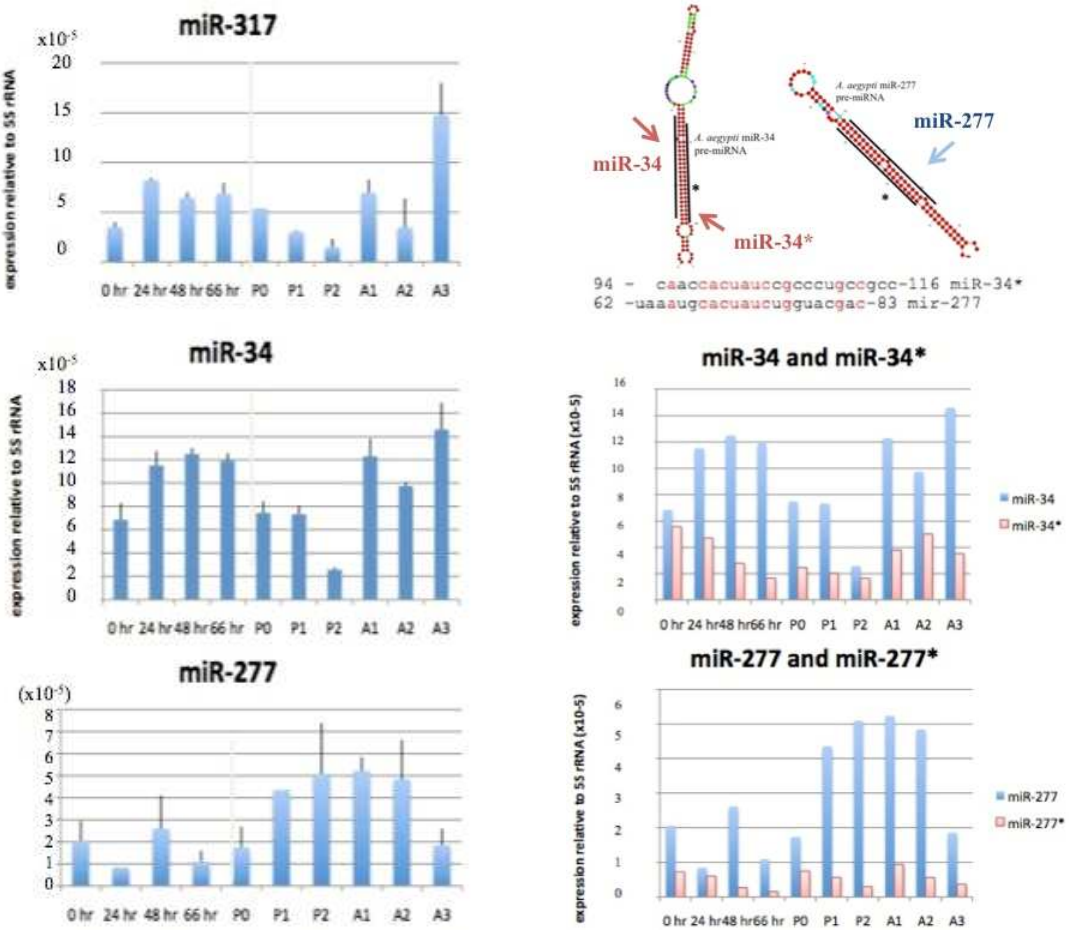

Figure 1.23 *miR-317, miR-277,* and *miR-34* expression during midgut metamorphosis: *miR-34* and ***miR-317*** were similar, but ***miR-277*** was low. ***miR-34*** and ***miR-277*** pre-miRNA hairpins - alignment of ***miR-34**** with ***miR-277*** (top right) suggested potential duplication then arm-switch. ***miR-34****(3' side of hairpin **pink**) and ***miR-277**** (5' side of hairpin-**pink**) *miR-34** expression was more abundant than *miR-277*, but *miR-277** was minimal in the midgut.

*miR-34**, the cleavage-product passenger-strand on the 3' side of the pre-miR-34 hairpin, was less abundant than *miR-34*, but more abundant than *miR-277*. *miR-34** and *miR-277* shared expression patterns, suggesting that *miR-34** might function in the midgut (Figure 1.23).

The lower abundance and different expression pattern of *miR-277* suggests *miR-277* may not be part of a common primary transcript that includes *miR-317, miR-277* and *miR-34*. In *D. melanogaster* an independent primary transcript was recently cloned that only encoded a single miRNA, *miR-277* ([72], Genbank FJ45605). By 3' RACE I cloned a transcript with a similar 3'

end in *Ae. aegypti* (Genbank KC897652). This suggested that, though located between *miR-317* and *miR-34*, *miR-277* may be transcribed independently in *Ae. aegypti*, as in *D. melanogaster* (Figure 1.24).

FIGURE 1.24 *Aae-pri-miR-277* 3' RACE product

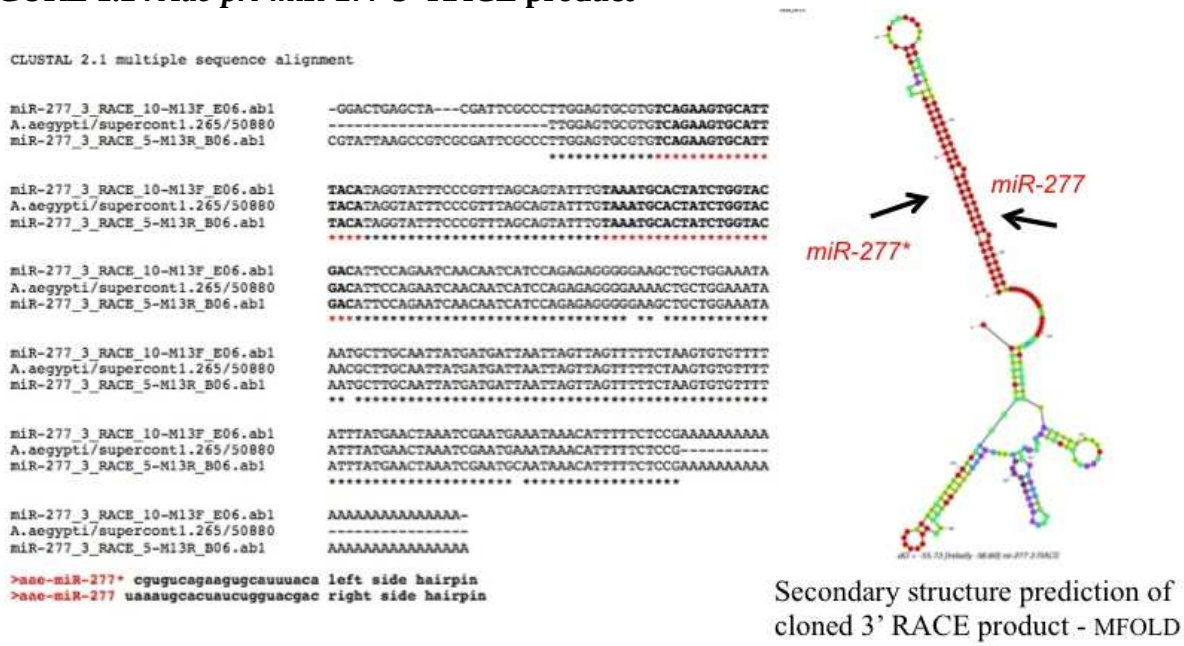

Figure 1.24 Sequence alignment of the *Aae-miR-277* 3' RACE-product (Genbank KC897652) with *A. aegypti* genomic DNA from Broad Institute (left), and predicted secondary structure of that 3' RACE product showing the hairpin structure of *miR-277* (right).

Genomic organization and expression pattern of *miR-100, let-7* and *miR-125* during metamorphosis

In *Ae. aegypti* (and many bilaterans), *miR-100, let-7* and *miR-125* are clustered in the same genomic locus, and may be coordinately expressed [73]. In *D. melanogaster,* the primary miRNA transcript that encodes *miR-100, let-7,* and *miR-125* has been cloned and characterized [23]. During *D. melanogaster* metamorphosis, *let-7* and *miR-125* levels increase in response to ecdysone signaling. Ecdysone elevates *let-7* and *miR-125* expression, but decreases the level of *miR-34* [22, 23, 25].

FIGURE 1.25 *miR-100, let-7, miR-125* in *Ae. aegypti*

Figure 1.25 A. ***miR-100, let-7* and *miR-125* are clustered** in the same genomic region in *Ae. aegypti* genome.

Figure 1.25 B. *miR-100, let-7, miR-125* expression in midgut 4th instar-adult

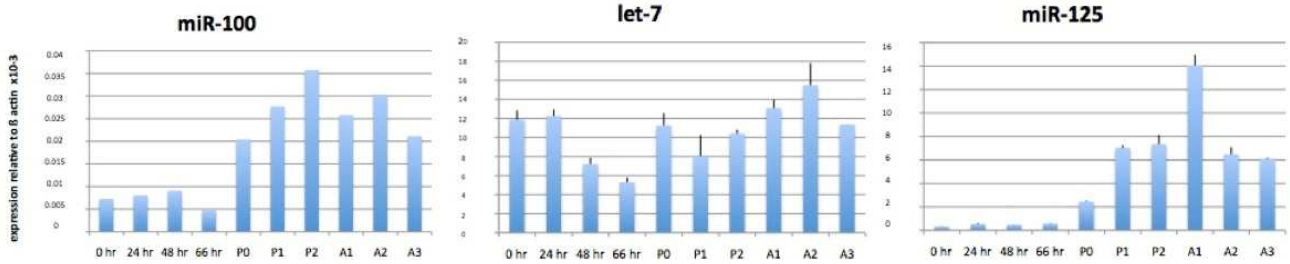

Figure 1.25 B *let-7, mir-125, miR-100*: Expression during midgut metamorphosis
In contrast to *miR-125* and *miR-100,* which increased mostly in the pupa and adult, *let-7* was also elevated during the larval stage.

Expression level of *miR-100, let-7* and *miR-125* during midgut metamorphosis.

let-7 transcript levels decreased during larval growth, then increased in the pupa and the adult (Figure 1.25 B). Unlike *let-7, miR-125* and *miR-100* expression levels were lower during the 4th instar. In pupal midguts, the expression levels of all three miRNAs increased.

***miR-14* expression during midgut metamorphosis**

In *D. melanogaster*, *miR-14* regulates fat metabolism and insulin production [74, 75]. In addition, *miR-14* targets the ecdysone receptor mRNA and is an autoregulator of ecdysone production [74]. Since ecdysone signaling is a key factor in the timing and control of metamorphosis, *miR-14* levels were investigated during mosquito metamorphosis. Of the miRNAs studied, *miR-14* was overall the most abundantly expressed in *Ae. aegypti* midgut. *miR-14* levels were lower during the feeding larval stage, then increased in the (non-feeding) pupa and adult (Figure 1.26).

FIGURE 1.26 *miR-14* expression in *Ae. aegypti* midgut 4th instar-adult

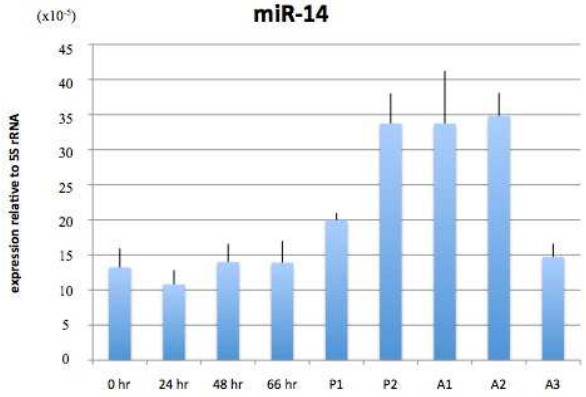

Figure 1.26 Expression of *miR-14* during midgut metamorphosis: *miR-14* was the most abundant miRNA in the midgut. *miR-14* increased in the pupa and in the newly-eclosed adult.

***miR-7* and *miR-190*: microRNAs that map to introns of protein-coding genes**

The genomic position of *miR-190*, and its expression during metamorphosis

miR-190 is located within the 12th intron of *AaegTALIN*. *TALIN* encodes a cytoskeletal protein involved in connecting cellular actin with extracellular-matrix integrin. Overall, the abundance of *miR-190* was relatively low. *miR-190* expression was highest in early 4th instar, decreased during the remainder of the instar, then increased slightly again in the adult (Figure 1.27). The expression of *TALIN* mirrored that of *miR-190: TALIN* mRNA levels were also low in the midgut.

Figure 1.27 Expression of *miR-190* and host gene *talin*

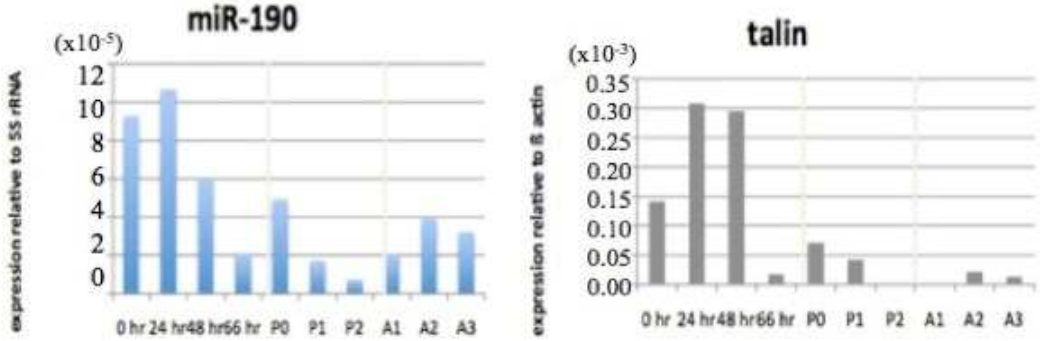

Figure 1.27 Expression of *miR-190* and its host gene *TALIN* during midgut metamorphosis: *miR-190* is located in an intron of the gene encoding *TALIN*. Both were expressed at low levels in the midgut. *miR-190* and *TALIN* levels were higher in early 4th instars than in pupae or adults.

The genomic position of *miR-7*, and its expression during metamorphosis

miR-7 is located in the last intron of heterogeneous nuclear ribonucleoprotein-K (*hnRNP-K*), an RNA-binding protein involved in translational regulation [76-78] (Figure 1.28 A). This ancient intronic location is conserved from insects to humans [79].

FIGURE 1.28 A *miR-7* in the last intron of *hnRNP-K:*

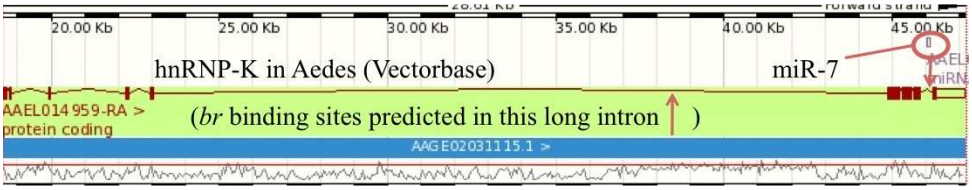

FIGURE 1.28 B Expression of *miR-7* and of host gene *hnRNP-K*

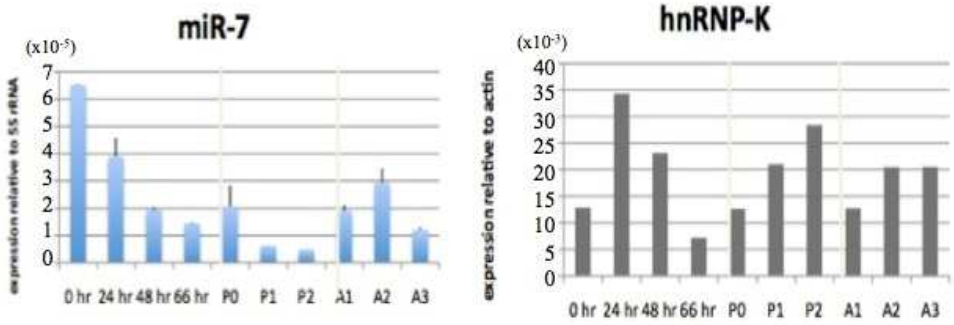

Figure 1.28 A *miR-7* is in an intron of ***hnRNP-K***; an evolutionarily conserved position. An independent promoter for *miR-7* may be in the long upstream (5-6) intron [76].
B. Expression of *miR-7* and of its host gene *hnRNP-K* in the midgut at metamorphosis: *miR-7* abundance was low in the midgut. Like *miR-190*, *miR-7* expression was highest in the early 4th instar. In contrast, *hnRNP-K* was abundantly expressed in the midgut, with an expression pattern that differed from *miR-7*.

The relative abundance of *miR-7* was low. *miR-7* expression level was highest in early 4th instars, then subsequently decreased, remained low in the pupal stage and then moderately increased in the adult (Figure 1.28 B). The expression of intronic miRNAs usually follows that of the host gene, but in the midgut both the expression pattern and the abundance of *miR-7* and *hnRNP-K* differed: *hnRNP-K* was abundantly expressed throughout midgut development, decreasing slightly at the larva-to-pupa and pupa-to-adult transitions.

Expression patterns of RNA-binding factors in the midgut of *Ae. aegypti* during metamorphosis: heterochronic gene homologs *lin-28* and *Brain Tumour (BRAT)*

BRAT, an RNA-binding translational regulator

BRAT is an RNA-binding factor from the tripartite motif and *Ncl*, *Ht2a,* and *Lin-41* (Trim-NHL) family. The NHL domain forms a beta-propeller that mediates protein-protein interactions. Members of the Trim-NHL family act as translational repressors [80]. BRAT binds miRISC component AGO1, and co-immunoprecipitates with the miRISC-associated deadenylase complex factor, NOT1 in *D. melanogaster* [80-82]. The level of *BRAT* expression in *Ae. aegypti* midgut dramatically increased near pupation (Figure 1.29 B). This expression pattern was repeatable, and was the opposite of *BR*, which sharply decreased near pupation (Figure 1.29 A). Expression of *BRAT* just at pupation suggested it might have a function in that process.

FIGURE 1.29 RNA-binding factor expression compared with *BR* isoform expression

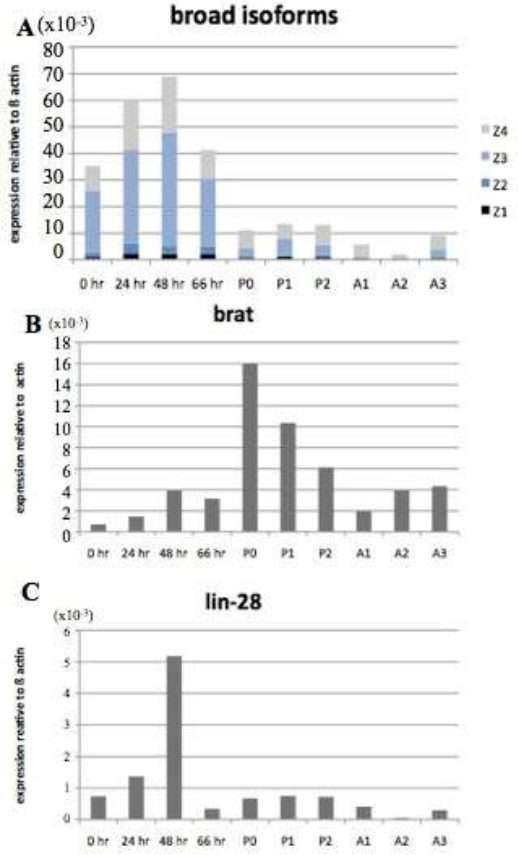

Figure 1.29 A. Total expression of *BR* isoforms in the midgut at metamorphosis. **B. *BRAT* (lin-41 homolog)** increased at pupation. When *BR* expression decreased, *BRAT* isoforms increased. **C. *LIN-28* expression** was similar to *BR*, but *LIN-28* transcript abundance was very low.

Midgut expression levels of *LIN-28*, an RNA-binding regulator of developmental timing

LIN-28 was first characterized as a developmental timing regulator in the *C. elegans* heterochronic pathway, and its role in developmental timing is highly conserved across species [83, 84]. LIN-28 binds *let-7* post-transcriptionally to inhibit *let-7* transcript expression and prevent differentiation [85]. While *let -7* function is associated with terminal differentiation [86], LIN-28 function is associated with an undifferentiated state [87].

LIN-28 expression in the mosquito midgut was similar to the *BR* expression pattern: it was highest in the first 48 hours of the 4th instar, declined towards the time of pupation, and remained low in the pupa and adult. However, *LIN-28* transcript abundance overall was much lower than *BR* and *hnRNP-K* (Figure 1.29 C).

DISCUSSION

A rationale and summary of midgut developmental histology

Micrographs of the developing midgut provided a visual record of morphological changes that occurred during metamorphosis and allowed study of midgut morphology and cellular composition. I first established what normal midgut development looked like as a baseline against which to later compare the results of hormone treatment or of dietary restriction.

I used basic techniques of dissection, staining, and microscopy to characterize and record midgut metamorphosis as a series of developmental changes over time. Imaging the midgut at different stages both documented and provided insight into the processes it undergoes during the transition from the larval stages to the adult. Correlating morphological changes with changes in expression patterns in well-fed, untreated larvae now can provide a baseline against which to compare morphological and expression-pattern changes in experimentally treated larvae. This is

a first step in exploring the molecular mechanisms that underlie the observed morphological changes.

As midgut remodeling progressed, coordinated changes occurred; small diploid adult midgut progenitor cells proliferated, obsolete larval cells detached from the basement membrane, and new cells differentiated to form adult structures.

FIGURE 1.30 Landmarks of the timing of metamorphosis in the midgut

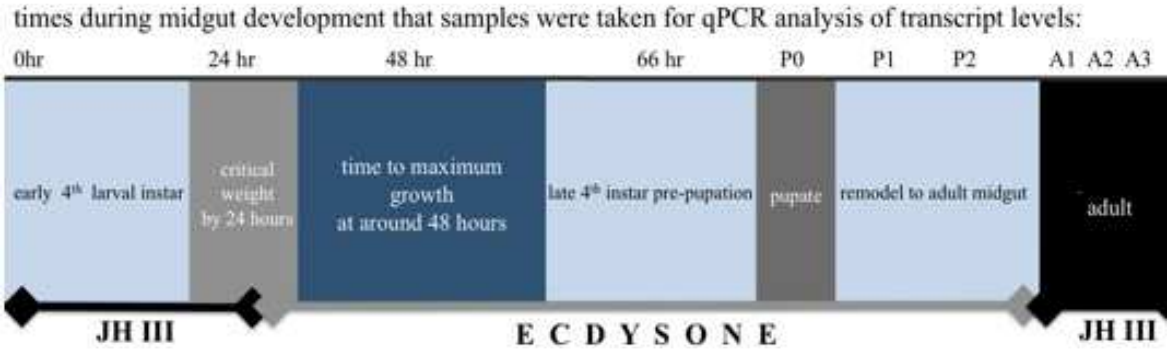

Figure 1.30 Sequence of developmental timing events during midgut metamorphosis correlated with sample times for expression analysis (sample times - written above).
0 hr: Early 4th instar - larval feeding and growth
24 hr: Continued larval feeding. Onset of cell proliferation by ~32 hours suggested that a commitment to pupate might have been made.
48 hrs: Larval feeding, fat body accumulation. Maximum midgut size ~48 hours.
66 hrs: Obsolete larval cells began to detach from the basement membrane into the lumen.
P0 hr: Pupation, no more feeding, the midgut was closed.
P0-P1: Obsolete larval cells filled the central lumen, and the outer nascent adult midgut was composed of small, newly proliferated cells.
P1-P2: The adult midgut formed, the larval cells inside the midgut were – reabsorbed? Adult structures formed, the male and the female midgut were different.
A1: Aquatic, non-feeding pupa eclosed to winged adult still reliant on larval nutrient reserves, not yet reproductively competent.
A2-A3: The young adult female mosquito in a preparatory state before the first blood meal. (Biosynthesis of juvenile hormone, synthesis of early trypsin mRNA.)

FIGURE 1.31 Summary of *BR* expression relative to miRNA and RNA-binding factors in
1. mainly **larvae** **2.** mainly **pupae and adults** **3.** mainly **larvae and adults**

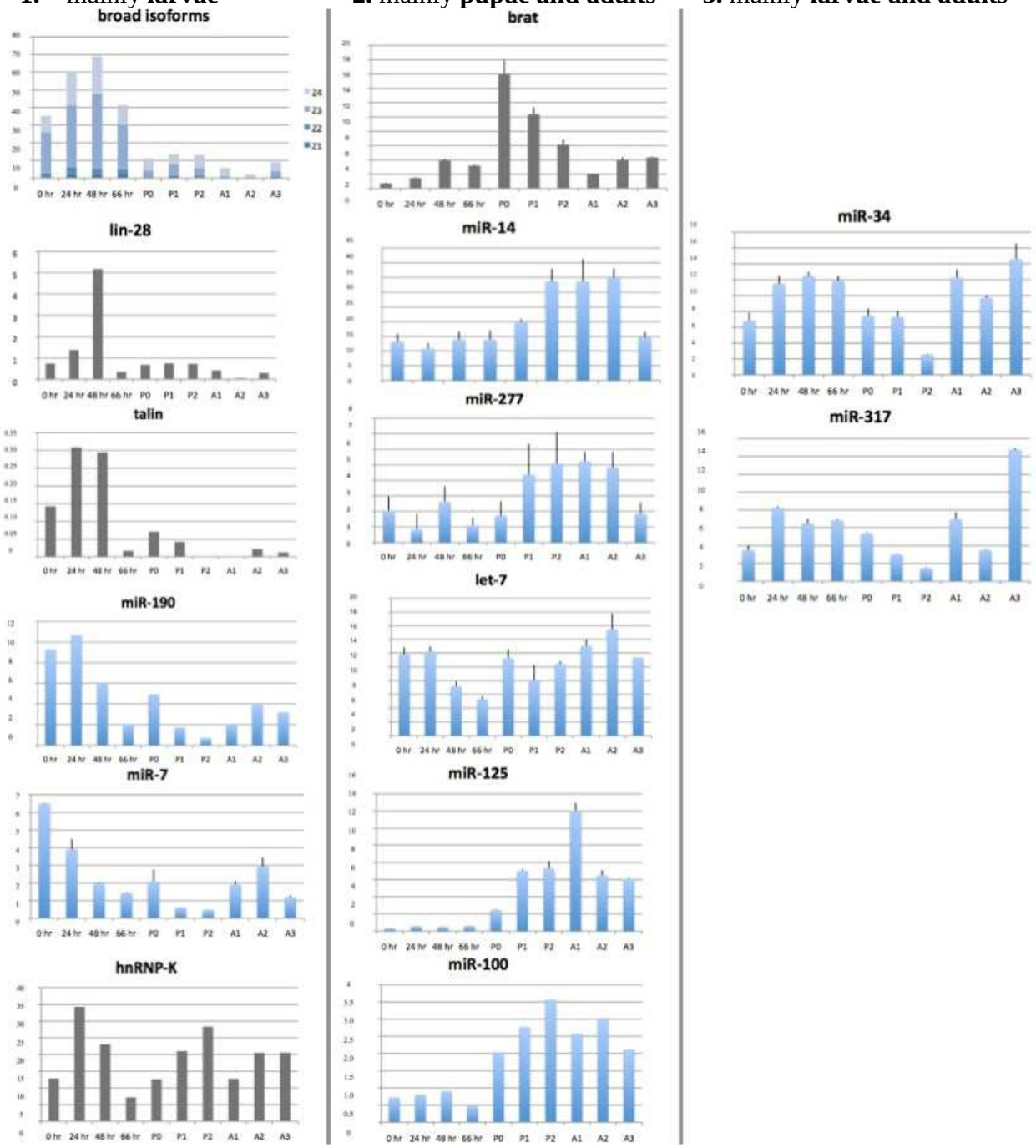

Figure 1.31 Summary of *BR* and RNA-binding factor expression in midgut of *Ae. aegypti*
***BR* isoform expression** (composite of 4 isoforms) – blue; **top left**.
Expression of mRNAs relative to ß actin ($x10^{-3}$) - **gray**
Expression of miRNAs relative to 5S rRNA ($x10^{-5}$) - **blue**

Expression patterns of miRNAs and RNA binding factors during midgut metamorphosis

The expression patterns of the miRNAs and RNA binding factors studied here can be loosely grouped into three categories: (1) those expressed mostly in larvae (2) those expressed mostly in pupae and in adults (3) those expressed mainly in larvae and in adults.

1. Factors expressed mainly in 4th instar larvae

Mosquito metamorphosis is initiated in 4th instar larvae. The miRNAs *miR-7* and *miR-190*, the transcription factor *BR*, and the RNA-binding protein *lin-28* were primarily expressed in 4th instars. *miR-7* and *miR-190* expression levels were highest in newly-molted 4th instars then gradually decreased over the course of the stage, however *lin-28* and *BR* expression increased over the first 2 days of the 4th instar, to peak around the time that ecdysone titers are the greatest, then decreased while ecdysone titers remained high.

miR-7

miR-7 has a well-documented role in patterning and development. *miR-7* is involved in regulating the timing of oocyte-follicle cell development, and targets the BTB-zinc-finger transcription factor **t**ram**t**rac**k** 69 (*ttk69*) to promote the transition from endoreplication to the selective amplification of the chorion genes for eggshell production [88]. *miR-7* is involved in the differentiation of photoreceptors during *D. melanogaster* eye formation [89]. In this context, *miR-7* expression is dependent on EGFR signaling. *miR-7* can regulate multiple effectors of EGFR signaling [90] as well as seven Notch target genes [76]. EGFR signaling promotes proliferation of adult midgut progenitor cells in the *D. melanogaster* larval midgut, and promotes intestinal stem cell division in the adult midgut [59, 91].

In the context of cell division, *Aae-miR*-7 was expressed in the early 4th instar larval midgut near

the onset of cellular proliferation (Figure 1.27 B). By analogy, *Aae-miR-7* may participate in cell proliferation during midgut remodeling. Although its expression level was low during the time of maximum diploid cell division, *miR-7* may be required to initiate cell division. In *D. melanogaster* follicle cells, the expression level of *miR-7* is also relatively low, suggesting that *miR-7* may have high regulatory efficiency [88]. Alternatively, *miR-7* may only be expressed in a subset of cells in the midgut, such as neuronal cells.

Based upon the critical weight model of metamorphosis, newly-molted 4th instars were hypothesized to have relatively high JH titers. Since *miR-7* transcripts were highest in newly-molted 4th instars, then decreased when the JH titer was expected to decrease, one explanation for this expression pattern is that *miR-7* may be JH-regulated. *miR-7* was expressed in the early 4th instar; so was *BR*. Since *miR-7* was predicted to target *BR*, *miR-7* might dampen *BR* translation in the midgut during the early 4th instar, before critical weight is reached.

miR-7 is located inside an intron of *hnRNP-K*, but, although *hnRNP-K* was highly expressed throughout midgut metamorphosis, *miR-7* was not (Figure 1.27). This uncoupled expression pattern also occurs in *D. melanogaster*, where a *Dme-miR-7* specific promoter was identified inside intron 5-6 of the *D. melanogaster* homolog of *hnRNP-K* (called *BANCAL*) [76]. *hnRNP-K* encodes a highly conserved RNA-binding factor with 3 KH domains and an RNA-binding RGG box, a domain structure shared by the Fragile X Mental Retardation Protein (FMRP), which acts with the RNAi machinery to repress translation of mRNA targets [92]. *hnRNP-K* transcripts are induced by ecdysone in *D. melanogaster*, and hnRNP-K may interact with *BR* during leg and wing morphogenesis [93]. hnRNP-K binds to C-rich regions, and is involved in translational silencing [94, 95]. Additionally, hnRNP-K is known be targeted by

viruses [78] and interacts with the Dengue virus core protein and the Chikungunya virus non-structural protein nsP2 [77, 96], two viruses carried by *Ae. aegypti* that cause human illness.

miR-190 and _talin_ expression levels were low in the late larva and the pupa

The expression patterns of *miR-190* and *miR-7* were very similar. *miR-190* expression peaked in the early 4th instar, when JH is hypothesized to still be present. *miR-190*'s intronic location inside the gene *TALIN,* and the similarity between their expression patterns suggests that they may be co-regulated. *miR-190* was predicted to have multiple binding sites on *BR*Z3 and Z4 3'UTRs.

LIN-28 The expression pattern of *LIN-28* was limited mostly to 4th instars, and highest expression was concurrent with the peak in the 4th instar ecdysone titer. The peak in *LIN-28* expression was also coincident with an increase in diploid cell proliferation and the attainment of maximum larval midgut size. LIN-28 is associated with an undifferentiated cellular state, while *let -7* is associated with terminal differentiation [86][83, 84]. LIN-28 binds *let-7* post-transcriptionally to inhibit *let-7* expression and prevent differentiation in human embryonic stem cells [85]. *LIN-28* was first characterized as a developmental timing regulator in the *C. elegans* heterochronic pathway, and its role in developmental timing is conserved across species [83, 84]. The reported interaction between LIN-28 and *let-7* in other species is very interesting and may have relevance to the results presented here. *let-7* is also a heterochronic gene in *C. elegans:* the *let-7* transcript was the second miRNA ever characterized. In *C. elegans*, *let-7* expression determines the onset of the adult developmental program [19]. *let-7* is highly conserved in metazoans, and up-regulation of *let-7* expression accompanies the onset of adult reproductive maturity [73, 97]. The timing of *let-7* expression in the pupal and adult midgut (Figure 1.25 B) was consistent with its conserved role in adult differentiation.

2. Factors expressed mainly in pupae and adults: RNA-binding factor *BRAT*, and *miR-14, miR-100, let-7, miR-125,* and *miR-277*.

Midgut metamorphosis in the pupa and adult includes the detachment of larval cells from the basement membrane and their subsequent degradation in the lumen, and the differentiation of diploid adult midgut precursor cells that will form the adult midgut. Nutrients stored in obsolete larval endoreplicated cells are digested and reused for adult development. In the early pupa the titer of ecdysone increases several fold over the 4th instar level, so hormonal stimulus for *BR* expression is present, but *BR* expression is minimal.

***BR* expression decreased then *BRAT* expression increased**

The time of *BR* expression was correlated with cell proliferation (Figure 1.13). The transient and dramatic up-regulation of *BRAT* near pupation was coincident with the down-regulation of *BR* (Figure 1.29).

In other organisms, *BRAT* function is associated with cellular differentiation, by translational silencing of factors that promote proliferation [98]. *BRAT* suppresses self-renewal in stem cell daughters, to promote their differentiation [99]. In *C. elegans*, developmental time progresses with the sequential and regulated increase and decrease of heterochronic cell-fate determinants [15]. *lin-41,* a *BRAT* homolog, is a key heterochronic gene in *C. elegans.*

During midgut metamorphosis, *BR* and *BRAT* may function as sequentially expressed developmental timing regulators (as heterochronic regulators). I hypothesize that BR may initiate the pupal program and the proliferation of adult midgut precursors, then BRAT might repress *BR,* terminate cellular proliferation and initiate the process of differentiation. This hypothesis of timing regulation is consistent with two lines of evidence in *D. melanogaster:* firstly, *BR* is

highly expressed in proliferating adult midgut precursors at the larva-pupa transition [60] and secondly, *BR* is upregulated prematurely in *BRAT* mutants [5].

Of the miRNAs studied, ***miR-14*** was the most highly expressed in *Ae. aegypti* midgut, particularly during the pupal and adult stages, when *BR* expression was low. *miR-14* is an arthropod-specific miRNA [100]. In *D. melanogaster*, *miR-14* has been implicated in a negative feedback loop involving the ecdysone receptor, where *miR-14* targets the ecdysone receptor (*EcR*), and ecdysone signaling reduces *miR-14* levels [74].

miR-100, let-7,* and *miR-125 may be coordinately regulated in mosquitoes. Their physical linkage was demonstrated in *D. melanogaster*, where the three miRNAs are co-transcribed in a common primary transcript, but they do not have the same abundance in the cytoplasm. This suggests that the pre-miRNAs of the primary transcript may be differently processed post-transcriptionally [23]. Data presented here suggest the expression patterns and relative abundance of *miR-100, let-7* and *miR-125* also differs in the mosquito midgut.

The expression level of ***miR-277*** was relatively low in the midgut, and *miR-277* expression was higher in the pupa and the adult than in the larva. *miR-277* is predicted to have numerous targets involved in development, growth factor signaling pathways, metabolism, and hormonal regulation [101-103]; therefore the expression of *miR-277* may be highly regulated. In the midgut, the *miR-277* expression pattern clearly differed from that of its two closest neighbors, *miR-317* and *miR-34*, and was highest in the pupal stage. This different expression pattern suggests *miR-277* may not be part of a common primary transcript that includes *miR-317, miR-277* and *miR-34*. In *D. melanogaster*, an independent primary transcript was recently cloned that only encoded a single miRNA, *miR*-(Genbank FJ45605) [72]. By 3' RACE I cloned a homologous product in *Ae. aegypti* (Genbank KC897652). This suggests that, although located

between *miR-317* and *miR-34*, *miR-277* might be transcribed independently in *Ae. aegypti*, as it is in *D. melanogaster* (Figure 1.24).

3. Factors expressed mostly in larvae and adults: *miR-317*, and *miR-34*

miR-34 and *miR-317* were expressed in the midgut throughout the larval stage. Their expression decreased in pupae, then had greatly increased in the adult by the third day after eclosing (Figure 1.23). While this expression pattern was not entirely consistent with hypothesized JH titer fluctuations, it does to some extent follow the pattern of *BR* expression. In *D. melanogaster*, *miR-34* was up-regulated by a juvenile hormone analog and down-regulated by ecdysone [25]. The results presented here are consistent with these mechanisms.

CONCLUSION

This expression analysis establishes a baseline of relative expression patterns. Potential relationships between the RNA binding factors and *BR* need to be further studied.

There is very likely a role for miRNAs in midgut development, and the heterochronic pathway homologs may be important regulators of the timing of mosquito midgut development. This study therefore provides a foundation for further investigation of the complex molecular regulatory interactions that underlie mosquito midgut metamorphosis.

TABLE 1.5 Summary of Chapter 1 - The expression of *BR* in the midgut of the mosquito *Ae. aegypti* and the expression of RNA binding factors that may modulate *BR* expression

knowledge gained	caveats/limitations/observations
1. The relative abundance of factors in the midgut was determined.	A. We do not know where they were localized B. Factors with a low expression level may still have an important function in a subset of cells (ex: enteroendocrine cells, or visceral muscle cells)
2. The expression patterns were established –we learned when a factor's expression peaked and when it decreased	A. We know expression at discrete time-points in a complex tissue composed of different kinds of cells B. We cannot relate the expression of one factor to that of another – for example, if *BR* decreased, and *BRAT* increased, the two events are not linked, just correlated – we cannot say *BRAT* caused *BR* to decrease, or *BR* decrease allowed *BRAT* to increase.
3. A rough outline of the course of midgut metamorphosis over time was established, which can be correlated with the expression analysis to allow a sense of what is happening in the developing midgut at a given expression point.	A. This did not confirm mechanistic molecular relationships between, for example, the expression of lin-28 and the proliferation of epithelial cells. B. Clues of molecular function can be derived from the literature, and also from the domain structure of the factor.
4. Bioinformatic and RNA structural analysis suggested possible relationships between *BR* and miRNAs (and RNA-binding proteins); coupled with co-expression in the same tissue this provides two lines of evidence to support hypotheses for molecular interactions.	A. Bioinformatic predictions are not reliable. Not enough is yet understood about the molecular interactions between miRNAs and their targets to rely on bioinformatic predictions. B. Sometimes miRNAs with perfect seed identity do not bind in vivo, while other miRNAs bind when not expected to.

MATERIALS AND METHODS

Mosquito culture

Ae. aegypti eggs (Orlando strain) were obtained from Louisiana Biologicals. Larvae were grown at 24ºC and fed a mixture of Tetramin chiclid food (4g) and bakers yeast (2g) in 500 mls distilled water. To obtain timed 4th instars, 2nd or 3rd instars were individually placed into 12X100 mm culture tubes containing approximately1 ml water and excess food. Late 3rd instars were checked every 2 hours, and the presence of the shed 3rd instar cuticle was taken as the start of the 4th instar.

Larval midgut staining

Midguts were dissected in phosphate buffer saline (PBS) and stained with either 4'6-diamdino-2-phenylindole (DAPI), phalloidin AlexaFluor 546 (Invitrogen/Molecular Probes) (5µl in 100µl PBS), orcein (midguts fixed in Carnoy's buffer) or methylene blue.

RNA extraction and purification

10-20 midguts were dissected in PBS then transferred to QIAzol Lysis reagent (Qiagen), heated briefly at 60ºC, vortexed then stored at -20º C until processing. Chloroform (0.2 volume) was added to separate phases. The samples were then mixed on a rotator for 15 minutes, and centrifuged for 20 minutes at 4ºC. The resulting aqueous phase was transferred to an RNAeasy mini-column, washed and DNase-digested on the column using the Qiagen RNAse-free DNase set (catalog 79254). Total RNA was eluted from the column with RNAse-free water (~30-50µl) then the total RNA yield was quantitated using the Quant-it RNA broad range assay kit (catalog Q10213; Invitrogen/Molecular Probes). 1 µg of total RNA was used for each sample in the reverse transcription reaction.

mRNA and miRNA expression analysis

FIGURE 1.32 Overview of expression analysis

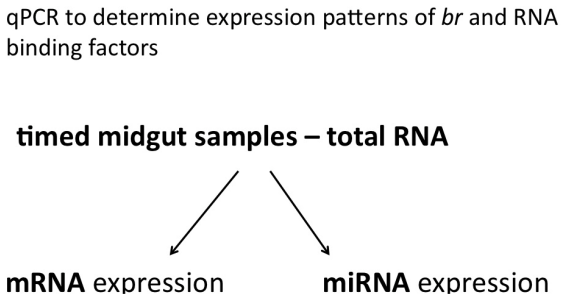

miRNA and mRNA expression was analyzed quantitatively using the miScript PCR System from Qiagen that includes the miScript Reverse transcription kit (catalog no. 218061) and the miScript SYBR Green PCR Kit (catalog 218075). These kits allow the detection of both mRNAs and miRNAs from the same total RNA sample. During the reverse transcription step miRNAs are poly-adenylated by poly(A) polymerase. Reverse transcriptase then converts RNA to cDNA using oligo-dT and random primers. The oligo-dT primers have a universal tag sequence on the 5' end; this universal tag allows miRNA amplification in the real-time PCR step. To amplify miRNA, the forward primers used are specific for the miRNA (see chart for primer sequences) and reverse primers prime the universal tag sequence appended during reverse transcription. **Real-time PCR** conditions on an MJ Research Opticon thermocycler were as follows: Hot start 95ºc for 15 min, then 35 cycles of: Melt-15 sec, Anneal- 30 sec, Extend-30 sec. This was followed by melt curve analysis to ensure that a single product was amplified that melted at the expected temperature (miRNAs tend to melt around 75ºC, depending on their CG content). *Ae. aegypti 5S rRNA* was used as the reference gene for the miRNA reactions. mRNA products were amplified using the same PCR conditions and either *Ae. aegypti ACTIN* or *Ae. aegypti RPS7* as the reference gene.

Quantitation of differences in the expression levels of target genes was calculated using the relative standard curve method, by re-writing the slope-intercept form of the line equation (**Y = mX + B**) to solve for X:

X = (Y-B) / m where **Y** = c(t) value,

M = slope

B = Y intercept

X = nucleic acid abundance

Calculations were set up in Excel spreadsheets using the raw data from the PCR analysis:

$$X = (c(T) - 20.89)/-3.5$$

then: anti-log of target x value is divided by the anti-log of the control (reference) gene:

$$= 10^{\text{x experimental}} / 10^{\text{x control}}$$

For the Chapter 1 expression charts, the reference gene for mRNA was *ß actin*, and the reference gene for miRNA was *5S rRNA*. Error bars show the standard error of 3 technical replicates. If no error bars are shown, 3 technical replicates were not performed.

Analysis of standard error for technical PCR replicates: Standard error = standard deviation of samples/√number of samples

TABLE 1.6 PRIMERS USED FOR PCR – miRNAs and control

miRNA	***A. aegypti* sequence (from miRBase)**
miR-317-2	5'TGAACAGCYGGYGGYAYCT3'
miR-277	5'TAAATGCACTATCTGGTAGAC3'
*miR-277**	5'CGTGTCAGAAGTGCATTTACA3'
miR-34	5'TGGCAGTGTGGTTAGCTGGTTG3'
*miR-34**	5'CAACCACTATCCGCCCTGCCGCC3'
miR-100	5'AACCCGTAGATCCGAACTTGTG3'
let-7	5'TGAGGTAGTTGGTTGTATAGT3'
miR-125	5'TCCCTGAGACCCTAACTTGTGA3'
miR-7	5'TGGAAGACTAGTGATTTTGTTGT3'
miR-14	5'TCAGTCTTTTTCTCTCTCCTAT3'
miR-190	5'AGATATGTTTGATATTCTTGGTTG3'
5S rRNA	5'GTCAACGATCATACCATGTTGAAA3'
U6 snRNA	5'GTCTTTGCTTCGGCAAGACATAT3'

Table 1.7 PRIMERS USED FOR PCR - mRNAs

mRNA	forward (5'-3')	reverse (5'-3')	accession number
BR Z1	TCACCACAAGGCGAGGACT	TCGTTCTGATCCACGGCAC	AY499537
BR Z2	GTTCACCACAAGGCTGCTC	GACGGCAACTAGTGGCAAG	AY499538
BR Z3	TCTCGGCAGCGTCCTCAT	ACAGCGTGTCGGATTGTTCG	AY499539
BR Z4	AACGGCACAAGGAGCAACAG	GGATGATGCAAAGGACTGGC	AY499540
BRAT	TGTCCACTTCACCCTCACAA	GACGAATGGTCCCAGACTGT	XP_001650044
LIN-28	TGCAAGTGGTTCAACGTGAT	GAAACCCCTCCATTTGAAGC	XP_001648803
hn-RNPK	GCAAGATTTTCACGCACACT	CGCTTTTATCCAGATTGATGAAG	EAT32806
TALIN	GAAGTTAAGGAAACGGACGAA	CTCTCGTTGAGCAGCATTTG	EAT42216
AGO1 shrt	ATTCGATGGGCGTAACAATC	CGTATGGGATCTGTGTCGTGTG	XP_001651170
AGO1-lng	GCCTCCAAGTCCGACTCA	AGTTCGTTTTGCATCAGTCC	XP_001662554
GW182	ATCTCATCGGAGGTGACTGG	ATACGGAACTGCTTGCTGCT	EAT40860
NOT-1	TCCCGTAACCGTATCTCGTC	TGTGTCTCAGCGAAGGATTG	EAT33966
ß ACTIN	GACTACCTGATGAAGATCCTGAC	GCACAGCTTCTCCTTAATGTCAC	XP_001655176
RPS7	ATGGTGGTCTGCTGGTTCT	ACCGCCGTCTACGATGCCA	EAT38624

Table1.8 Databases and software used

Software/database	purpose	Website URL
mfold	nucleic acid folding and hybridization prediction	http://mfold.rna.albany.edu/?q=mfold
CLUSTALW	multiple sequence alignment/ tree	http://www.genome.jp/tools/clustalw/
miRBase	Database of miRNA sequences and annotation	http://www.mirbase.org/
Broad Institute *Aedes*	*A. aegypti* genome database	http://www.broadinstitute.org/annotation/genome/aedes_aegypti.2/Home.html
Vectorbase *Aedes*	*A. aegypti* genome database	https://www.vectorbase.org/organisms/aedes-aegypti

CHAPTER 2

The effects of juvenile hormone and ecdysone on *BR* and RNA-binding-factor expression and on midgut metamorphosis

BACKGROUND

To investigate potential relationships between *BR* and candidate RNA regulators, and to learn more about the role of *BR* as a developmental timing switch in *Ae. aegypti*, I studied the effect of the juvenile hormone analog methoprene and the ecdysone analog RH2485 on midgut metamorphosis, and on the expression of *BR* and RNA-binding-factors.

Since juvenile hormone (JH) represses *BR* response to the molting hormone ecdysone and delays pupal development [7, 10, 104], and since ecdysone stimulates *BR* expression, I hypothesized that inappropriate exposure to methoprene and to RH2485 might give insight into the roles of juvenile hormone and ecdysone in the potential regulation of *BR* transcripts by RNA-binding factors.

The JH titer is not known in *Ae. aegypti* larva or pupa, but JH increases in early adult

JH levels are known in the newly-eclosed adult female mosquito, where JH directs reproductive maturation (Figure 2.6B). JH increases in the adult during the first two days after eclosion, and remains high until the blood meal [105, 106]. JH biosynthesis in the early adult is dependent on the teneral reserves (nutrient stores) carried over from larval feeding [107].

The JH titer has not been determined for *Ae. aegypti* larval or pupal stages, but juvenile hormone esterase (JHE), which degrades JH, is expressed in the midgut during the larst larval instar. JHE plays a critical role in reducing juvenile hormone levels. In 4^{th} instar larvae JHE gradually increases, and reaches a peak at around 42 hours after the molt [108].

1. Effect of Juvenile hormone and methoprene on gene expression

Methoprene is a juvenile hormone analog used as a larvicide and also as an experimental tool to understand the action of juvenile hormone. Methoprene interferes with normal metamorphosis and remodeling of the midgut in *Ae. aegypti* [63, 109].

FIGURE 2.1 Methoprene, Juvenile Hormone

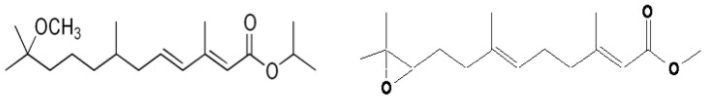

Methoprene **Juvenile Hormone III**

Figure 2.1 A comparison of the chemical structures of methoprene (left) and JHIII (right)

Methoprene has greater activity than JH

The level of JH in the hemolymph of most insects typically ranges from 0.3-180 nM, with the maximum level of JH III activity at ~25-35 nM [110]. In *D. melanogaster*, the 50% effective dose (ED_{50}) of methoprene was measured at 5 picomoles/puparium, while the ED_{50} of JHIII was 143 picomoles/puparium in the same assay [111]. Methoprene may have higher activity relative to JHIII because methoprene is more resistant to enzymatic degradation by JH esterase [110].

How juvenile hormone may inhibit *BR* expression

A methoprene-resistant mutant was discovered in *D. melanogaster*, **me**thoprene-**t**olerant (*MET*), that encodes a basic helix-loop-helix, Per-Arnt-Sims (bHLH-PAS) domain transcription factor with a small, hydrophobic binding pocket that is able to bind JHIII with high affinity [112, 113]. To test the hypothesis that the JH analog methoprene interferes with *BR* function at metamorphosis though *MET*, mutant flies were treated with methoprene [114].The resulting phenotypes of *MET* mutants were the same as those of flies with defects in *BR* function. That is, *MET* mutants phenocopied *BR* mutants. This finding placed *MET* in a signaling pathway that connects JH with *BR* [114].

The JH receptor may be a heterodimer, of which *MET* is an obligate component and another bHLH transcription factor is a variable partner. In *Ae. aegypti* newly-eclosed adults, *MET* forms a heterodimer with the hormone receptor coactivator *FISC* (ß-***F****ushiTarazu*-F1 **I**nteracting **S**teroid-receptor **C**oactivator) or with another bHLH factor, *CYCLE*, to induce the expression of Kruppel-Homolog1 (*KRH)*, a C2H2 zinc finger transcription factor thought to act downstream of *MET* to repress *BR* [115, 116]. Heterodimerization of *MET* with different partners may explain the pleiotrophic effects of JH [115, 116]. In the *Ae. aegypti* early adult, the *MET*/*FISC* heterodimer binds the promoter of the *EARLY TRYPSIN* gene to induce its expression in a JH-dependent manner [115].

FIGURE 2.2 Effects of JH and JHA signaling on *BR* expression
JH inhibits premature metamorphosis via *BR* Methoprene re-upregulates *BR* in the pupa

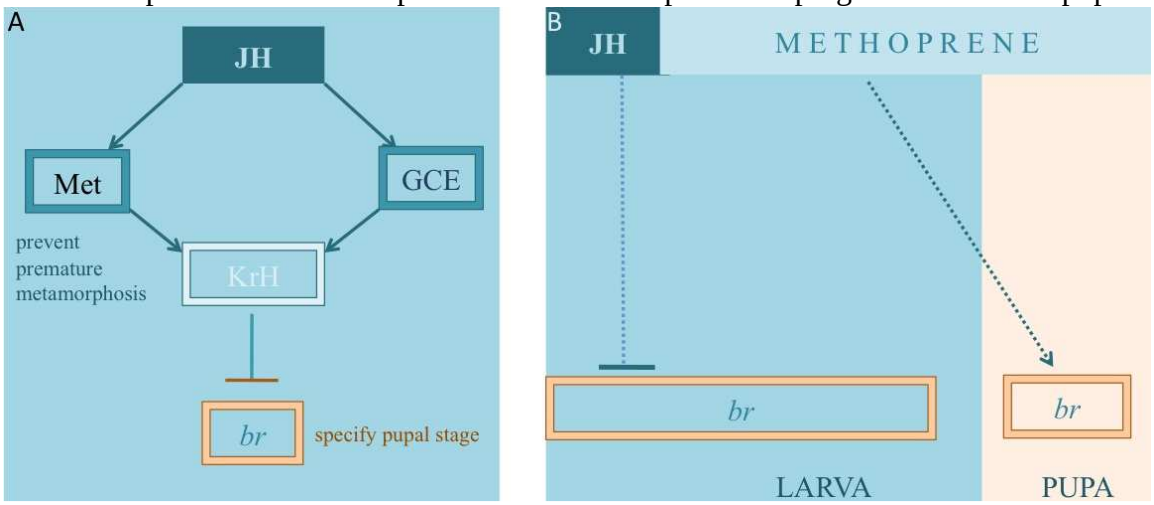

Figure 2.2 A. JH signals through *MET* and *KRH1* to block precocious *BR* expression and inhibit early metamorphosis in the *D. melanogaster* larva [104, 117].
B. Adding exogenous JH or methoprene causes inappropriate *BR* re-expression in the pupa, when *BR* is not normally expressed [104]. In the *Ae. aegypti* midgut, methoprene causes a reiteration of the larval program and inhibits larval tissue histolysis in the pupal midgut [109].

Perhaps metamorphosis in *Ae. aegypti* follows a more ancestral pattern. In *D. melanogaster*, metamorphic changes occur in the late last instar, after larval growth has ended. *DmelBR* is directly induced at the beginning of the wandering stage, when larvae leave the food [118], but in *Ae. aegypti*, metamorphic changes overlap larval growth and feeding [62, 119]. In more basal

holometabolous insects, such as flour beetle *T. castaneum* and mosquito *Ae. aegypti*, *BR*Z3 isoform is expressed at low levels during the early larval instars (Figure 2.3) then up-regulated during the final larval instar. This may reflect an ancient evolutionary identity for *BR*Z3 [120], the most distal isoform in the *BR* locus (Figure 1.3), and seemingly the most JH-compatible.

FIGURE 2.3 *BR*Z3 expression in the early larval instars of *Ae. aegypti*

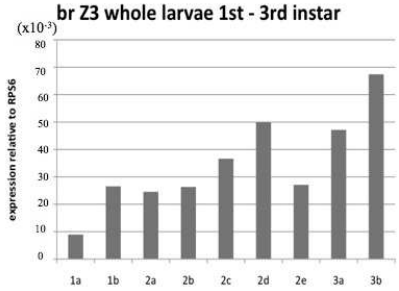

Figure 2.3 *BR*Z3 expression in the first three larval instars (1a-early 1st instar, 1b-late 1st instar; 2a-early 2nd, 2b-early-mid 2nd, 2c-late-mid 2nd, 2e-late 2nd, 3a-early 3rd, 3b-mid 3rd)

2. Effect of Ecdysone and ecdysone analog RH2485 on gene expression

The insect steroid hormone ecdysone induces and coordinates molting and metamorphosis in insects [7, 121-124].

Ecdysone biosynthesis in *Ae. aegypti*

Pro**t**horacico**t**ropic **h**ormone (PTTH) is a neurohormone that stimulates production of ecdysone in insects [69]. In *D. melanogaster*, ecdysone is synthesized in the ring gland, a neuroendocrine gland that includes the prothoracic gland, the corpora cardiaca, and the corpora allata, described by Marguerite Vogt in 1930. In *Ae. aegypti*, PTTH is expressed in the brain, and its highest expression occurs around 24-36 hours in the 4th instar [125], after the critical weight is reached. No specific site of ecdysone biosynthesis has been identified in *Ae. aegypti* larvae [125]. The prothoracic gland is reported to be inactive in the 4th instar, though there is coordinated and synchronous release of ecdysteroids from the thorax and the abdomen [125, 126]. In the adult female after the blood meal, ecdysone is synthesized in the ovary [127].

Evidence that insulin signaling affects ecdysone biosynthesis comes from experiments in *D. melanogaster*, where over-expression of phosphatidylinositol 3-kinase (*PI3K*), a downstream effector kinase in the insulin pathway, causes larvae to attain critical weight earlier, and to metamorphose into tiny adults [128]. Enhanced insulin signaling in *D. melanogaster* increases the expression of the ecdysone biosynthetic enzymes disembodied (*DIB*) and phantom (*PHM*), which are induced by BR [129, 130]. In *Ae. aegypti*, insulin signaling also regulates ecdysone biosynthesis [131], and eight insulin-like peptides (ILPs) have been identified - of these, ILP6, ILP5, and ILP2 are found in the larval abdomen [131].

Several RNA-binding factors in this study may be involved in insulin signaling. In mouse, ***let-7*** represses the insulin receptor, and this repression is blocked by LIN-28. Antisense *miR-7* in the mouse embryo reduces insulin expression in the developing pancreas [132]. *Dme-miR-14* binds and represses *SUGARBABE*, a zinc-finger transcription factor that regulates the expression of ILPs in neurosecretory cells in *D. melanogaster* brain in response to nutritional cues [74]. *Dme-miR-14* directly binds a complementary, conserved site in the 3'UTR of *SUGARBABE* [74].

FIGURE 2.4 Conservation of *miR-14* binding site on *Ae. aegypti SUGARBABE* 3'UTR

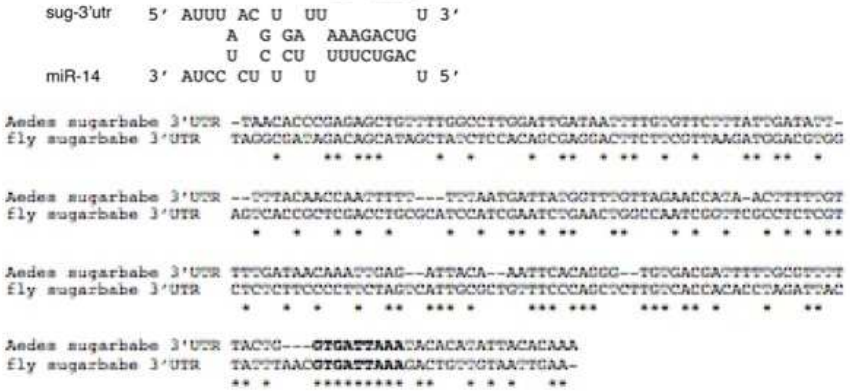

Figure 2.4 *miR-14* binding prediction on *AaegSUGARBABE* 3'UTR, showing 8 complementary pairs in the seed region predicted by RNA Hybrid [133]
Alignment of the 3' UTR of *AaegSUGARBABE* with *DmelSUGARBABE* 3'UTR, a *bona fide* biological target of *miR-14* binding in **conserved region** (**bold**) [74]

Alignment of *DmelSUGARBABE* with the *Ae. aegypti* homolog (Figure 2.4) shows that the *miR-14* binding sites are identical. Conservation of the *miR-14* binding motif suggests *Aae-miR-14* might also target *AaegSUGARBABE* to regulate insulin signaling. *Aae-miR-14* was highly expressed in pupal and adult midguts when ecdysone levels decrease (Figure 1.25).

Transmission of ecdysone signaling by the ecdysone receptor

How does a single hormone circulating in the hemolymph coordinate morphological change in diverse tissues at different times? An early understanding of ecdysone regulation of gene expression came from the observation that if ecdysone is added to the large polytene chromosomes of *D. melanogaster* salivary glands in tissue culture, a puffing response results [3, 134-136]. Ashburner hypothesized that an intracellular ecdysone receptor receives the ecdysone signal, and proposed that a hierarchical cascade of transcription factors responds to that signal. These factors then activate downstream factors, and autoregulate their own promoters to allow a sequential progression of gene activation. It was subsequently shown that the early-puff gene products indeed include three ecdysone-responsive (at 2^{-9} M) transcription factors: *E75* [137] , *E74,* [138], and *BROAD* [68].

The ecdysone receptor heterodimer

The cellular response to ecdysone is mediated by a heterodimer composed of two nuclear hormone receptors, the ecdysone receptor (*EcR*) [139, 140], and Ultraspiracle (*USP*), an ortholog of the vertebrate retinoic acid receptor (*RXR*) [141, 142]. Nuclear receptors belong to an ancient transcription-factor family. They share a common domain structure, which includes a conserved DNA binding domain (DBD), a central hinge region, and a ligand binding domain (LBD) [143]. Nuclear receptors activate or repress transcription of target genes by direct recognition of specific cis-regulatory regions [144]. The ecdysone receptor binds ecdysone in a flexible ligand-

binding pocket [145], but *EcR* by itself cannot bind ecdysone, it must first form a heterodimer with *USP* [146].

Response to ecdysone is tissue and cell-type specific

The two ecdysone receptor isoforms in *Ae. aegypti, EcRA* and *EcRB*, differ in their N-terminal activation domains and 5' UTRs [147, 148]. Differential expression of *EcR* and *USP* isoforms allows different tissues and developmental stages to have distinct responses to ecdysone circulating in the hemolymph [149]. The two *EcR* isoforms vary in sensitivity to ecdysone; *EcRB* responds to low levels of ecdysone, and seems to be the first-responder to rising ecdysone titers [148]. The *USPA* and *USPB* isoforms also differ from each other only in their N-terminal activation domain and 5'UTR. Thus each isoform of *EcR* and of *USP* recognizes the same cis-regulatory region with their DNA binding domains, but may vary in their induction and their partners due to differences in their promoter regions and activation domains.

The EcR heterodimer in the larval mosquito midgut

In *Ae. aegypti* midgut, *USPA* expression increases around 48 hours after the last larval molt, and *EcRB* also increases towards the end of the 4th instar [150]. *EcRB* and *USPA* may form the heterodimer that transduces the ecdysone signal in the midgut during metamorphosis.

Co-repressors and co-activators of the EcR heterodimer

The EcR/USP heterodimer interacts with co-repressors or co-activators to coordinate the ecdysone response. A co-repressor attaches in the absence of a ligand [151] then, when ecdysone binds, the EcR ligand-binding domain undergoes a conformational change, and releases the co-repressor to recruit a co-activator [152]. In *Ae. aegypti,* the co-activator FISC may mediate crosstalk between JH and ecdysone signaling. FISC interacts with MET via its PAS domain in the presence of juvenile hormone [153], but binds the EcR/USP heterodimer with its

conserved LXXLL nuclear-receptor-binding motif in the presence of ecdysone [153, 154]. Like *BR*, *FISC* responds to both JH and ecdysone.

FIGURE 2.5 EcR/USP heterodimer co-activators and co-repressors

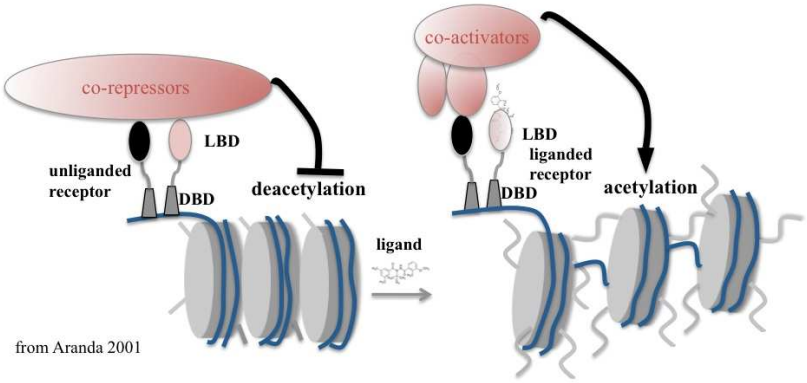

Figure 2.5 Ecdysone binding causes EcR/USP heterodimer to change local chromatin from repressed to open.

Ecdysone levels in the mosquito *Aedes aegypti* during metamorphosis, and Juvenile Hormone levels in the newly eclosed female adult

FIGURE 2.6 A Ecdysone levels in *A. aegypti* larva and pupa determined by the Palli lab **[69]**

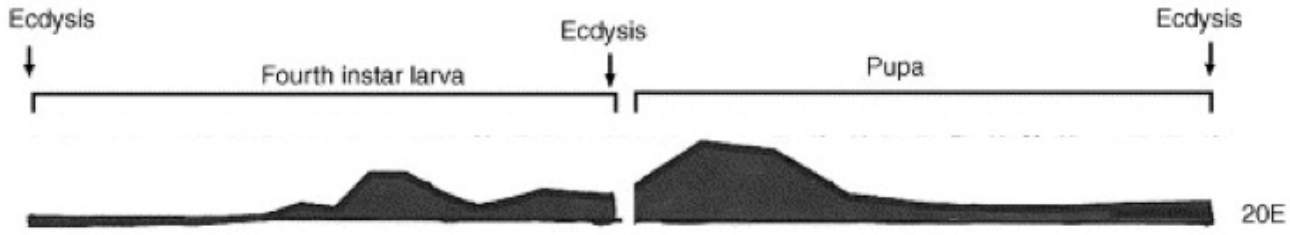

FIGURE 2.6 B Juvenile hormone levels in newly eclosed pre-vitellognenic female adult [66]

Larva Pupa Adult

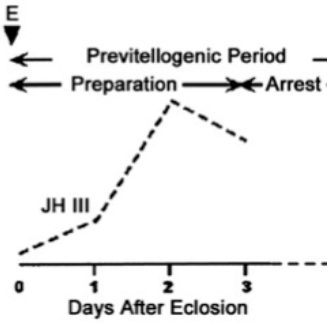

Figure 2.6 A. Ecdysone levels rise in 3 peaks in the middle and late 4th instar, then there is a high peak of ecdysone in the early pupa within 15 hours, after which ecdysone levels decrease [69]. B. **JH** levels are not known in larva or pupa. In newly-eclosed adult females, **JH** levels increase during the first two days after emergence, then slowly decline (Raikhel lab) [66].

1. RESULTS: Treatment of mosquito larvae with methoprene, a juvenile hormone analog

To determine the effect of juvenile hormone on survival, fed larvae were treated with the juvenile hormone analog methoprene, or with an equal volume of the solvent as a control. Larvae were treated at 24 hours after the molt, because the level of JH was expected to normally decrease then, after the critical weight was reached, and when JH esterase increased.

The effect of methoprene on survival and midgut development

Methoprene-treatment of larvae caused an interruption in midgut development, and ultimately resulted in death approximately a day after pupation (Figures 2.7 and 2.8).

FIGURE 2.7 Survival after treatment with methoprene, or treatment with solvent alone

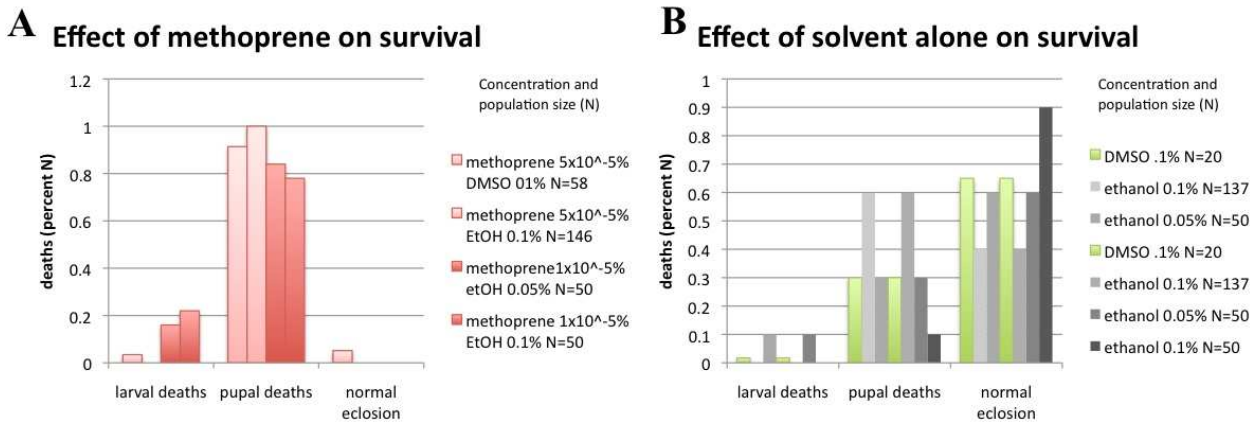

Figure 2.7 A. Effect of methoprene on survival. At the concentrations tested, most methoprene-treated larvae died after pupating. **B.** Some DMSO (green) and ethanol (gray) controls also died as pupae, though many eclosed to normal adults. Concentrating the stock solution to 2µl methoprene/ml ethanol allowed less ethanol to be used in the experiment, resulting in fewer pupal deaths in the controls, while methoprene still killed at the pupal stage.

DMSO was used to dissolve methoprene, however, DMSO itself affected larval viability. Later, ethanol was substituted as the solvent for methoprene. Concentrating the stock solution decreased pupal deaths in the controls, because less ethanol was added in the experiment. In the following expression analyses, both untreated and ethanol-treated controls were included for comparison with the methoprene-treated sample.

Midgut phenotype In untreated individuals, the midguts shrank and the gastric cecae contracted during pupation. Concurrent with these changes was the appearance of a yellowish meconium in the midgut lumen, likely composed of detached larval epithelial cells. The pupal midgut was smaller than the larval midgut, and had no peritrophic membrane. In contrast, midguts of pupae developed from methoprene-treated larvae still had intact gastric cecae, midguts remained large, and no meconium. There was no peritrophic membrane (Figure 2.8). In short, the pupal midgut had a larval phenotype, except for the absence of the peritrophic membrane. Pupae from methoprene-treated larvae appeared straightened, as if their midgut was too large to fit into their cuticle, and their swimming movements were irregular.

FIGURE 2.8 A. Phenotype of untreated larval and pupal midgut (left) and of pupal midgut of a larva treated with methoprene (right)

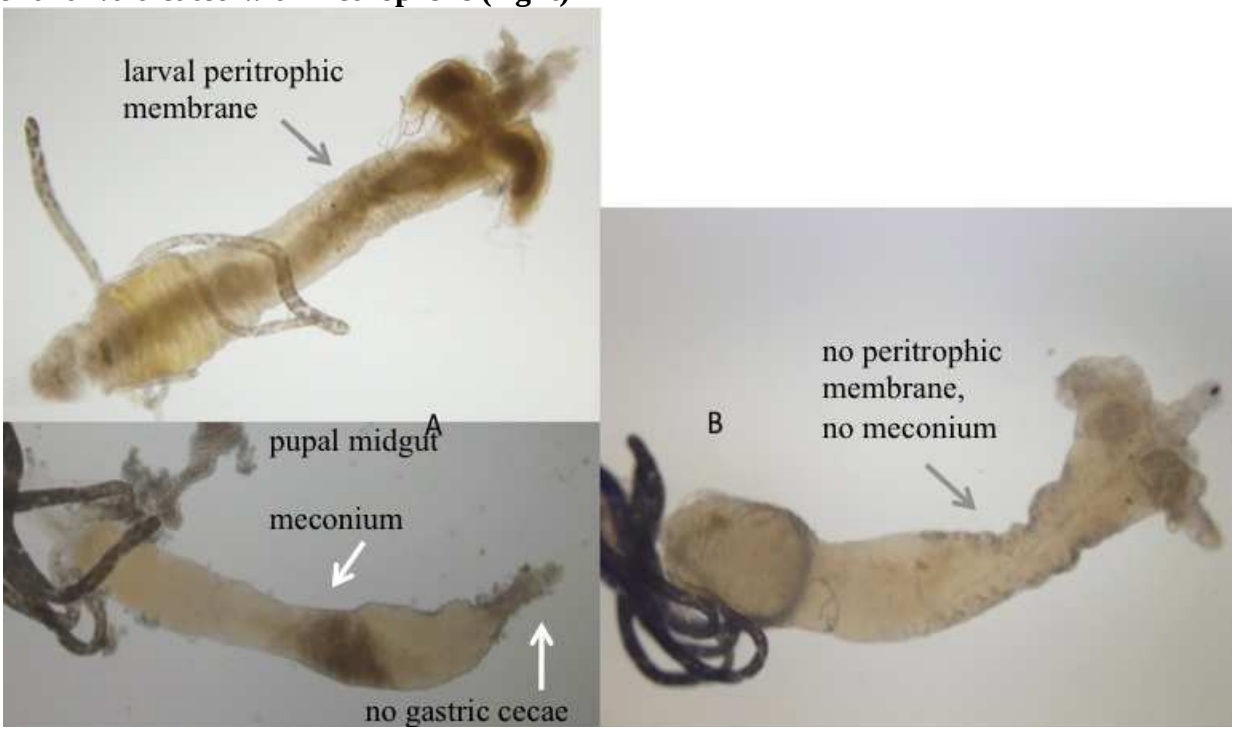

A. Untreated larval midgut (left top) and pupal midgut (left bottom) ~15 hr after pupation. Meconium (detached larval cells) visible inside midgut, no gastric ceacae. **Pupal midgut (right) from methoprene treated larva** had a larval phenotype; no meconium, gastric cecae still intact.

FIGURE 2.8 B Midgut epithelial cells from a pupa treated with methoprene as a larva:

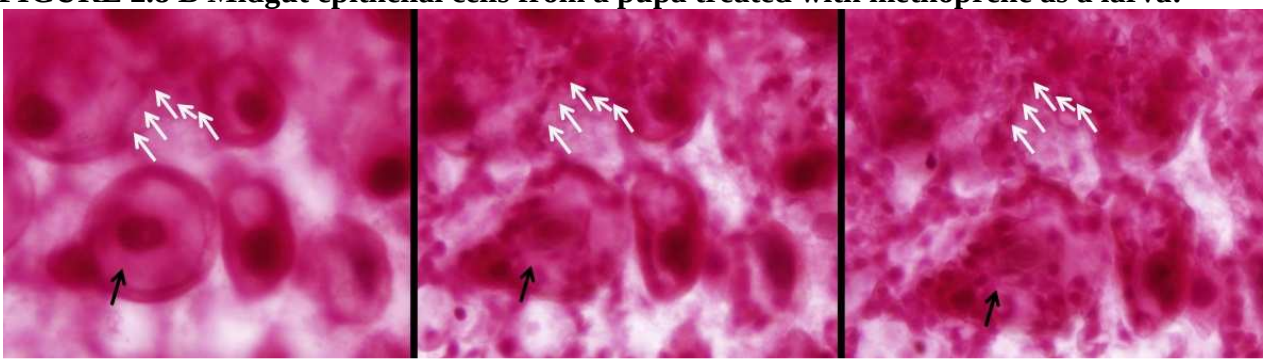

B. Seen at 3 different focal planes, **large larval cells (black arrow)** and **small diploid adult precursors (gray arrows)** were crowded together on the basement membrane (orcein staining).

FIGURE 2.8 C Midgut epithelial cells from a pupa treated with methoprene while a larva

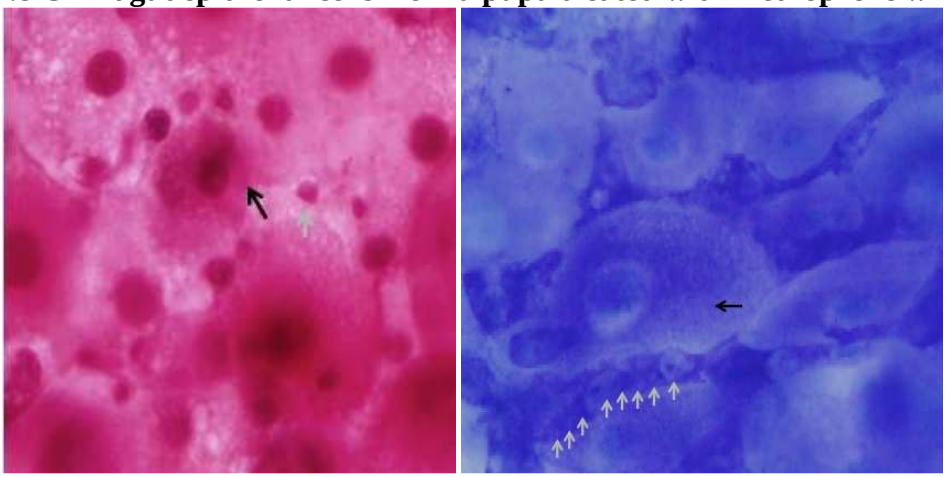

Figure 2.8C. Disordered diploid cells surrounded still-intact large larval cells in the pupal midgut. Orcein stain shows intact chromatin in pupal polytene cell nuclei. In pupal midgut, **larval cells (black arrow)** remained attached while numerous **adult midgut precursor cells (gray arrows)** surrounded them. (Compare with Figure 1.13) Orcein and methylene blue stains.

Methoprene-treated larvae, after pupating, had midguts that retained the large polytene epithelial cells, while the small diploid adult precursor cells surrounded them. This caused the pupal midgut to become crowded and disordered (Figure 2.8C). The gastric cecae didn't shrink, and larval epithelial cells failed to detach from the basement membrane.

The effect of methoprene treatment on midgut *BR* expression during metamorphosis

To determine the effect of methoprene on expression of *BR* and RNA-binding factors, larvae were treated with methoprene at 24 hours after the molt to 4th, and midgut samples were taken at intervals until the treated individuals died, approximately one day after pupating. Midgut

development of methoprene-treated larvae appeared normal before they pupated. Larval midgut *BR* expression was highest around 48 hr then decreased toward pupation (Figure 2.9). In midguts of post-molt pupae developed from methoprene-treated larvae, *BR*Z3 and Z4 expression was substantially higher than it was in midguts of pupae developed from untreated larvae at 3-15 hours after pupation. *BRZ1* and *Z2* levels were low, and Z1 expression was inconsistent. Because of the low level of expression, differences between control and methoprene-treated expression of *BRZ1* may have been beyond the ability of the assay to determine. Elevation of *BR* expression in *Aaeg.* pupal midguts of methoprene-treated larvae has been previously reported [155].

FIGURE 2.9 *BR* isoform expression in midguts of methoprene-treated larvae

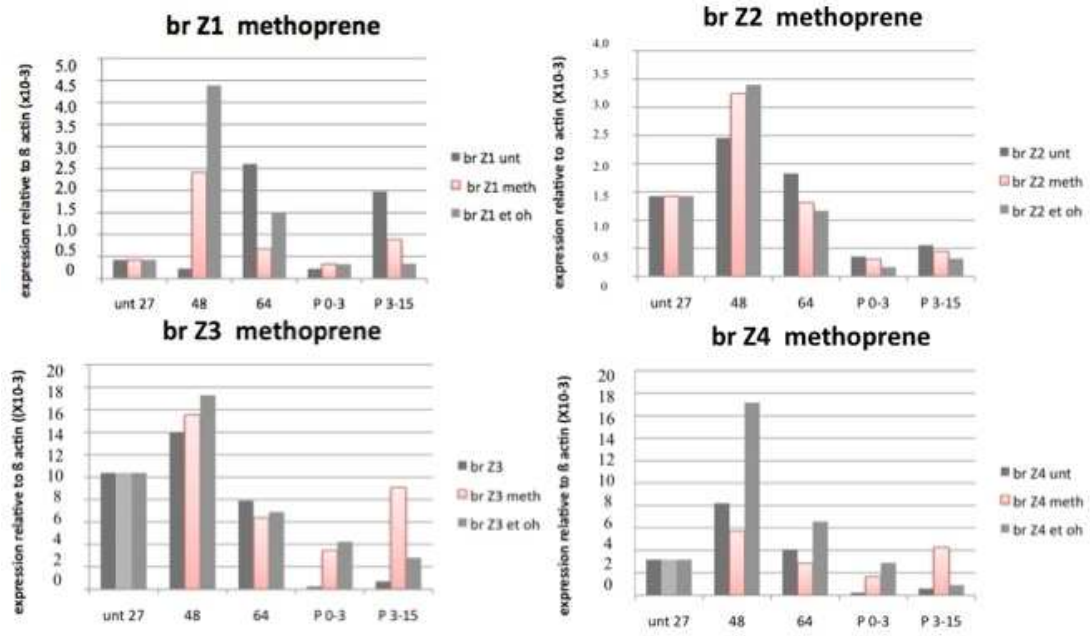

Figure 2.9 *BR* isoform expression in methoprene-treated larvae In methoprene-treated larval midguts, ***BRZ*3 & Z4 increased in the pupa (red)** In untreated and control larval midguts, *BR* expression peaked at 48 hr then decreased before pupation. EtOH – ethanol unt - untreated 4th instar: 27 hr, 48 hr, 64 hr, p 0-3 - pupa 0-3 hr, p3-15 - pupa 3-15 hr

Methoprene treatment and miRNA expression in the midgut

The effect of methoprene on miRNA expression was evaluated in multiple experiments using DMSO or ethanol as solvents, and results of these experiments were consistent with data presented here.

Effect of methoprene treatment on midgut *miR-317, miR-277* and *miR-34* expression

The expression levels of *miR-317* and *miR-34* in methoprene-treated larvae were higher in the controls near pupation. There was a three-fold increase in *miR-34* expression in the midguts of the pupae developing from methoprene-treated larvae (Figure 2.10). miR-277 levels were low.

FIGURE 2.10 Effect of methoprene treatment on *miR-317, miR-277* and *miR-34* expression during metamorphosis

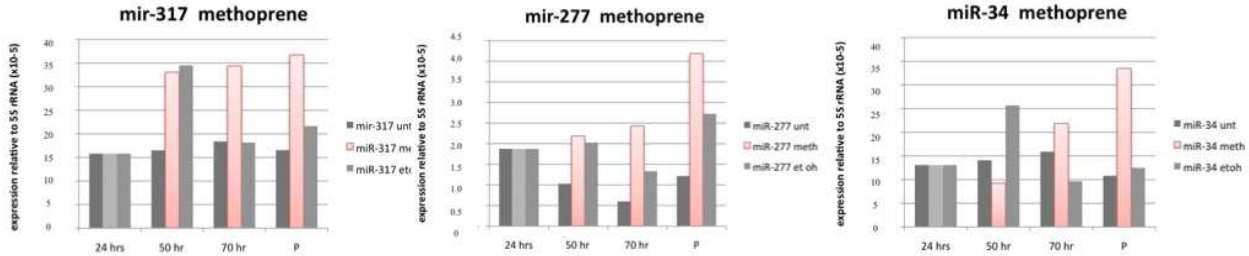

Figure 2.10 *miR-34* was up-regulated in the pupal midgut by methoprene
untreated: gray left methoprene-treated: red middle EtOH control: gray right

The effect of methoprene treatment on midgut *miR-14* expression levels

Methoprene didn't greatly affect *miR-14* expression in the larval midgut, but the treated larvae had elevated *miR-14* transcript levels in the pupal midgut.

FIGURE 2.11 Effect of methoprene treatment on *miR-14* expression in the midgut

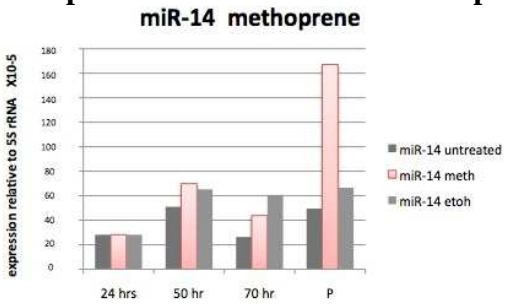

Figure 2.11 *miR-14* was upregulated in pupal midguts by methoprene treatment of larvae
untreated: gray left methoprene-treated: red middle EtOH control: gray right

The effect of methoprene treatment on *let-7* and *miR-125* expression levels

At pupation the expression of let-7 and miR-125 was similar in methoprene-treated larval midguts and in the ethanol controls.

Note that methoprene-treated pupae died before the normal pupal elevation of *let-7* and *miR-125* expression (shown – gray bars to right, Figure 2.21).

FIGURE 2.12 *let-7* and *miR-125* expression in midgut of methoprene-treated larvae

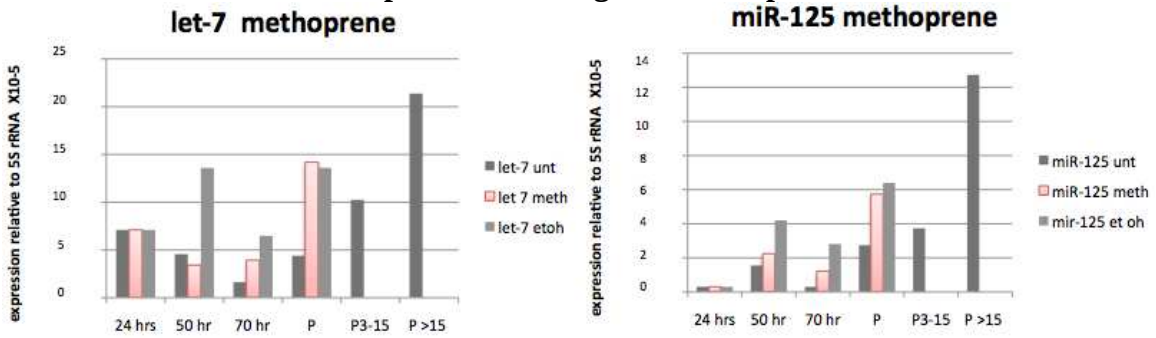

Figure 2.12 *let-7* and *miR-125* expression after methoprene treatment *let-7* and *mir-125* expression levels were not greatly affected by methoprene treatment.
untreated: gray left methoprene-treated: red middle EtOH control: gray right

Methoprene treatment and the midgut expression level of the RNA-binding factor *BRAT*

Figure 2.13 shows that methoprene treatment of larvae may have delayed the normal increase in *BRAT* expression that occurred near pupation in untreated larvae. This result agreed with earlier experiments using DMSO as a solvent.

FIGURE 2.13 Effect of methoprene treatment of larvae on *BRAT* expression in the midgut

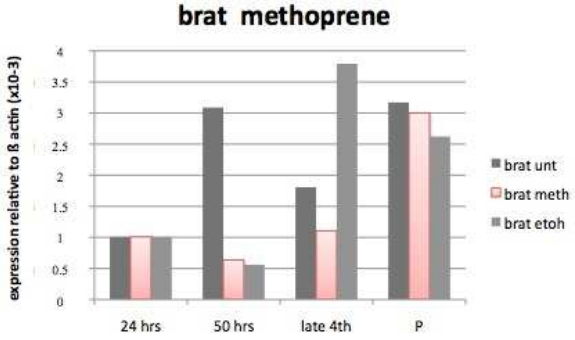

Figure 2.13 Methoprene treatment of larvae delayed the increase in *BRAT* expression near pupation.

DISCUSSION - Effect of methoprene on midgut development and gene expression

In insects, ecdysone signaling induces *BR* transcription, but in the presence of JH, pupation is delayed. JH represses *BR* transcription through *MET* and Kruppel-homolog (*Kr-H1*) [156, 157]. This is why Lynn Riddiford and others consider *BR* a "JH-dependent switch between larval and

pupal programs" [156]. Perhaps the responsiveness of *BR* to both JH and ecdysone underlies the ability of *BR* to control the timing of pupation.

In this study, the time of methoprene exposure is based on Nijhout's theory (1994) that attaining the critical weight triggers a drop in JH levels, such that a subsequent increase in ecdysone titers induces a metamorphic molt. JH analog treatment of the larva after 24 hours post-molt would be inappropriate and might prolong larval developmental time. The larva-like phenotype of the pupal midgut in methoprene-treated larvae supported this hypothesis.

Midgut remodeling did not occur in the pupa when the 4th instar larva was treated with methoprene, and treatment resulted in a concurrent, larva-like up-regulation of *BR* and *miR-34* transcripts in the pupal midgut. Another possible effect of methoprene treatment was a delay in *BRAT* expression in the pupal midgut of treated individuals. These results were similar to those described in *C. elegans,* where retarded heterochronic gene mutants reiterate stage-specific events, so that subsequent development is delayed, or never occurs [20]. Treatment with methoprene caused a heterochronic shift in *Ae. aegypti* midgut development so that physiological and molecular events that normally occurred in 4th instars reocurred in the pupal midgut.

The pupae do not feed, so methoprene would not enter the midgut, but it is possible that molecular effects of larval treatment might have persisted in the pupal midgut because methoprene had higher activity than JH, and resisted enzymatic degradation by JH esterase.

A central focus of this thesis is to try to better understand what causes *BR* levels to decrease at the end of the 4th larval instar. Ashburner proposed that early genes autoregulate, and that the protein products of the early ecdysone-induced genes bind their own promoters to down-regulate their own transcription to allow the sequential progression of the transcription factor cascade that is the molecular underpinning of metamorphosis [3].

To explain methoprene's inhibition of pupal development, and the up-regulation of *BR* and *miR-34* in the pupal midgut of methoprene-treated larvae, I hypothesize that methoprene treatment leads to translational regulation of *BR* transcripts. This hypothesis implies that normally, in pre-critical-weight 4th instar larvae, JH restrains *BR* translation in order to prevent premature metamorphosis, by acting through RNA-binding factors to limit *BR* translation into protein. The observed physiological effects of methoprene treatment might result from the repression of *BR* translation, and are consistent with this hypothesis.

The *miR-34* expression pattern was somewhat similar to that of *BR* in the larva. As in *D. melanogaster* [25], *Aae-miR-34* may respond to both JH and ecdysone signaling, as *BR* does, but in the opposite way (induced by JH, repressed by ecdysone). JH has been studied intently in insect development for more than thirty years, yet there are few known effectors of JH signaling. One way that JH may influence the timing of *BR*-induction of pupal programming is through *MET* and *Kr-H1*-mediated repression of *BR*, but there may be other JH pathways not yet defined: *miR-34* may be a miRNA mediator of JH signaling.

FIGURE 2.14 Summary of expression in midgut of untreated vs methoprene treated larvae

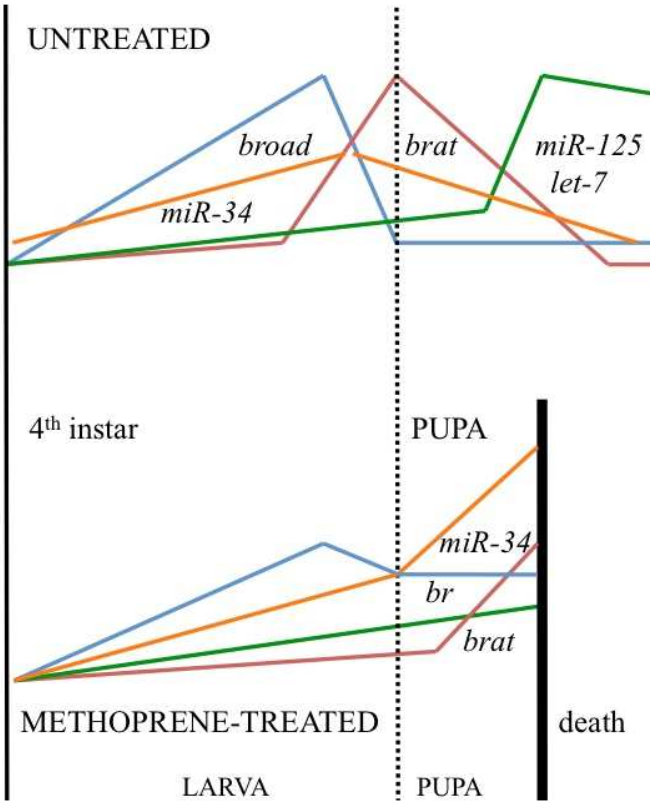

Figure 2.14 In untreated larvae, *BR* and *miR-34* transcript levels peaked then decreased, *BRAT* transcripts peaked at pupation, then *miR-125* and *let-7* transcripts increased (top).
In methoprene treated larvae, *BR* expression levels increased again in the pupa, *BRAT* peak was delayed, *mir-34* was elevated, and pupa died before upregulation of *miR-125* and *let-7* (bottom). ***miR-34*-orange *BR*-blue *BRAT*-red *let-7* and *miR-125*-green**

Discrepancies in reported expression levels

A critical flaw in the experimental design was that, although the methoprene experiments were repeated in independent experiments, the experiments could not be directly compared because the samples were not taken at the same developmental times. This precluded statistical analysis of the results to evaluate their validity. The pupal death of the controls was also problematic. However, the main conclusions drawn from the experiments were derived from results consistent with earlier experiments using DMSO as a solvent. In each methoprene-treatment experiment, *BRZ3* and *miR-34* were up-regulated in the pupa, while *miR-125* and *let-7* expression levels were not greatly affected by methoprene treatment. The methoprene-treatment expression charts show

a single example of the qPCR data obtained. There were discrepancies between the untreated and the ethanol-treated controls. I first used DMSO as a solvent for methoprene, but DMSO had adverse effects on larval survival, so I subsequently used ethanol. One possible explanation for differences in the expression levels of the controls is that ethanol treatment may have delayed larval development, making the ethanol-treated expression levels out-of-phase with the untreated levels. In a study in *D. melanogaster*, ethanol affected developmental progress, and an ethanol-free environment reduced development time [158].

CONCLUSION – Effect of methoprene on midgut development

Methoprene treatment caused a retarded developmental phenotype in the pupal midgut. *BR* and *miR-34* transcripts were expressed inappropriately in the pupa at a time they should normally have disappeared. Additionally, the expression of the RNA-binding-factor *BRAT*, which typically increased near pupation, was delayed in the midguts of methoprene-treated larvae. Treatment of the larvae with the juvenile hormone analog methoprene caused a reiteration of the larval midgut developmental phenotype, and resulted in persistent *BR* expression. In the pupal midgut *BR* transcripts did not fully decrease, and midgut remodeling did not occur.

2. RESULTS: The effect of methoxyfenozide, an ecdysone analog, on midgut development

Although it has a different chemical structure (Figure 2.15), the diacylhydrazine agonist methoxy-fenozide (RH2485) acts as an ecdysone analog that mimics the binding properties of ecdysone. RH2485 binds in the flexible ligand-binding-domain pocket of the ecdysone receptor [159]. However, RH2485 is not easily metabolized, disrupts metamorphosis, and kills a treated insect [160]. Synthetic insect growth-regulators are used as biorational insecticides and also as tools of discovery to learn about the biological activity of ecdysone [123].

FIGURE 2.15 Methoxyfenozide vs 20-hydroxy-ecdysone

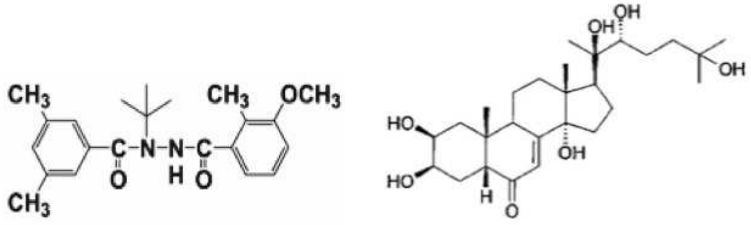

methoxyfenozide (RH2485) **20--hydroxyecdysone**

Figure 2.15 A comparison of the molecular structure of methoxyfenozide and 20-hydroxy ecdysone shows that they have quite different molecular structures.

Effect of ecdysone analog methoxyfenozide (RH2485) on *BR* expression

The ecdysone agonist RH2485 was used to determine if inappropriate exposure would affect the pattern of *BR* expression during midgut metamorphosis. Under normal conditions, ecdysone titers peak about 48 hours after the last larval-larval molt. I exposed larvae to RH2485 earlier, at 24 hours after the molt, by placing staged larvae in containers of water with RH2485 added (final concentration of about 135nM), and food. *Ae. aegypti* larvae treated with RH2485 were unable to complete the pupal molt, and died as larvae or during pupation.

Phenotype of the midgut of larvae treated with RH2485

Most of the dead larvae had pigmented respiratory trumpets. Cuticle pigmentation was variable, and frequently RH2485-treated larvae had abnormal dark markings on their cuticle, in contrast to

cuticles of untreated larvae. There was also evidence of premature imaginal disc development, and eye development seemed advanced: in RH2485-treated larvae a wider crescent of pigmented pre-adult ommatidia surrounded the larval ocelli in than in the controls, but this difference was not quantitatively compared. In some larvae, a structure resembling the larval hindgut extended from the anal papillae (Figure 2.16A). Dissected midguts of treated larvae often had anterior and medial muscular constrictions. Many larvae began, but could not successfully complete, the pupal molt. The larval headcaps of treated larvae remained attached, though the pupal cephalothorax formed. The disastrous result of this attachment was that the cuticle could not be completely shed (Figure 2.16C). The onset of pupation was delayed in these larvae, and most died 3-5 days after treatment with RH2485. Melanotic patches observed in the RH2485-treated larvae when they died (Figure 2.16D) seemed to phenocopy *D.melanogaster* mutants defective for the ecdysone inactivation enzyme Cyp18a1; such mutants have melanotic masses resulting from local concentrations of ecdysone [161].

FIGURE 2.16 Phenotype of RH2485 treatment in the midgut

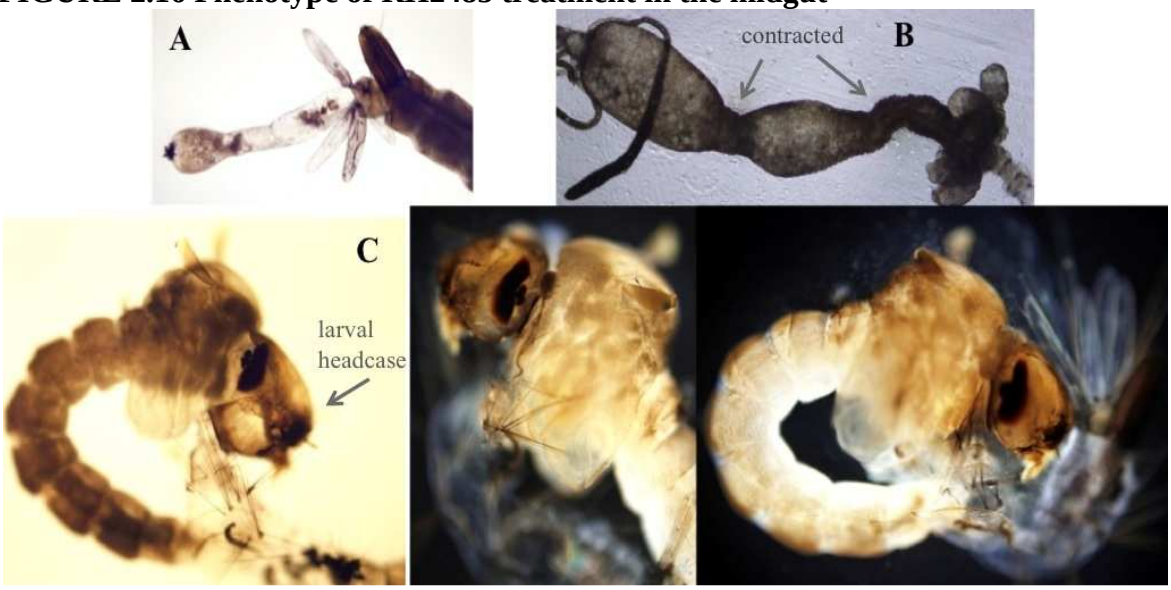

Figure 2.16 Phenotype of RH2485 treatment in the midgut **A.** Early-developed hindgut extruded from anal papillae **B.** RH2485-treated larval midgut **C.** Larva with pupal thorax, unable to complete molt, with larval head-case stuck on. Note extent of eye development.

FIGURE 2. 16 D. Phenotype of RH2485 treatment in the midgut

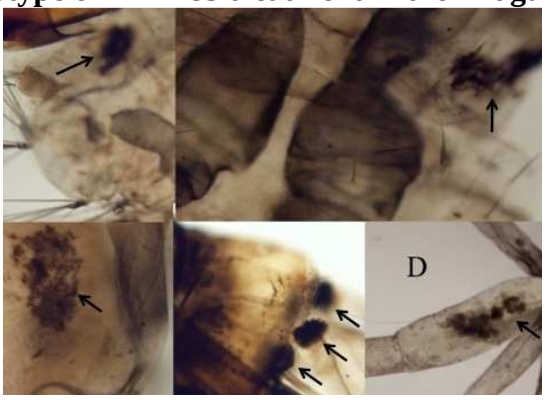

Figure 2.16 D. Phenotype of RH2485 treatment in the midgut: dark melanotic patches (arrows) on RH2485-treated larval cuticle

Effect of RH2485 treatment on *BR* expression in the midgut

The expression level of the *BR* isoforms was analyzed by qPCR with midgut RNA samples from control and RH2485-exposed larvae treated by the regime described above. This inappropriate exposure to RH2485 at 24 hours after the molt was expected to occur approximately 24 hours before the endogenous peak in ecdysone titer. The 24 hr midgut RNA expression levels shown in the charts are the pre-treatment levels. Late-4th samples were taken at the onset of pupation, when RH2485-treated larvae were trying to molt (Figures 2.16, 2.17). After approximately 26 hours exposure to RH2485 (at 50 hrs into the 4th instar, when *BR* expression normally peaked) *BR* expression in the treated larvae was unexpectedly lower than in untreated larvae. In the late 4th instar midgut, the levels of the *Z1, Z2*, and *Z3* isoforms were similar in both the treated and the untreated control samples, but in RH2485-treated larvae, *BR*Z4 levels remained elevated at the larval molt, while *Z4* decreased in untreated larvae.

Results of three subsequent experiments with RH2485 in larvae that were refed after starvation were consistent with the results reported here for *BR*, miRNA and *BRAT* expression.

FIGURE 2.17 *BR* expression in RH2485-treated larval midguts

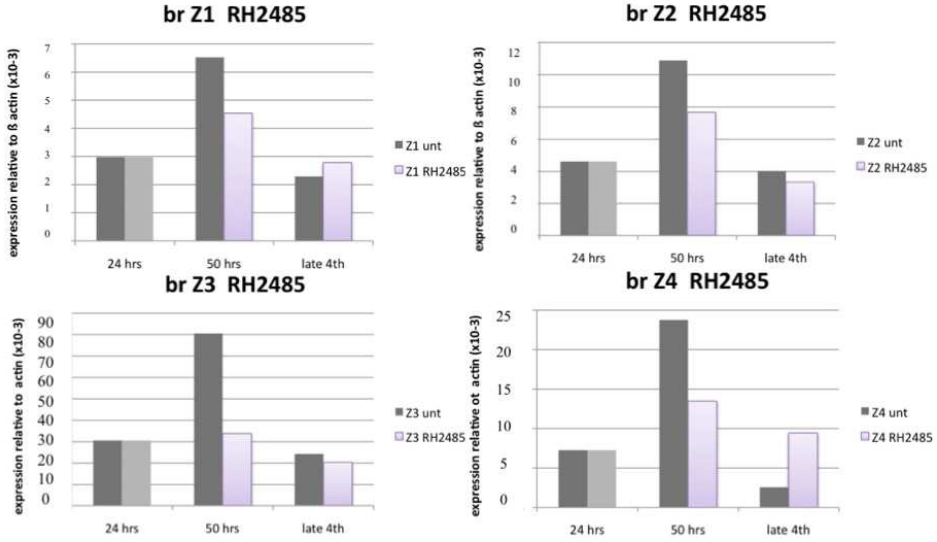

Figure 2.17 *BR* expression in RH2485-treated larvae was lower at ~50 hr than in untreated larvae. In RH2485-treated larvae, Z4 was higher in late 4th, compared to Z4 in transcript levels in untreated larvae. RH2485-treated larvae died at pupation. RH2485-purple untreated-gray
Note: A related *BR* expression analysis of the midguts from starved larvae, re-fed and treated with RH2485, or re-fed and left untreated, gave the following result:

FIGURE 2.18 *BR* expression after starvation when treated with RH2485

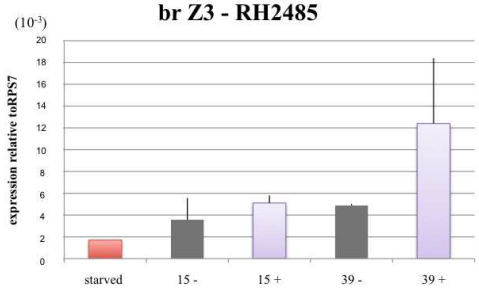

Figure 2.18 *BR* expression increased in RH2485-treated midguts when larvae were re-fed after starvation. RH2485 treatment elevated *BRZ*3 expression at 39 hr after re-feeding, in contrast to *BRZ*3 expression in untreated larvae at 39 hours.

One interpretation of these results is that RH2485 treatment may have caused a peak in *BR* expression earlier than normally expected in untreated re-fed larvae. This would and support the hypothesis that treatment with RH2485 may accelerate *BR* expression during recovery from starvation and re-entry into midgut metamorphosis.

Effect of RH2485 exposure on *miR-317, miR-34,* and *miR-277* expression

In the same experiments miRNA expression levels were determined. Figure 2.19 shows that *miR-317* and *miR-277* expression was relatively unaffected by RH2485; their control and

RH2485-treated levels were similar. However, during the course of exposure, *miR-34* increased in control larvae but in RH2485-exposed larvae, *miR-34* decreased. The overall abundance of *miR-277* was low.

FIGURE 2.19 Expression of *miR-317, miR-277 & miR-34* in RH2485-treated larvae

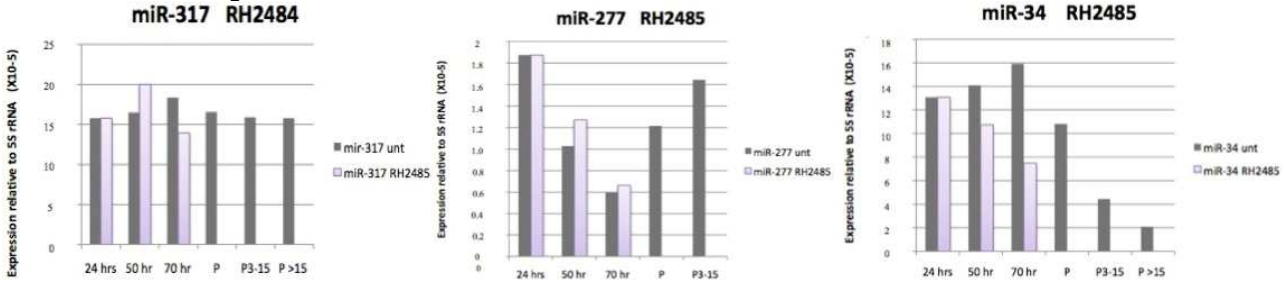

Figure 2.19 *miR-317, miR-277* and *miR-34* Expression levels of *miR-317* and *miR-277* were not greatly affected by treatment with RH2485, but *miR-34* levels decreased in late 4th in RH2485-treated larvae. *miR-277* was overall less abundant.
Untreated - gray RH2485-treated - purple

Effect of RH2485 exposure on *let-7* and *mir-125* expression

Both *let-7* and *miR-125* were elevated in RH2485-treated midguts (Figure 2.20). However, this increase was moderate compared to the normal up-regulation of *let-7* and *miR-125* observed later in untreated pupae (gray bars to right).

FIGURE 2.20 *let-7* and *miR-125* in RH2485-treated larvae

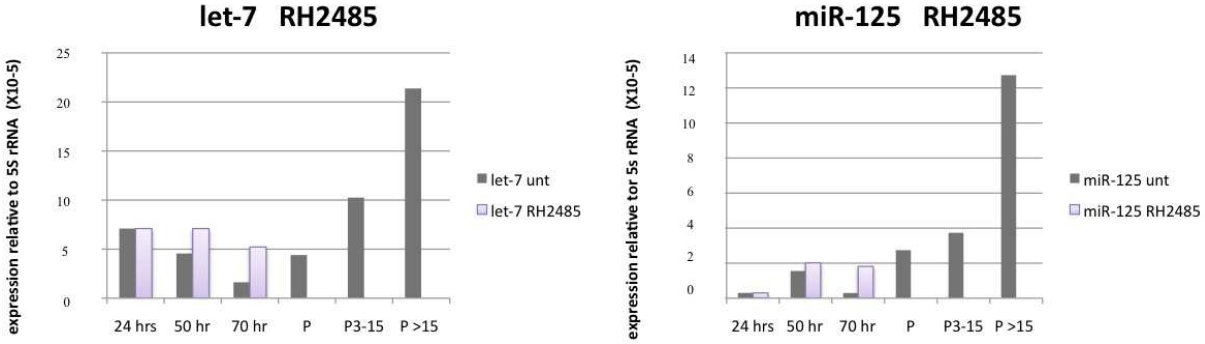

Figure 2.20 A. *let-7* and *miR-125* expression levels were elevated in RH2485-treated larvae, but treated larvae died before the pupal peak of *let-7* and *miR-125* that normally occurred in untreated midguts.

Effect of RH2485 exposure on *miR-14*

Treatment with RH2485 did not greatly affect the expression of *miR-14* in the midgut (Figure 2.21).

FIGURE 2.21 *miR-14* expression levels in RH2485-treated larvae

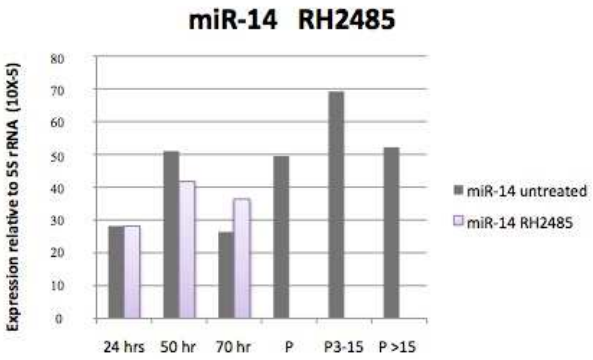

Figure 2.21 RH2485 treatment had little affect on *miR-14* expression.

RH2485-treatment and *BRAT* expression levels in the midgut

In RH2485-treated larvae *BRAT* expression was higher at 70 hr. *BRAT* increased at pupation in untreated midguts (Figure 2.22).

FIGURE 2.22 Expression of RNA-binding factor *BRAT* in midguts of RH2485-treated larvae

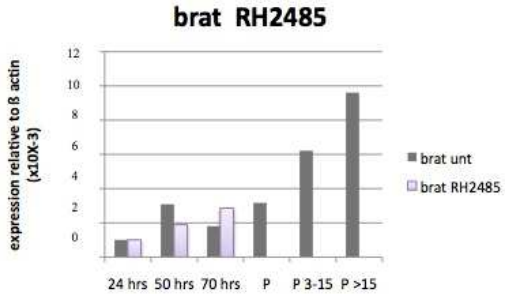

Figure 2.22 Expression of RNA-binding factor *BRAT* in midguts of RH2485-treated larvae The expression of *BRAT* was highest at 70 hours in RH2485-treated larvae. In untreated larvae *BRAT* levels increased in the pupa. (purple - RH2485-treated gray - untreated).

DISCUSSION - Effect of RH2485 on midgut development

After treatment with RH2485, subsequent pre-pupal development became uncoordinated. Ultimately, treated larvae were unable to pupate because, although the pupal cephalothorax formed, the animals were unable to separate from the larval headcase (Figure 2.16 C).

Effect of RH2485 on *BR* expression levels

It is possible that RH2485 treatment shifted *BR* expression earlier than it normally occurs in untreated larvae, such that a peak in *BR* expression was not observed at the 50 hr sample time in

RH2485-treated larvae (Figure 2.18). Alternatively, the higher level of RH2485 may actually repress *BR*, because *BR* is not normally expressed in the early pupa when the ecdysone level is highest. Premature developmental midgut phenotypes that resulted from ecdysone analog treatment might correlate with the decrease in *BR* expression, just as, in untreated larvae, *BR* expression decreases near pupation (Figure 1.21).

Effect of RH2485 on miRNA expression levels

The data reported here can be grouped as follows:

TABLE 2.1 Effect of RH2485 on miRNA expression levels

Effect of RH2485	**Expression unaffected by RH2485 treatment**	**Expression elevated by RH2485 treatment**	**Expression decreased by RH2485 treatment**
miRNA	miR-14, miR-317, miR-277	let-7, miR-125	miR-34

Elevated miRNA expression

In both control and experimental larvae, the expression levels of *let-7* and *miR-125* were relatively low during the 4th instar. Under normal developmental conditions the ecdysone titer rapidly increases just after the pupal molt, as do the *let-7* and *miR-125* expression levels. RH2485 treatment resulted in an earlier increase in the *let-7* and *miR-125* expression, in 4th instar larvae.

Decreased miR-34 expression

Like *BR, miR-34* also decreased after exposure to RH2485. Further experiments need to be done to resolve BR expression levels between the time of treatment and 50 hours after the 4th instar to determine if and when a peak in *BR* expression occurs.

FIGURE 2.23 Expression patterns in the midgut
untreated larvae (top) methoprene-treated larvae (middle) RH2485-treated larvae (bottom)

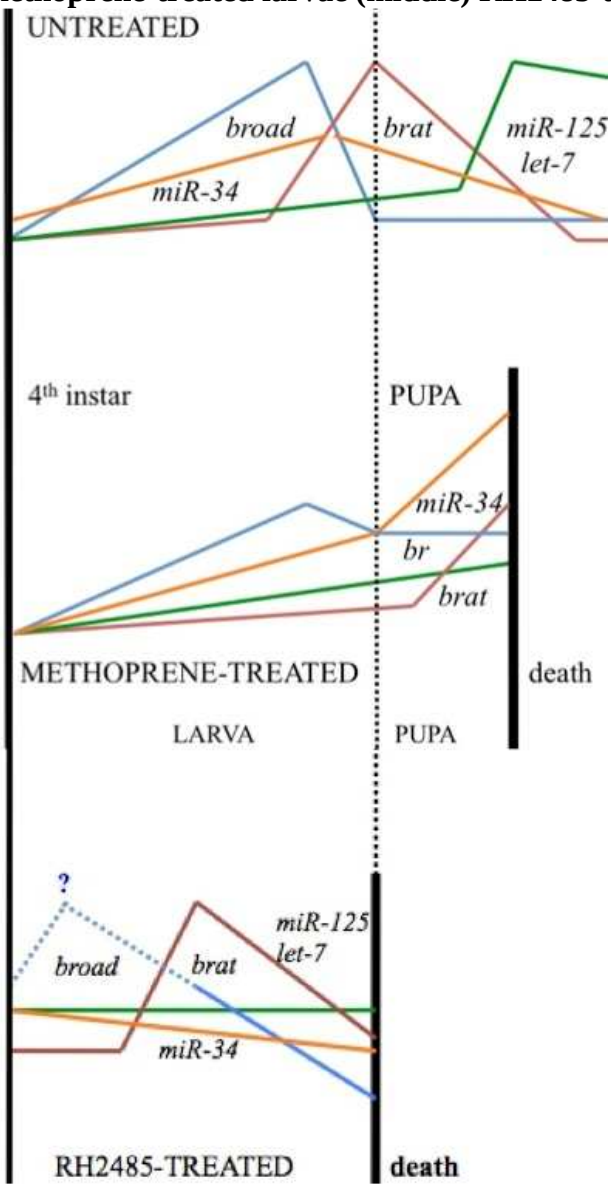

Figure 2.23 Expression pattern summary
In **untreated larvae (top),** *BR* transcript levels increased then decreased, then *brat* transcripts increased, then *let-7* (and *miR-125*) transcripts increased.
In methoprene treated larvae (middle chart), *BR* expression levels increased again in the pupa, *BRAT* was never upregulated, and the pupa died before the upregulation of *let-7* and *miR-125* (bottom**). Expression patterns expanded over time.**
In RH2485-treated larvae (bottom chart), *BRAT* expression increased earlier, *let-7* levels increased, and there was no peak of *BR* observed (possible earlier peak indicated in dotted blue lines). **Expression patterns compressed over time.** The expression pattern of these midgut developmental timing regulators when treated with hormone analogs suggests they may have undergone heterochronic shifts, with the JHA analog methoprene slowing and the ecdysone analog RH2485 accelerating expression patterns.
***miR-34* - orange** ***BR* - blue** ***BRAT* - red** ***let-7* and *miR-125* - green**

SUMMARY: Treatment of larvae with methoprene and with RH2485

Changes in *BR* expression in midguts when larvae were treated with the JH and ecdysone hormone analogs suggested that *BR* was responsive to both methoprene and to RH2485. When larvae were treated with methoprene, pupal midguts retained larval characteristics, such as the presence of gastric cecae and the persistent attachment of larval epithelial cells to the basement membrane. Methoprene-treated larvae may have undergone a shift in developmental progression where the timing of midgut development was delayed or repeated.

When treated with RH2485, larvae underwent early hindgut development, early midgut contraction and perhaps premature delamination of larval epithelial cells from the midgut basement membrane. RH2485-treated larvae appeared to have precocious development, suggesting a heterochronic shift where the timing of midgut development accelerated.

These changes in the pace of developmental progress in the midgut when larvae were treated with hormone analogs were consistent with the canonical roles for juvenile hormone (to maintain the *status quo)* and for ecdysone (to initiate change).

MATERIALS AND METHODS

Timing of control and treated larval cohorts:

Cohorts of 50 larvae that attained 4th instar within 5 hours of each other (timed by appearance of cast off 3rd instar cuticles in tube) were collected and amply fed. At 24 hours 4th instar they were distributed at 50 larvae/container into100 ml distilled water and the following treatments:

Treatment with methoprene: 4 µl of methoprene (technical grade) was added to 2 mls of ethanol, well-vortexed and stored at -20ºC. 50 µl of this stock solution was then added to the experimental100 ml of distilled water, to obtain a final concentration of ~ 2x10 $^{-8}$ methoprene in the larval water. When the larvae reached 24 hrs 4th instar, 50 larvae were added to this container and fed. When DMSO was used as a solvent, 2µl of technical grade methoprene was dissolved in 2 ml of DMSO, well-vortexed, and stored at -20ºC. This stock solution was used at a concentration of 1µl/1ml distilled water (individual larvae in tube) or at 100µl/100 ml distilled water to treat cohorts of ~50 larvae.

Treatment with RH2485: Methoxyfenozide (Fluka) was first dissolved in ethanol at a concentration of 50 mg/ml. 1 µl of this stock solution was added to 100 ml of distilled water for a final concentration of about 135nM. When the larvae reached 24 hrs 4th instar, 50 larvae were added to this container and fed.

Ethanol-treated larvae: When the larvae reached 24 hrs 4th instar, 50 larvae were added to a container of 100ml distilled water and 50µl ethanol, and fed.

DMSO-treated larvae: When the larvae reached 24 hrs 4th instar, 50 larvae were added to a container of 100ml distilled water and 100µl of DMSO and fed.

Untreated larvae: When the larvae reached 24 hrs 4th instar, 50 larvae were added to a container of 100ml distilled water and fed.

Timed samples: Approximately15 midguts from each treatment condition were dissected in PBS, placed in 300µl Qiazol lysis reagent, vortex, briefly heated to 65ºC, vortexed again, then stored at -20ºC.

RNA extraction, reverse transcription, and PCR were as described in Chapter 1.

CHAPTER 3

The effect of starvation and nutrient restriction on *BR* and RNA-binding factor expression

Evidence is presented in Chapter 2 that both the ecdysone analog RH2485 and the juvenile hormone analog methoprene can alter *BR* expression, suggesting that, in the *Ae. aegypti* midgut, *BR* may integrate information from diverse signaling pathways to control developmental timing [1, 60].

The duration of the larval phase is affected by nutrient availability [9, 162]. I hypothesized that suboptimal nutrient conditions might delay the onset of pupation by altering the time when *BR* is expressed. To test this hypothesis, experiments were done to investigate the role of nutrition in the expression of *BR* and RNA-binding factors in the *Ae. aegypti* midgut under the following conditions:

1. Starvation

2. Re-feeding after starvation

3. Fed nutrient-restricted diets

4. Starvation then treatment with RH2485

BACKGROUND

Current models concerning regulation of larval growth and metamorphosis in insects

Current models concerning the regulation of growth and development propose that metamorphosis is initiated after the insect has attained a critical weight [122]. Nijhout defined critical weight as “the minimum weight at which further feeding and growth are not required for a normal time-course to metamorphosis and pupation”. Once the critical weight is reached, JH levels decrease, and a subsequent peak in ecdysone specifies a pupal molt [122, 163]. Although JH concentration in mosquito larvae has not been determined, based on work in other insects I

hypothesized that, by analogy JH is present in the early 4th instar until the critical weight is reached.

Ae. aegypti 4th instar larvae must feed for approximately 24 hours after the molt from 3rd to attain a critical weight of 2.7-3.2 mg. [9, 125, 162]. *Critical weight* thus is an approximate size threshold based on the mass and feeding time required for a 4th instar larva to commit to pupate. Hereafter, critical weight in *Ae. aegypti* larvae refers to a minimum larval mass that provides sufficient reserves for the larva to pupate. After the critical weight is reached ecdysone biosynthesis is initiated, and the larva commits to pupal development, even if starved later [164, 165]. If nutrients are available after the critical weight is reached there is a final growth period, and larval growth continues until a peak in the ecdysone titer, when growth ceases and the larva pupates [166].

In the midgut of fed larvae, *BRZ*3 is expressed in late 3rd and 4th instars. *BR* expression remains relatively low until ~24 hours, when it begins to increase. The increase in *BR* expression coincides with the attainment of critical weight, and the first small peak of ecdysone (Figure 3.1). The peak in *BR* expression around 48 hours after the molt coincides with the pre-pupal peak in ecdysone level (Figures 1.21 and 3.1) and the attainment of maximum weight [9, 162].

FIGURE 3.1 Developmental timescale 4th instar - pupa with Palli lab ecdysone titers

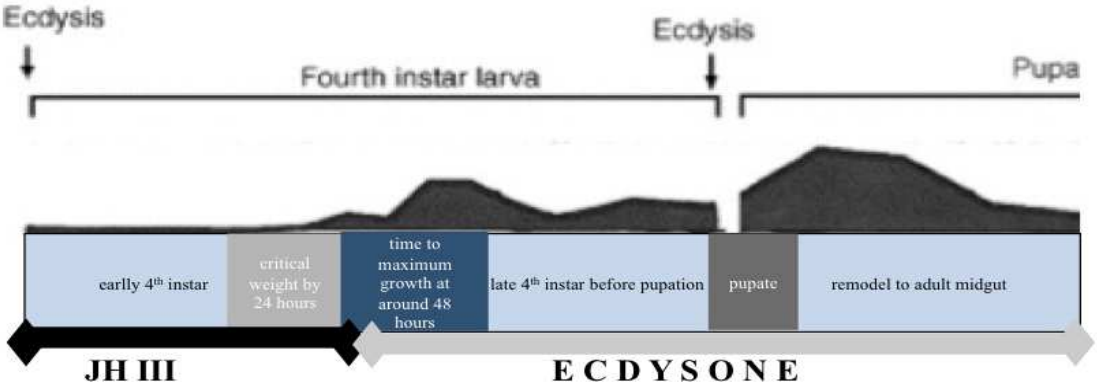

Figure 3.1 Sequence of developmental phases during midgut metamorphosis relative to ecdysone titer fluctuations [69] JH levels not known, only hypothesized.

1. RESULTS: Response of 4th instar larvae to prolonged starvation

Mosquito larvae with constant access to food pupate within 3 days of the 4th instar molt when raised at 25ºC. However, if starved before the critical weight is reached, larvae enter a state of developmental arrest and can live for 2-3 weeks or more, but never pupate [125, 162]. If re-fed, most larvae resume development, pupate, and become adults.

Expression of *BR* during the state of developmental arrest induced by starvation

If *BR* controls the timing of pupation in *Ae. aegypti*, what happens to *BR* transcripts during starvation-induced developmental arrest? This study of the effect of starvation on the expression patterns of *BR* and RNA-binding factors during larval development was done to better understand the larva-to-pupa transition in the *Ae. aegypti* midgut and the roles of *BR* and candidate regulators of *BR* during the larval response to food scarcity.

Morphology of starved larvae

If starvation began before the critical weight was attained, 4th instars did not pupate. If starvation conditions continued, larvae began to die around 2 weeks after the withdrawal of food, but some larvae remained alive for more than a month.

Larvae starved for 14 days have a transparent cuticle, little visible imaginal disc development in the thorax, and no visible fat body accumulated beneath the cuticle. They are less active than fed larvae, and although they avoid light and go to the bottom in response to movement, they mostly rest still in the water. Their midguts are thin and delicate with a transparent epithelium, suggesting a lack of accumulated lipids. Extensively branched trachea attach to the midgut. The peritrophic membrane remains intact. After 14 days without nutrients, both DAPI and methylene blue staining showed small diploid adult precursor cells *without* cytoplasmic projections, encircling larger endoreplicated enterocytes, particularly in the posterior midgut of starved

larvae (Figure 3.2D). Although starved larvae are unable to pupate, over time some changes do occur in the midgut (Figure 3.2).

FIGURE 3.2 Morphological response of 4th instar larvae to prolonged starvation

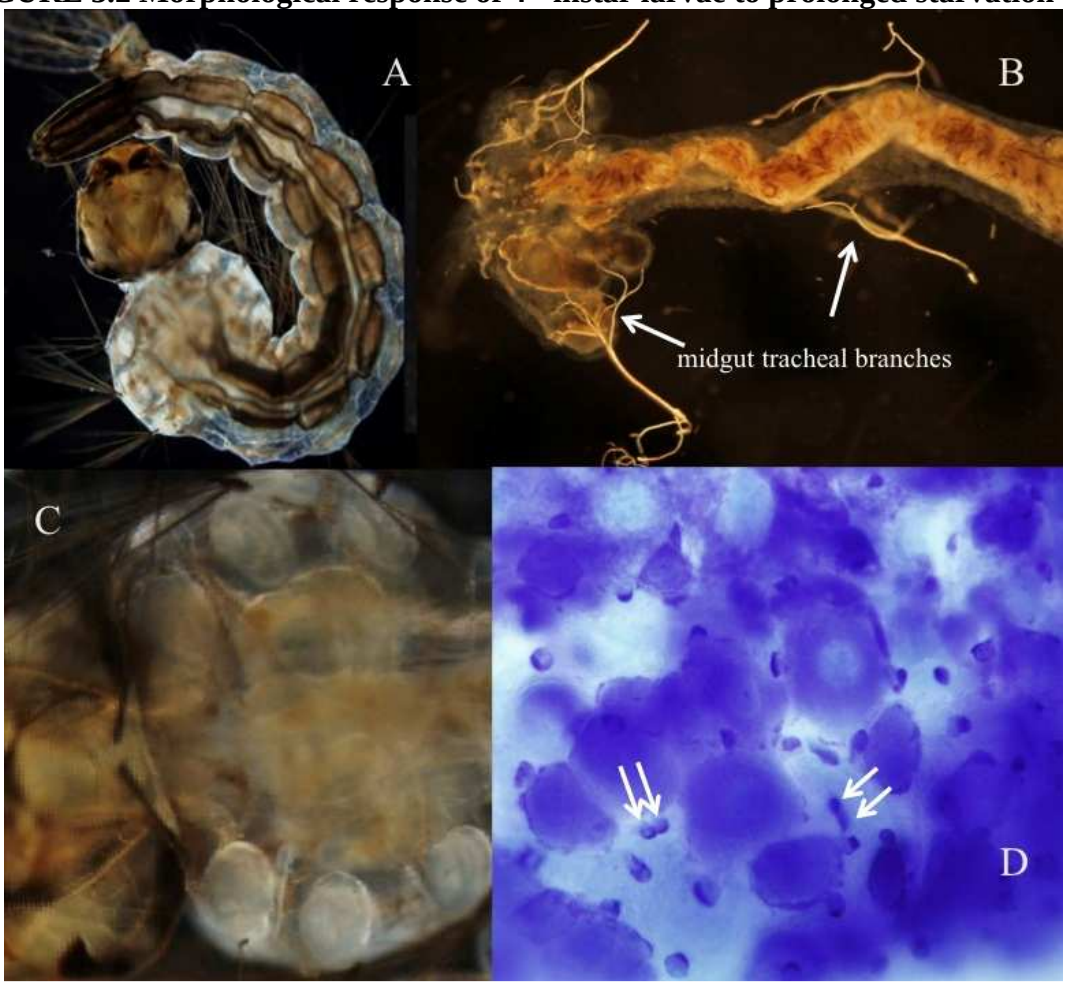

Figure 3.2 A. 14 day starved larva with transparent cuticle **B.** Translucent 18 day starved midgut: branching trachea (arrows) and intact peritrophic membrane. **C.** Transparent larval thorax (ventral view) revealing undeveloped peripheral imaginal discs and (central) midgut gastric cecae. **D.** Midgut epithelial cells: large larval enterocytes and small, often paired diploid adult precursor cells (arrows) without cytoplasmic extensions.

***BR* isoform expression during starvation - larval midguts after 4th instar molt**

During the first 7 days of starvation, *BR* transcript levels remained similar to the initial early 4th instar level before starvation, with Z3 still the most abundant isoform. After 14 days of starvation *BR* transcript levels decreased, but remained present. Figure 3.3 shows *BR* expression levels just at the molt (pre-starvation), and at 24 hours in fed 4th instars, after the critical weight was

reached (gray bars). Red bars show expression levels after 7 and 14 days of starvation. These experiments were repeated at least three times and the results were consistent and reproducible.

FIGURE 3.3 *BR* isoform expression in the 4th instar larval midgut during starvation

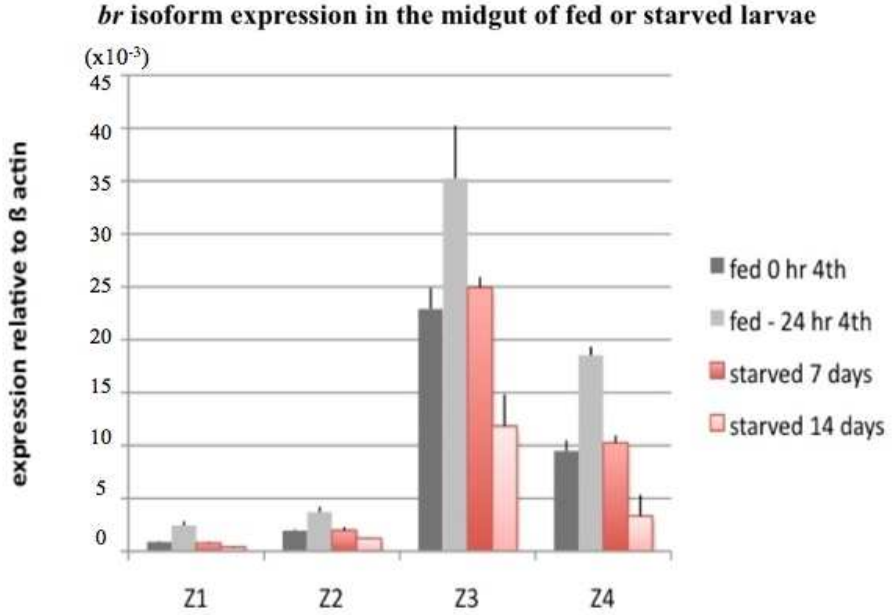

Figure 3.3 *BR* isoform expression after 7 days of starvation remained approximately at the same level as when the larva molted to the 4th instar, then decreased after 14 days of prolonged starvation. In fed larvae, *BR* expression levels increased 24 hours after the molt to 4th.
FED sampled at 0hrs, 24 hrs - **gray** **STARVED** sampled at 7 days, 14 days – **red**

miRNA expression in the midgut of starved larvae

The effect of starvation on miRNA expression was evaluated. The experiments were repeated (with the exception of miR-34* and miR-277*) and the results reported here were reproducible**.**

miR-14 expression during starvation The expression of *miR-14* clearly increased during starvation. This suggests that *miR-14* may have a function during starvation (Figure 3.4).

FIGURE 3.4 *miR-14* expression in starved larvae, compared to fed levels 4th instar

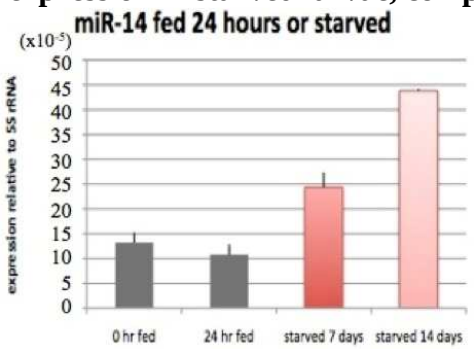

Figure 3.4 *miR-14* levels increased in larval midguts after 7 days of **starvation**, and further increased after 14 days (**red).**

Expression of *miR-317, miR-34* and *miR-277* during starvation

When larvae were starved, midgut expression levels of *miR-317* and of *miR-34* increased over time. In contrast, expression of *miR-277* decreased after the beginning of the 4th instar, and remained low in both starved and fed larvae. *miR-277* expression was substantially lower than *miR-317* and *miR-34*. While the expression of *miR-34* increased in starved larvae, *miR-34** did not, and neither did *miR-277**, suggesting they were not needed during starvation (Figure 3.5 C).

FIGURE 3.5 *miR-317, mir-277,* and *mir-34* expression in starved larval midguts

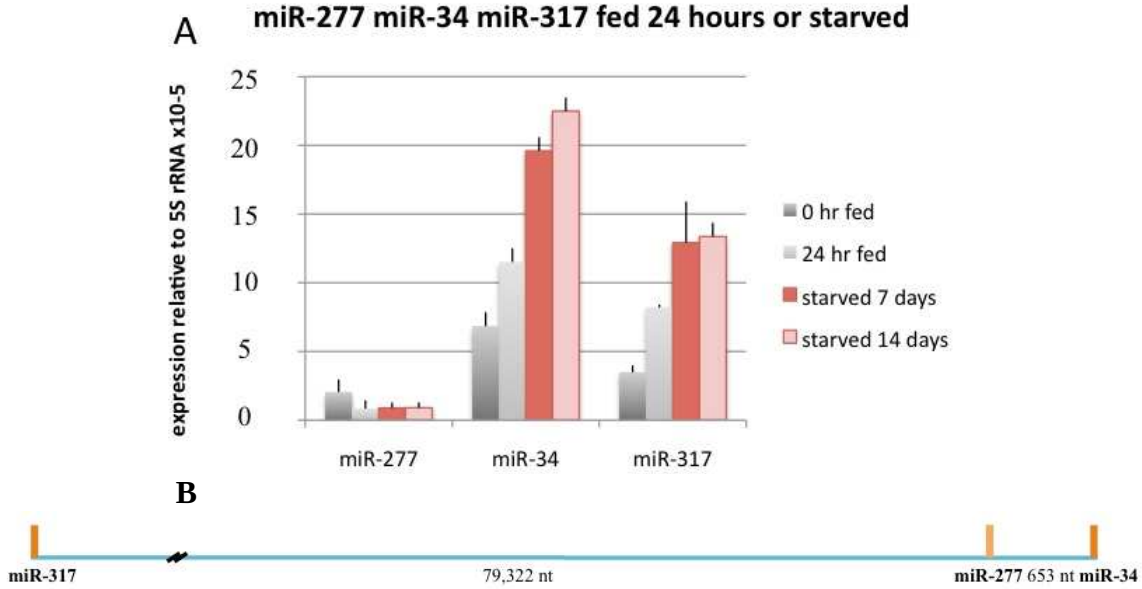

Figure 3.5
A. *miR-317, mir-277,* and *mir-34* expression in starved larval midguts. miR-34 increased 4-fold in starved larvae. B. *miR-317, miR-277* and *miR-34* cluster in *Aaeg* genome.

C. Expression of *mir-277 and of *miR-34** in starved larvae**

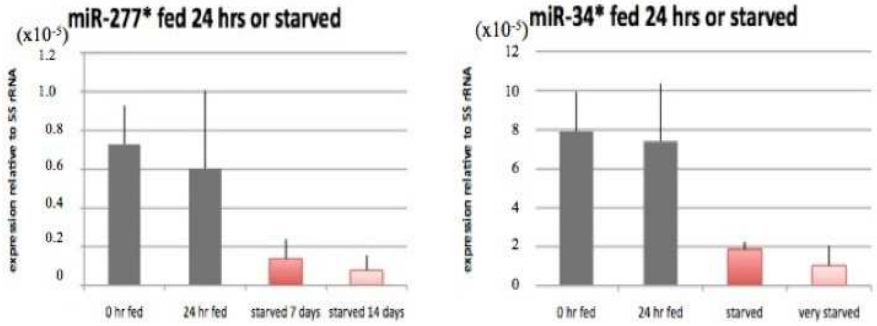

Figure 3.5 C. The expression of *mir-277** and of *miR-34** decreased during starvation.

Expression of *miR-100, let-7,* and *miR-100* during starvation

The expression of *miR-100, miR-125,* and *let-7* decreased over time in starving larvae.

FIGURE 3.6 *let-7* cluster expression in starved larval midguts
A *miR-100, let-7* and *miR-125* expression in starved larvae

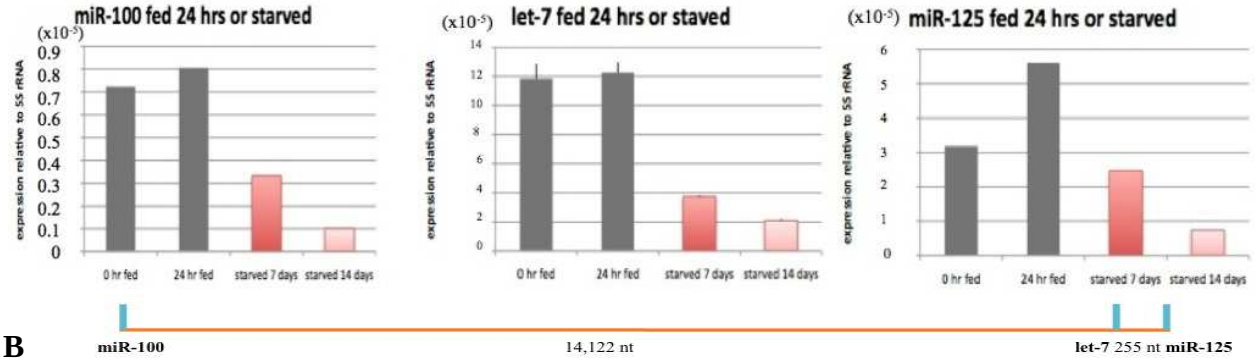

Figure 3.6 A. Expression of *miR-100, let-7* and *miR-125* decreased in starved larval midguts.
B. *miR-100, let-7,* and *miR-125* are clustered in the *Ae. aegypti* genome

Expression of *miR-7* and host gene *hnRNP-K* in the midgut during starvation

The expression of *miR-7* sharply decreased, while *hnRNP-K* decreased only slightly.

FIGURE 3.7 *miR-7* and *hnRNP-K* expression levels in starved larvae

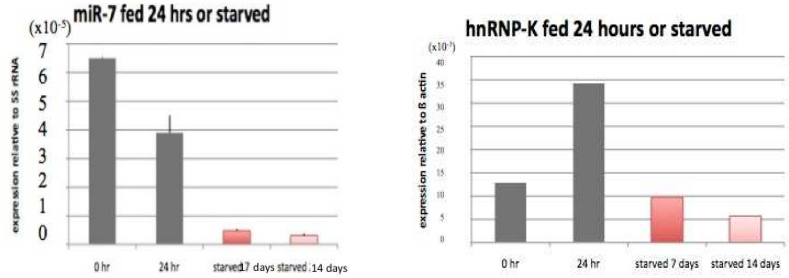

Figure 3.7 *miR-7* and *hnRNP-K* expression levels decreased in starved larvae, compared to fed larval expression levels in early 4th instars.

Expression of *miR-190* and host gene *TALIN* during starvation

In starved larvae, as in fed larvae, *miR-190* and *TALIN* expression was similar. Transcript levels of *miR-190* decreased during starvation (Figure 3.8), and the expression of host gene *TALIN*, which encodes a cytoskeletal protein connecting actin with integrin, also decreased. Like *miR-7*, in larvae fed a normal diet *miR-190* expression was highest in the early 4th instars.

FIGURE 3.8 *miR-190* and *talin* expression in starved larval midguts

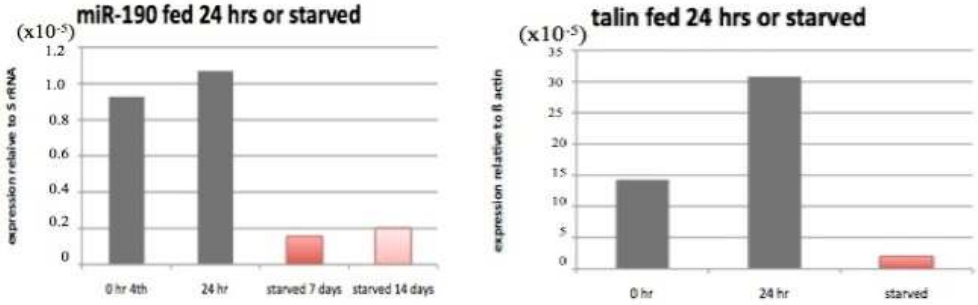

Figure 3.8 *miR-190* and host gene *TALIN* transcripts decreased in starved larval midguts

Expression of *BRAT* during starvation

In the fed-larval midgut, *BRAT* expression pattern was inversely correlated with *BR* expression (Figure 1.28). *BRAT* expression in the midgut was delayed by methoprene treatment, and accelerated by treatment with RH2485 (Figure 2.21). When larvae were fed a normal diet, *BRAT* sharply increased near pupation. After two weeks of starvation, *BRAT* transcripts remained at nearly the same level as they were at 24 hours in fed 4th instar larvae (Figure 3.9).

FIGURE 3.9 RNA-binding factor *BRAT* expression in starved larval midguts

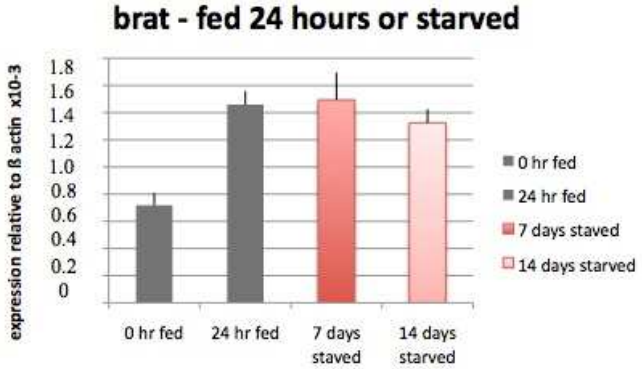

Figure 3.9 *BRAT* expression levels did not decrease during starvation.

Expression of *lin-28* during starvation

During starvation, *LIN-28* expression level was negligible, suggesting that, like *let-7*, *LIN-28* function was not required during starvation; during starvation the midgut is in a state of developmental arrest.

FIGURE 3.10 *LIN-28* expression in starved larval midguts (vs fed levels 4th instar)

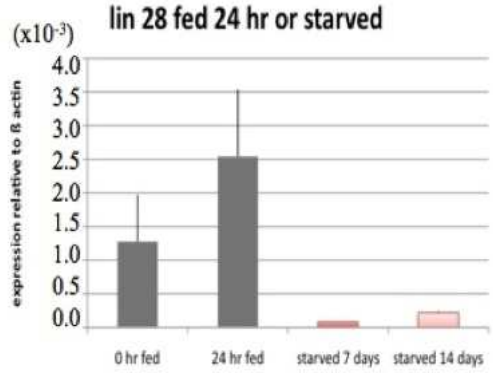

Figure 3.10 *LIN-28* transcript levels were very low in midguts of starved larvae, while they increased in fed larvae until ~ 48 hours 4th instar.

2. RESULTS: Response of 4th instar larvae to RE-FEEDING after starvation

When the starved larvae were re-fed, they completed the larval phase and pupated. To determine midgut transcript expression levels in starved 4th instar larvae after re-feeding, larvae were isolated late 3rd instar, allowed to molt to 4th, then starved. After a week of starvation they were re-fed a normal diet (yeast and fish food) and sampled at 5, 21, 30, 42, 56, and 64 hours after re-feeding.

Female larvae that had been starved and re-fed became smaller adults than the female adults developed with adequate nutrition throughout development (Figure 3.11). There was less difference between the sizes of the males when they were fed or starved-then-re-fed.

FIGURE 3.11 Phenotype of adults that developed from starved and re-fed larvae

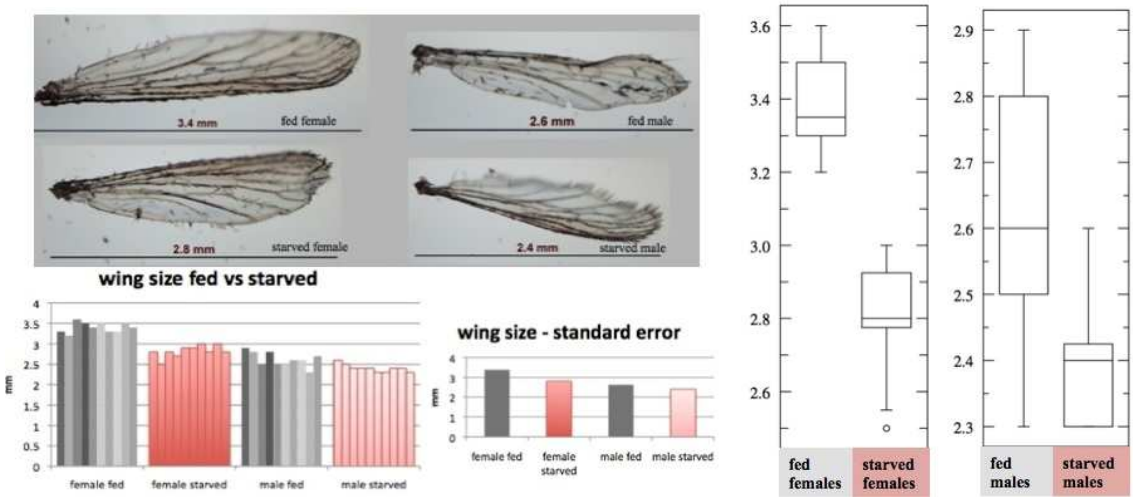

Figure 3.11 Top: Wings of fed, and of starved-then-refed adult female and male mosquitoes Female adults resulting from larvae starved 7 days then re-fed had smaller wings than those resulting from larvae that were never starved. **Bottom: Average wing size:** the average wing size was 3.4 mm in fed females vs 2.82 in starved females; and was 2.62 mm in fed males vs 2.4 in starved males (N=10 each group). **Sexual dimorphism**: there was a greater difference on average between the female wing sizes (0.58mm, p<.0001, t=9.21) than between the male wing sizes (0.22mm, p = 0.0032, t=3.4 http://www.physics.csbsju.edu/stats/t-test_bulk_form.html

***BR* isoform expression in the midgut of larvae starved 7 days, then re-fed**

When re-fed, *BR*Z3 expression levels at first decreased, then increased around 42 hours. The peak of *BR* expression occurred around 56 hours in the midgut of re-fed larvae (Figure 3.12). A comparison of *BR*Z3 expression in well-fed larvae (Figure 1.21) with larvae that were re-fed after starvation shows that, in the midgut of the well-fed larvae, Z3 levels increased around 24 hours, and a *BR*Z3 expression peak occurred around 48 hours, while in re-fed larvae, Z3 began to increase later, near 42 hours, and the peak in Z3 expression occurred around 56 hours. Thus the peak of *BR*Z3 expression in re-fed-larvae was delayed if compared with the expression peak in un-starved larvae.

FIGURE 3.12 *BR* isoform expression in the midgut of larvae that were starved then refed

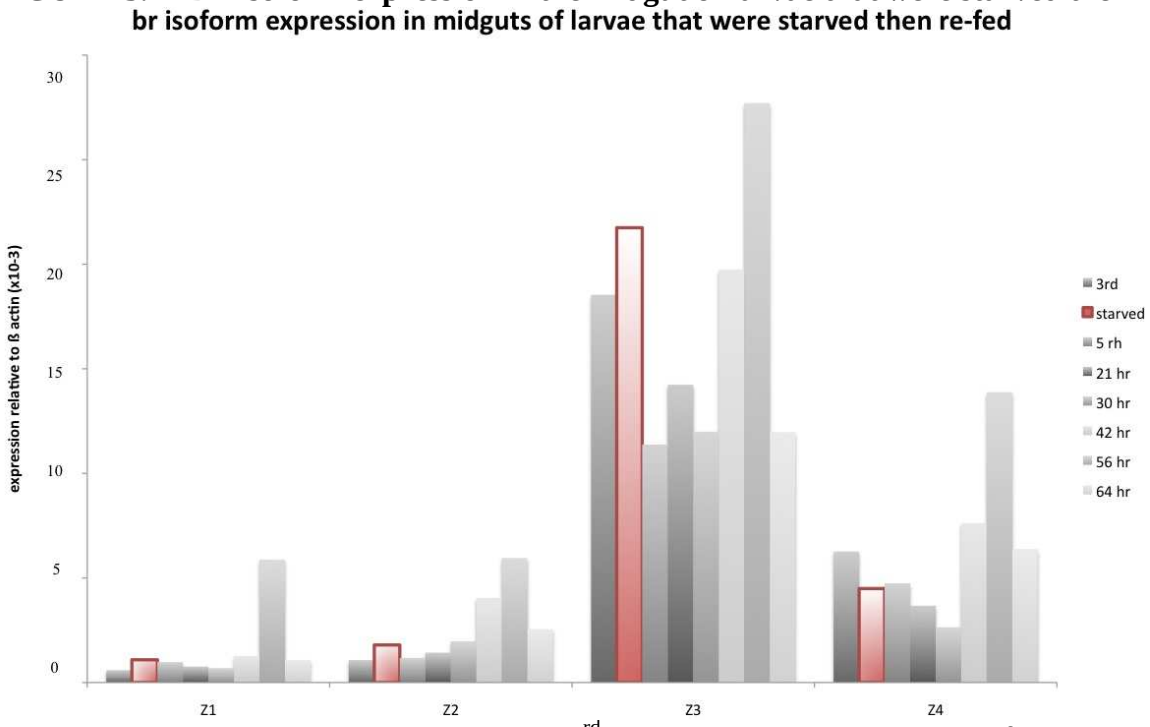

Figure 3.12 Fed larvae were sampled at late 3rd instar, starved 1 week, then re-fed and sampled at 5, 21, 30, 42, 56, and 64 hours after refeeding. *BR* transcript expression level starved 7 days (red) was higher than when feeding resumed. It took 42 hours after feeding resumed to bring *BR* expression beyond the starved level; ***BR*** expression was highest at 56 hr after re-feeding. **STARVED: red RE-FED: gray**, right of red

miRNA expression in the midgut of larvae that were starved 7 days then re-fed

Expression of *miR-14* in midguts of starved then re-fed larvae

miR-14 expression increased after re-feeding. Following an initial increase upon re-feeding, *miR-14* expression decreased again 30 hours after being re-fed (Figure 3.13).

FIGURE 3.13 *miR-14* expression in midguts of larva re-fed after starvation

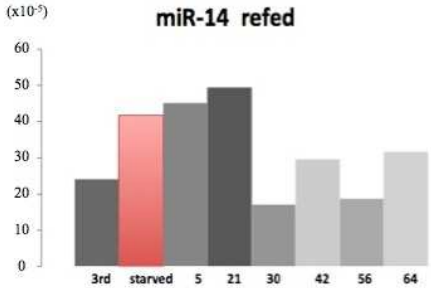

Figure 3.13 *miR-14* expression levels increased during starvation, remained high until 21 hr after re-feeding, then decreased. (gray bars right of red bar – hours after re-feeding)

Expression of *miR-317, miR-34* and *miR-277* in midguts of starved then re-fed larvae

In fed, starved, then re-fed larvae, the expression level of *miR-277* was consistently low. *miR-317* and *miR-34* transcripts were elevated in midguts of larvae starved for 7 days. When starving larvae were re-fed, expression of *miR-317* and *miR-34* decreased over a period of 30 hours, and remained low for the duration of the 4th instar (Figure 3.14). This suggested *miR-34* and *mir-317* may have a special function during starvation not needed in the larval midgut after feeding resumes. As in normally fed larvae, re-fed *miR-34* and *miR-317* transcript levels decreased towards pupation (Figure 1.23).

FIGURE 3.14 Relative expression of *miR-317, miR-277* and *miR-34* in midguts of larvae re-fed after starvation

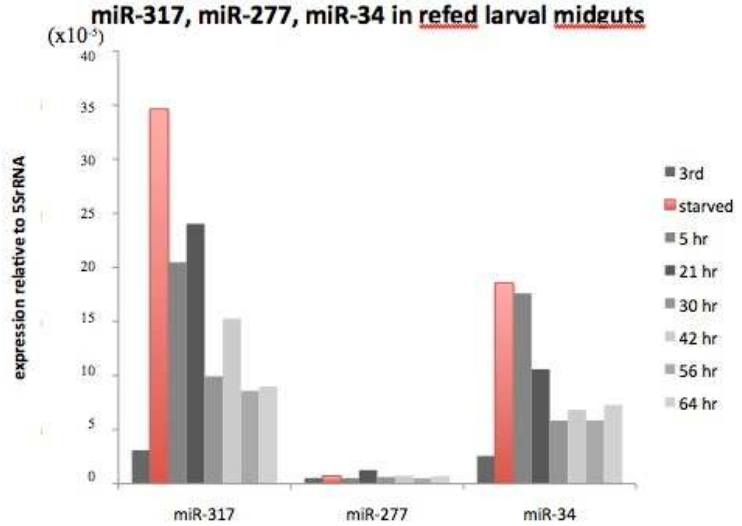

Figure 3.14 Expression of *miR-317* and *miR-34* was high in midguts of larvae starved for 7 days. When re-fed, expression levels gradually decreased over 30 hr. The abundance of *miR-277* was low in comparison to *miR-317* and *miR-34*.

Expression of *miR-100, let-7* and *miR-125* in midguts of starved then re-fed larvae

When starved larvae were re-fed, by 21 hours after re-feeding *let-7* and *miR-125* resumed expression levels comparable to normal levels during the 4th instar (Figure 1.25). In larvae re-fed after starvation, *let-7* was more abundant than *miR-125* (Figure 3.15).

FIGURE 3.15 *let-7* and *miR-125* expression in midguts of larvae re-fed after starvation

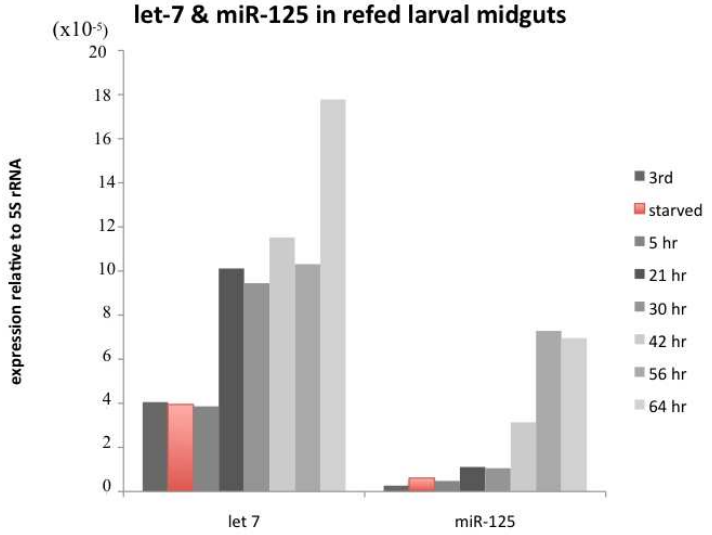

Figure 3.15 When larvae were re-fed after starvation, *let-7* and *miR-125* expression levels increased in the midgut.

Expression of *miR-7* and *hnRNP-K* in midguts of starved then re-fed larvae

miR-7 is located in an intron inside *hnRNP-K*. In re-fed larvae expression levels of *miR-7* and *hnRNP-K* increased at first, then decreased towards the end of the 4th instar. This pattern was similar to *miR-7* and *hnRNP-K* expression in fed larvae (Figure 1.28). The overall abundance of *miR-7* was low, while *hnRNP-K* expression level was higher.

FIGURE 3.16 *miR-7* and *hnRNP-K* expression in midguts of starved then refed larvae

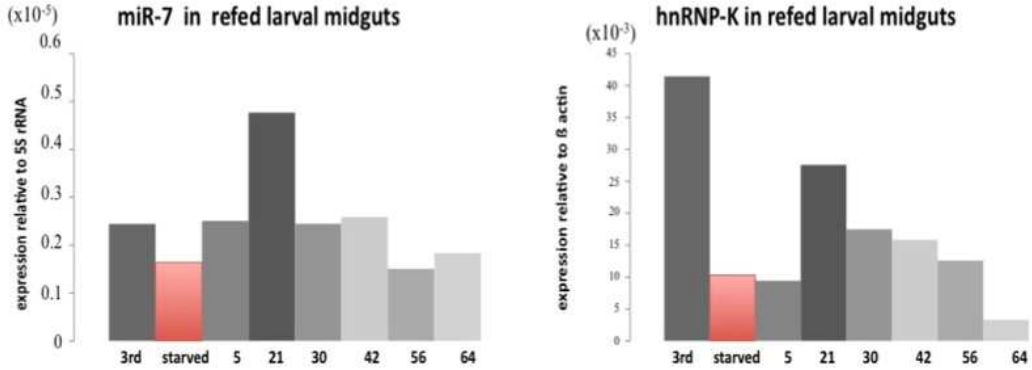

Figure 3.16 The expression levels of *miR-7* and its host gene *hnRNP-K* followed a similar pattern. Both were reduced in starved larvae, and both peaked at 21 hours after re-feeding. Numbers on the X-axis of the charts indicate sampling time (hrs after re-feeding)

Expression of *miR-190* and host gene *TALIN* in midguts of starved then re-fed larvae

miR-190 expression level decreased in the midgut at 5 hours after re-feeding, then increased. In the midgut of normally-fed larvae, and also in re-fed larvae, miR-190 expression was highest around 24 hours, then decreased after that (Figures 1.27, 3.17).

FIGURE 3.17 *miR-190* expression in midguts of larva re-fed after starvation

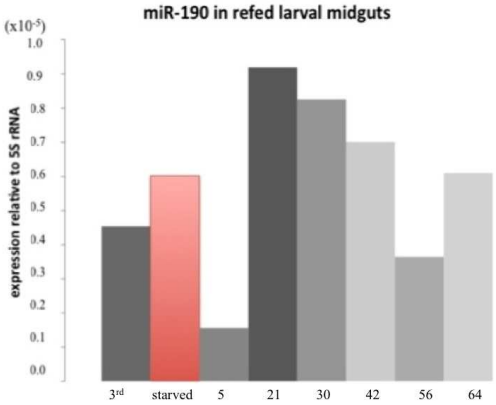

Figure 3.17 5 hours after re-feeding, *miR-190* expression levels dropped, then increased to a peak level at 21 hours after re-feeding. Numbers on the X-axis of the chart indicate sampling times (hrs after re-feeding)

Expression of RNA-binding-factor *BRAT* in midguts of starved then re-fed larvae

BRAT transcript levels were moderately elevated in the midguts of starved larvae. When larvae were re-fed, *BRAT* decreased, then increased again towards the end of the 4th instar, at 56 and at 64 hours. In fed larvae, *BRAT* normally strongly increased at pupation.

FIGURE 3.18 *BRAT* expression levels in midguts of larvae that were starved then re-fed

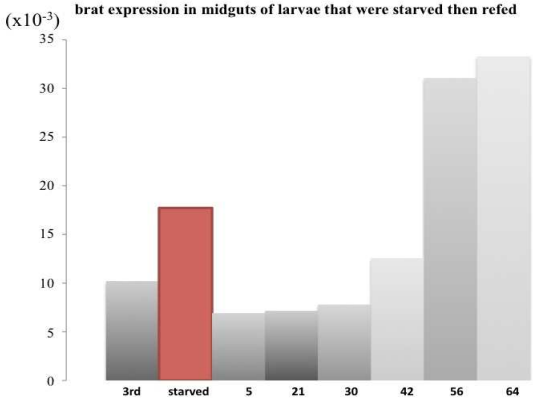

Figure 3.18 *BRAT* transcripts were slightly elevated during starvation, decreased when feeding was resumed, then increased again in late 4ths, at 56 and 64 hours. Numbers on the X-axis of the chart indicate sampling times (hrs after re-feeding)

1 & 2 DISCUSSION: The effects of (1) Starvation and of (2) Starvation then re-feeding on larval development and gene expression

1. Starvation

When starved in the early 4th instar, larvae underwent an extended developmental pause, during which the expression of *BRZ*3 transcripts was maintained at a moderate level. During starvation the expression of *let-7, miR-125, miR-7, miR-190, hnRNP-K, TALIN* and *LIN-28* clearly decreased, while the expression levels of *miR-14, miR-317,* and *miR-34* increased (Table 3.1).

TABLE 3.1 Expression levels in the midgut after prolonged starvation

expression level in midgut	**increased or unchanged** after prolonged starvation	**decreased** after prolonged starvation
miRNA	***miR-14, miR-317, miR-34***	***miR-277, miR-7, miR-190, miR-100, let-7, miR-125***
mRNA	***br, brat***	***lin-28, hnRNP-K, talin***

Up-regulation of *miR-34, miR-317,* and *miR-14* during starvation and increased expression of these miRNAs in response to methoprene may be related. Since starvation was initiated during a period of larval development when JH levels are relatively high, one could imagine that starvation conditions led to persistently high levels of JH and this resulted in increased levels of *miR-34* and *miR-14* expression, just as observed with methoprene exposure. Up-regulation of *miR-34* and *miR-14* during starvation (and, to a lesser extent, *miR-317*) was consistent with the possibility that juvenile hormone may regulate gene expression during starvation, and added support for the hypothesis that JH mediates a balance state [65] between survival and developmental progression in response to starvation in *Ae. aegypti* 4th instar larvae.

miR-34* and *let-7* in the regulation of dauer diapause in *C. elegans

Dauer diapause in the nematode is an alternative stage caused by environmental cues such as food, temperature and dauer pheromone [167]. Dauer larval progenitor cell lineages arrest at the end of the second larval stage [168]. Studies of miRNA expression during dauer diapause have shown that *miR-34* expression is up-regulated in diapause states, while *let-7* is down-regulated [168, 169].

miR-34 and *let-7* are among the most ancient and the most highly conserved miRNAs found in metazoans [170]. The molecular regulatory mechanisms that control dauer diapause in *C. elegans* may play similar roles in the starvation-induced developmental arrest of *Ae. aegypti*. The similar expression patterns of the ancient miRNAs *miR-34* and *let-7* in *C. elegans* and *Ae. aegypti* larvae confronting starvation suggested that these miRNAs might be part of an evolutionarily-conserved molecular response to nutrient scarcity. Alternatively, other factors, such as adipokinetic hormone, may mediate developmental arrest during mosquito development [171].

Larvae re-fed after starvation

The pattern of miRNA expression after the regimen of starvation and re-feeding was similar to the pattern obtained under conditions of continuous feeding. As in normally fed larvae, upon re-feeding *miR-14, miR-34,* and *miR-317* were the most abundant miRNAs in the larval midgut. *let-7* and *miR-125* expression levels remained low during the 4th instar in re-fed larvae*; let-7* and *miR-125* normally increased in the pupal stage. Generally, for all transcripts assayed, there was a slight delay after starvation before normal expression patterns resumed (Figure 3.19). This result agreed with previous studies done in 4th instar *Ae. aegypti* larvae that were starved then re-fed [162].

BR transcripts began to increase around 42 hr, and *BR* expression peaked around 56 hr. By 64 hr after re-feeding, *BR* transcripts had decreased, suggesting that the larvae might soon pupate. Seemingly, after re-feeding, a period of readjustment is required before a normal *BR* expression pattern resumes (Figure 3.19, bottom panel).

FIGURE 3.19 Developmental time to pupation in fed and starved then re-fed larvae

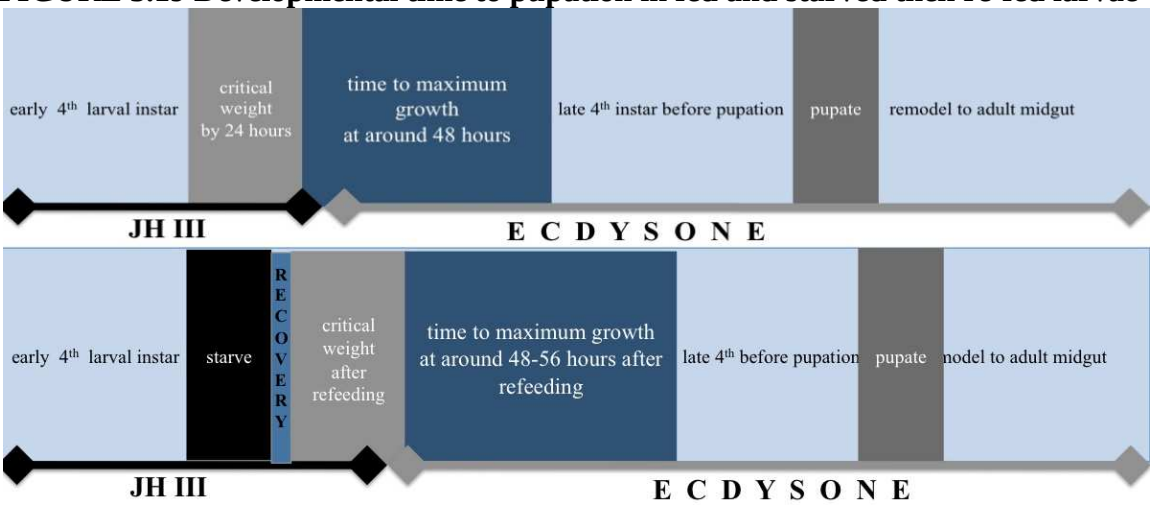

Figure 3.19 A hypothetical model for control of developmental timing by nutrition - modified from Layalle [165] Transcript levels changed when the larvae were starved. When re-fed, after an initial delay, transcript levels resumed normal expression patterns. **Top**: Developmental progression of fed larvae. **Bottom**: Developmental progression of starved then re-fed larvae, showing a **recovery period** before development resumes. (JH regulation is hypothetical)

While developmentally arrested, starved larvae may need to be ready to respond rapidly if nutrients become available. This might explain why *BR* transcripts were maintained during starvation. If *BR* is needed for commitment to pupate, a requirement for *de novo* transcription of *BR* upon re-feeding might delay developmental progress, which could decrease survival rates in a nutrient- restricted environment.

Translationally-repressed mRNAs accumulate in cytoplasmic foci called **P**rocessing bodies (P-bodies), or other sub-cellular localizations in which miRISC components *Ago1* and *GW182* and miRNAs are found [18]. I hypothesize that, during starvation, miRNAs and miRISC may target

BR transcripts to a sub-cellular location to protect them from degradation or autophagy, and if nutrients become available, *BR* transcripts are released and translated.

3. RESULTS: Response of starved 4th instar larvae when re-fed nutrient-restricted diets

Is there a nutritional cause of developmental arrest? To determine if larvae on nutrient-restricted diets are able to pupate, and how *BR* transcript abundance correlates with available nutrients, larvae were fed different diets according to the following design:

FIGURE 3.20 Experimental design – effect of nutrient restriction on the ability to pupate

Figure 3.20 After molting to the 4th instar, larvae were starved 11 days, then divided into four groups and fed 3 different diets: **2% sucrose** (carbohydrate), **peptone** (amino acids) - 500 µl of a stock solution of 0.1g peptone/ml, in 100ml distilled water, or fed a **normal diet** (fish food and yeast). The fourth cohort was **not fed** (prolonged starvation). At 48 hours after re-feeding, larvae from each group were dissected, then RNA was extracted from midguts, reverse transcribed and used as template for qPCR. Remaining larvae in each group were checked daily for pupation.

To determine how nutrient content and abundance affects pupation, I starved 4th instar larvae for 11 days, then divided them into 4 groups according to the following feeding regimes: peptone only, sucrose only, complete diet, or no food. After 48 hrs (6 hours after the increase in *BR* expression at 42 hours in re-fed larvae), midguts were dissected from each cohort for PCR analysis, and remaining larvae were scored for their ability to pupate (Figure 3.21).

The effects of nutrient restriction after starvation on larval development and gene expression (2 independent biological experiments gave similar results)

Four days after being re-fed, the cohort re-fed a normal diet had all pupated. About 70% of the larvae that were fed peptone also pupated by then, and all fed peptone had pupated by 8 days after being re-fed peptone. Unexpectedly, three weeks after being re-fed, the larvae fed only 2%

sucrose began to pupate, and all larvae in this cohort had pupated 25 days after re-feeding. Starved larvae never pupated and died as larvae by the 45th day, if not before (Figure 3.21). In this experiment there was no control for the possibility that microorganisms might grow in the water of the larvae fed only 2% sucrose, to provide a nutrient source that would sustain them. But after a long time, the larvae in 2% sucrose did pupate, while those that were unfed never did. One cannot conclude that metabolism of sugar enabled pupation, but this result reaffirms that the time to pupation is dependent on the nutrient resources [172], and that larvae with fewer available nutrients take longer to pupate.

FIGURE 3.21 Ability to pupate when fed different diets

A **B**

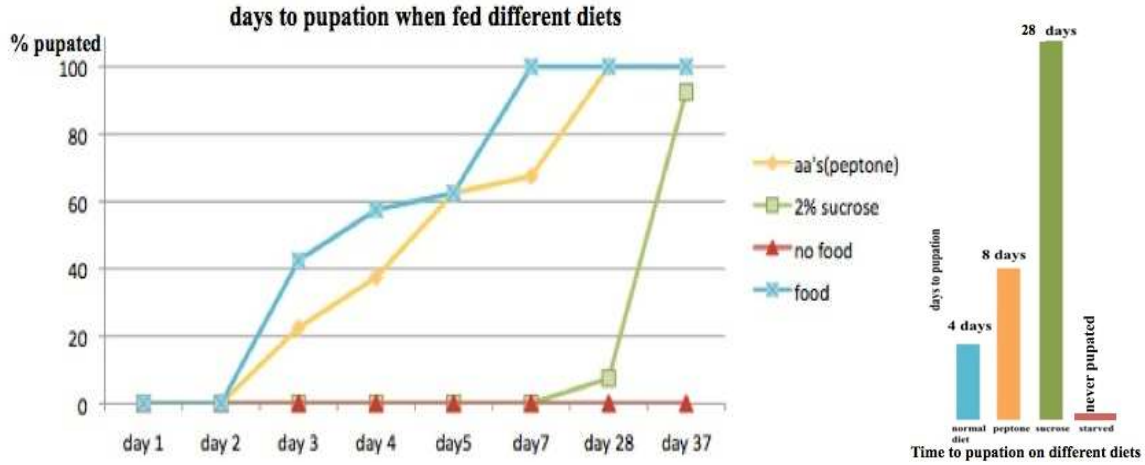

Figure 3.21 A. Time to pupation after re-feeding (days) when fed **normal diet (blue),** fed **peptone only (orange**), or fed **2% sucrose (green**). **Starved** larvae never pupated (**red, black) B.** Bar graph shows relative duration of time before pupation when fed different diets

BR expression in the midguts of larvae re-fed with various diets

*BR*Z3 and Z4 expression increased 48 hours after re-feeding in the midguts of larvae that were re-fed a normal diet. *BR* expression was also up-regulated in midguts of larvae that were re-fed only peptone. These results were reproducible.

FIGURE 3.22 *BR* expression in midgut at 48 hrs in larvae re-fed various diets

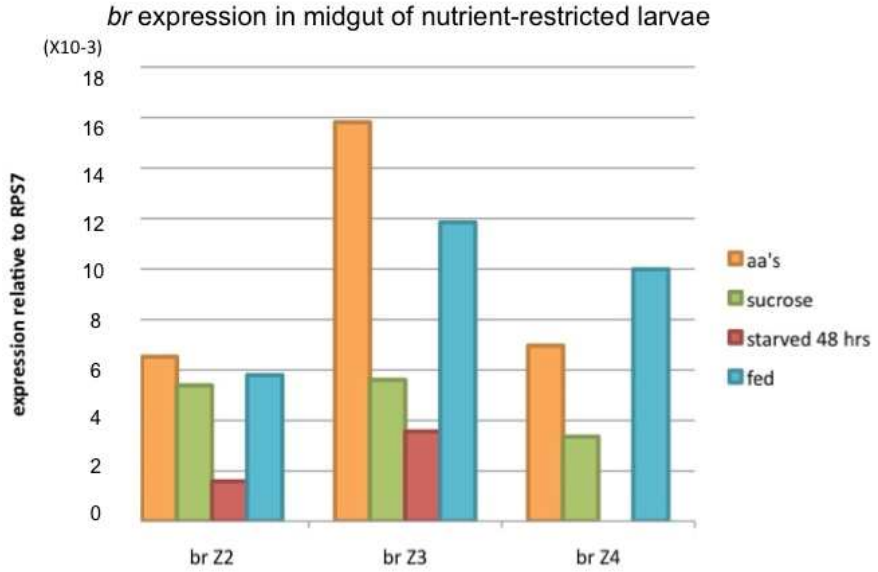

Figure 3.22 After re-feeding, *BR*Z3 and Z4 transcripts **increased** in larvae re-fed a **normal diet (blue**) and also in larvae fed **peptone only (orange**). Z2 transcript levels had not increased at 48 hr sample time. In larvae fed **sucrose only (green**) *BR* transcripts remained low (**starved, red**).

Larvae that were fed a normal diet subsequently pupated. Unexpectedly, larvae fed only peptone also pupated (Figure 3.21). *BR* expression in midguts of larvae fed sucrose was lower than in the larvae fed normal food or peptone. Thus, *BR* expression varied in larvae when they were fed different diets.

miRNA expression in midguts of larvae re-fed nutrient restricted diets

Expression of *miR-14* in larvae re-fed on various nutrient-restricted diets

miR-14 transcripts strongly increased in starved larvae (Figure 3.23). *miR-14* expression was also high in the 2% sucrose-fed larvae, but low in the peptone-fed larvae, and lowest in the larvae fed a normal diet. Thus, *miR-14* expression was inversely nutrient-dependent: the greater the nutrient restriction, the higher the expression of *miR-14* in the midgut. This result was reproducible. *BR* had the opposite expression pattern: *BR* was highest in the larval midguts re-fed a normal diet, and lowest in starved larvae.

FIGURE 3.23 *miR-14* expression at 48 hrs in larvae re-fed a nutrient-restricted diet

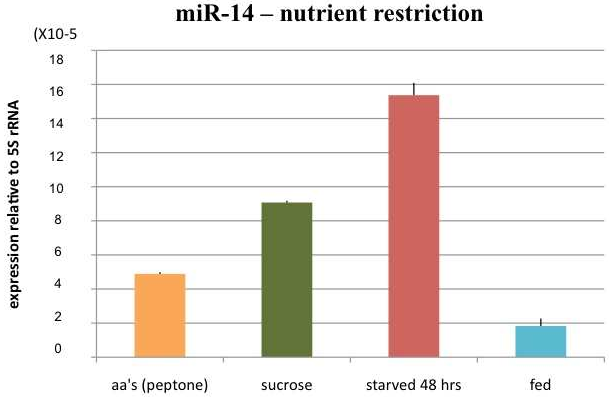

Figure 3.23 *miR-14* expression in midguts of larvae fed nutrient-restricted diets

Expression of *miR-317, miR-277,* and *miR-34* in larvae re-fed nutrient-restricted diets

Like *miR-14, miR-34* was clearly up-regulated during starvation. *miR-34* expression differed from *miR-317* and *miR-277* levels, which did not specifically increase in the starved larvae.

FIGURE 3.24 *miR-317, miR-277,* and *miR-34* expression in larvae re-fed a nutrient-restricted diet

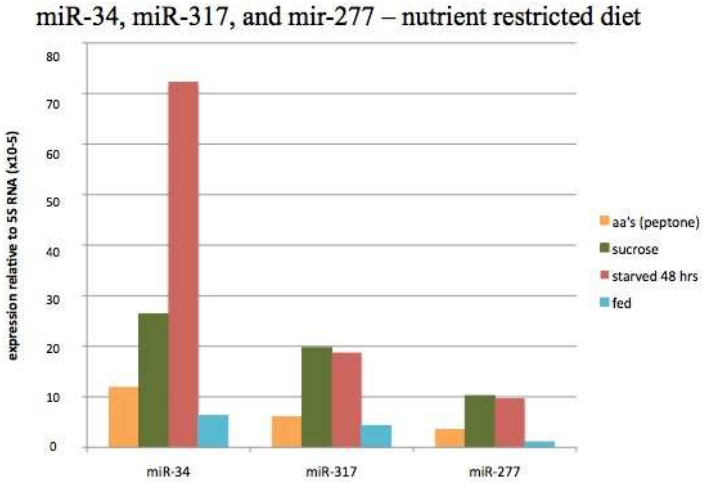

Figure 3.24 *miR-34, miR-277,* and *miR-317* expression in larval midguts when re-fed restricted nutrients after 11 days of starvation *miR-317* and *miR-277* were higher in starving larvae and in larvae fed **2% sucrose (green**). *miR-317* and *miR-277* decreased in larvae re-fed **peptone (orange**), and re-fed a **normal diet (blue)** *miR-34* was also higher when re-fed sucrose than when re-fed peptone or a normal diet, but much more than *miR-317 and miR-277*, **miR-34 was sharply elevated in the midguts of starved larvae.**

A biological replicate experiment gave similar results to the first: as in the initial experiment, *miR-317, miR-277, miR-34*, and *miR-14* expression levels were higher in the starved and sucrose-only larvae, and the levels of *miR-34* and *miR-14* were specifically elevated in starved larvae.

The expression of *BR*Z3 followed the opposite pattern: highest in the larvae re-fed a normal diet and in the larvae re-fed peptone, lower in the larvae re-fed sucrose, and lowest in the midguts of starved larvae.

3. DISCUSSION: Effect of nutrient restriction on larval development and gene expression

Peptone (protein hydrolyzed to amino acids) provided sufficient nutrients to allow larvae to pupate, although larvae re-fed peptone took longer to pupate than those re-fed a normal diet. More surprisingly, after 3 weeks, the larvae in 2% sucrose pupated. Starved larvae never pupated.

In larvae re-fed a normal diet after starvation, *br* expression increased. These larvae subsequently pupated. *BR* was also elevated in larvae fed peptone, and increased *BR* expression was followed by pupation of this cohort several days later. These results suggested that up-regulation of *BR* may correlate with subsequent pupation, and demonstrated a connection between *BR* expression and nutrient status, since larvae fed sucrose had lower *BR* levels and long-delayed pupation, while starved larvae had the lowest *BR* transcript levels, and never pupated. *BR* expression seems to be nutrient-status-dependent in *Ae. aegypti*. These results are consistent with the proposed role for *BR* as a molecular marker of commitment to pupate.

The *miR-34* and *miR-14* expression pattern was the inverse of *br* expression

In contrast to the *BR* expression pattern, *miR-34* and *miR-14* transcript levels were highest in starved larvae, and elevated in sucrose-fed larvae, but lower in larvae fed peptone, and lowest in larvae re-fed a normal diet. Coincident up-regulation of *miR-34* and *miR-14* during nutrient depletion in these experiments further supported the hypothesis that they both function in the midgut to promote survival or developmental arrest during starvation and nutrient insufficiency.

HYPOTHESIS: *miR-14 and miR-34* might mobilize lipids during starvation

Control of lipid metabolism is a central issue in development and plays an important role in hormone biosynthesis [173] and in the response to starvation [174]. During starvation-induced autophagy, cellular stores of triglycerides in the form of lipid droplets are modified by lipases to release fatty acids [175]. These fatty acids undergo ß-oxidation in the mitochondria to produce ATP [176]. This results in the mobilization of stored fat for energy.

A better understanding of the regulation of this process may be valuable in *Ae. aegypti*, because the Dengue virus induces autophagy in order to change cellular lipid metabolism to release free fatty acids and generate ATP, and this process is required for efficient Dengue virus replication in cell culture [176].

miR-14 expression was up-regulated in the midgut during starvation. *miR-14* may be important in the regulation of lipid metabolism in the *Ae. aegypti* midgut, because in *D. melanogaster*, a *miR-14* deletion greatly increases levels of triacylglycerides (TAG) and diaclyglycerides (DAG) [75] . Additionally, *Aae-miR-34* was sharply up-regulated in the midgut of starved larvae. Human *miR-34 (miR-34A)* is associated with elevated free fatty acids and impaired nutrient-induced secretion of insulin from pancreatic ß cells [177]. *miR-34A* targets SIRT1, a regulator of lipid and glucose metabolism [178]. Thus, *miR-14* and *miR-34* may both act to mobilize fatty acids in the midgut during starvation. The functions of *miR-14* and *miR-34* in the midgut aren't known, but further investigation of their roles may have relevance for the control of Dengue viral replication.

4. RESULTS: Response of starved 4th instar larvae to treatment with ecdysone analog RH2485

When larvae were re-fed after starvation, midgut metamorphosis was re-initated. A response to nutrient availability might have stimulated translation of ecdysone biosynthetic enzymes to produce ecdysone, then ecdysone might have signalled for committment to pupation. To see if the ecdysone analog RH2485, alone, could bypass the need for nutrients to elicit pupation, larvae were starved for two weeks. Half of the starved larvae were then treated with the ecdysone analog RH2485 to a final concentration of ~135nM, and the other starved larvae were left untreated. Samples were taken from the two groups at 48 hours after treatment in order to determine the effect of RH2485 on transcript expression levels and larval development.

Survival and phenotype at pupation of starving larvae that were treated with RH2485

Most larvae treated with RH2485 died within 5 days, with pre-pupal characteristics. In contrast, untreated starved larvae died gradually over time as growth-arrested, undeveloped larvae.

FIGURE 3.25 Survival of larvae treated with RH2485 or left untreated

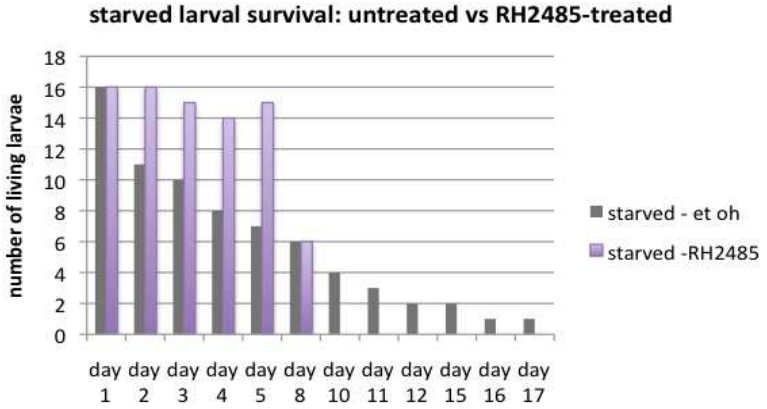

Figure 3.25 17-day-starved larvae were treated with RH2485 or left untreated. Treated larvae all died within 6 days of treatment, while the number of living, untreated larvae decreased gradually over time.

When starved larvae were treated with RH2485 alone, they underwent pre-pupal development, including growth of imaginal discs and pigmented respiratory trumpets, precocious cuticular

pigmentation and advanced eye development. Bodies of treated larvae appeared contracted (Figure 3.26B). These developmental changes occurred in the absence of food and resulted from treatment with the ecdysone analog alone.

FIGURE 3.26 Phenotype of starved larvae treated with methoxyfenozide (RH2385)

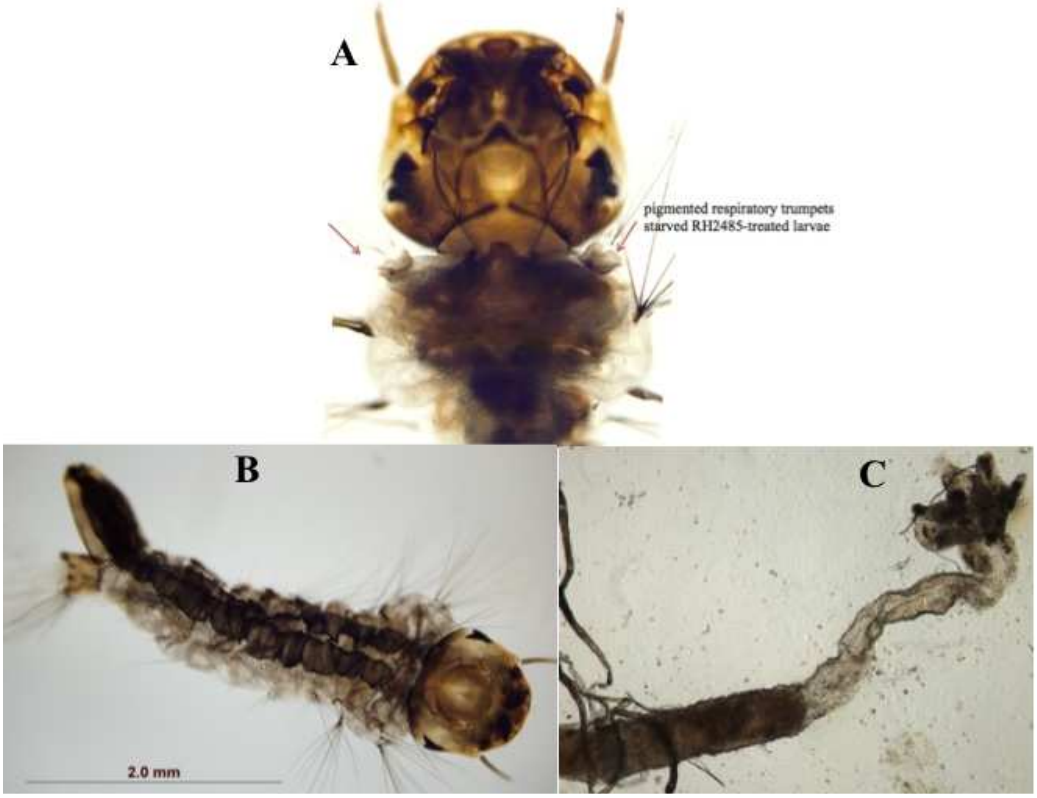

Figure 3.26 A. Pigmented respiratory trumpets in RH2485-treated starved larvae **B.** Contracted body phenotype of starved larvae given RH2485 **C.** Midgut of RH2485-treated starved larva. Epithelial cells detached from anterior midgut, and posterior midgut appeared to be filled, perhaps, with the detached epithelial cells.

***BR* and RNA-binding factor expression in midgut of starved larvae treated with RH2485**

Unexpectedly, at 48 hours after treatment *BR* transcripts were low in the midguts of larvae treated with ecdysone analog RH2485, while the expression of *BRAT, hnRNPK* and *LIN-28* was elevated (Figure 3.27).

FIGURE 3.27 *BR* and RNA binding factor expression in starved, RH2485-treated larvae

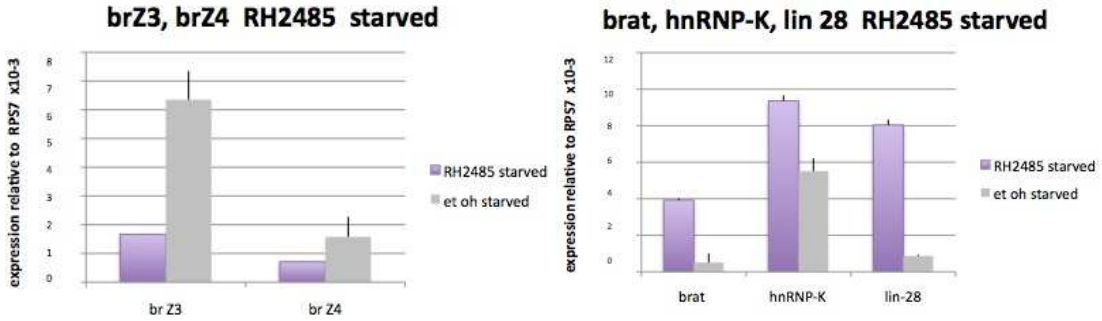

Figure 3.27 A. At 48 hours *BRZ*3 and Z4 levels were lower in starved, RH2485-treated larvae, but levels of ***BRAT, hnRNP-K*** and ***LIN-28*** increased in midguts of treated larvae. **Control**-starved larvae-**gray** starved larvae treated with **RH2485-purple**

miRNA expression in the midgut of starved larvae treated with methoxyfenozide (RH2485)

miR-34 and *miR-317* expression levels were not greatly affected by treatment with RH2485, and neither was the expression of *miR-14*, *miR-7*, or *miR-190*. In contrast, expression of *let-7* and *miR-125* clearly increased in the starved larvae treated with RH2485 (Figure 3.28B).

FIGURE 3.28 miRNA expression in the midgut of starved larvae treated with RH2485

A **B** **C**

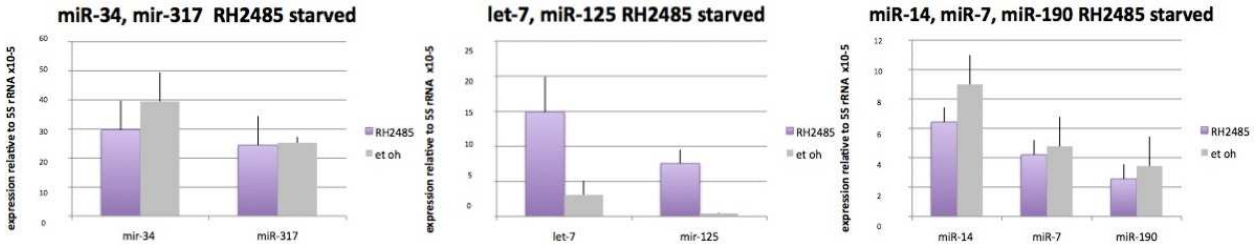

A. *miR-34* and *miR-317* **B. *let-7* and *miR-125*** **C. *miR-14, miR-7,* and *miR-190***

Figure 3.29 (A) *miR-34* and *miR-317* and **(C) *miR-14, miR-7,* and *miR-190* expression levels were not greatly affected** by treatment with RH2485.
B. In contrast, ***let-7* and *miR-125* levels were elevated** in starved larvae at 48 hours after treatment with RH2485. untreated **control-gray** **RH2485-purple**

4. DISCUSSION: Effect of RH2485 on starved larval development and gene expression

Starved larvae, at 48 hours after treatment with RH2485, had elevated midgut expression levels of *BRAT*, *let-7*, and *miR-125* transcripts. In contrast, *BR* expression was low in RH2485-treated starved larvae. In normally-fed larvae, *BR* transcript expression peaked around 48 hours in the 4th instar larval midgut, then declined sharply before pupation (Figure 1.21). Additionally, *BRAT*

levels increased at pupation, and *let-7* and *miR-125* increased after pupation in the midguts of normally fed larvae. Up-regulation of *BRAT*, *miR-125* and *let-7* all followed a decrease in *BR* expression. Perhaps *BR* expression was low in RH2485-treated larvae because *BR* peaked earlier, *before* the 48-hour sample time.

Though starving, RH2485-treated larvae might have made a molecular commitment to pupate, because at 48 hours after treatment, the midguts had characteristic pre-pupal transcript-expression patterns. The developmental phenotype of the treated larvae supported this hypothesis: though starved for more than 2 weeks, treated larvae showed the definitive marks of pre-pupal development: pigmented respiratory trumpets, and well-developed imaginal discs. RH2485 treatment may have caused unfed larvae to undergo a heterochronic shift that accelerated development even without the support of nutrients (Figure 3.29). Clearly, in these long-starved larvae, commitment to pupate wasn't dependent on the attainment of a critical weight, but was initiated solely by the ecdysone analog signal, and pre-pupal development progressed in the absence of nutrients.

FIGURE 3.29 Hypothetical model of RH2485-mediated acceleration of development

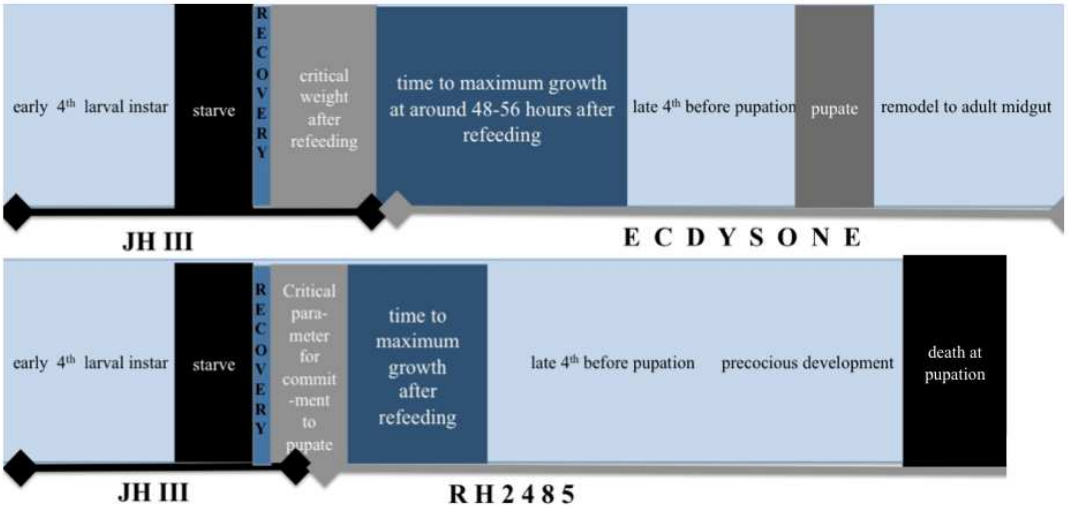

Top: Developmental progression of starved then re-fed larvae **Bottom:** RH2485 shortens the time of critical commitment to pupate and accelerates pre-pupal development

CONCLUSION: These starvation and nutrient-restriction expression studies offer insight into coordinated molecular responses that occur during midgut development. While these experiments don't reveal the function of *BR* or *miR-14* and *miR-34*, they do link their transcript abundance to key phases of growth and survival and demonstrate that, consistently and in a context-dependent manner, these factors respond to nutrient and hormonal signals which direct the timing of development.

HYPOTHESIS: JH controls the timing of pupation through miRNA expression and *BR*

While few factors have been shown to be directly regulated by JH [5], *BR* and a subset of the miRNAs in this study may be amongst those that are. JH-mediated targeting of *BR* mRNA by *miR-34, mir-317* and/or *mir-14* during starvation and in the early 4th instar larvae would present a novel mechanism for JH regulation of developmental timing though *BR.*

After eclosing, it takes a few days for the adult female mosquito to mature before becoming competent to take a blood meal. During that time, JH initiates the transcription of *EARLY TRYPSIN*. *EARLY TRYPSIN* mRNA accumulates in midgut epithelial cells until the blood meal, when it is rapidly translated to digest the blood [179]. Thus there is a stockpile of *EARLY TRYPSIN* mRNA ready for the blood meal, when it is needed and translated.

To explain *BR* transcript levels in the midgut during starvation, when *BRZ*3 transcript levels didn't decrease while other ecdysone-regulated transcripts did, I propose an analogous situation: if *BR* is required for the commitment to pupate, it may be critical to maintain a pool of *BR* mRNA transcripts in order be able to quickly respond if nutrients become available, as it might take too long or require unavaliable resources to transcribe new *BR* mRNA. *BR* transcripts might be sequestered in the starving larva, perhaps by miRNA and miRISC components, until nutrient

or ecdysone signals end the starvation-induced hold on developmental growth. Then translation of BR could release the larva from the developmental quiescence imposed by starvation, and commit the larva to pupate, by BR transcription-factor-induced regulatory changes of the molecular developmental program. In the absence of ecdysone signaling, developmental quiescence during starvation might be a JH-mediated, *status quo* state. If there is a gatekeeper, then *BR* may be that gatekeeper, and act to integrate the opposing but interconnected forces of JH (*status quo*) and ecdysone (change).

MATERIALS AND METHODS

Reference genes used for standardization during starvation

During starvation, the expression levels of the reference genes changed slightly.

For example, here actin c(T) values [**c**ycle **T**hreshold value - the number of PCR cycles required for fluorescence to exceed background levels and begin exponential amplification] increased slightly in the starved samples [the higher the c(T) value, the lower the copy number present in the sample]:

FIGURE 3.30 c(T) values of reference genes under starved and fed conditions

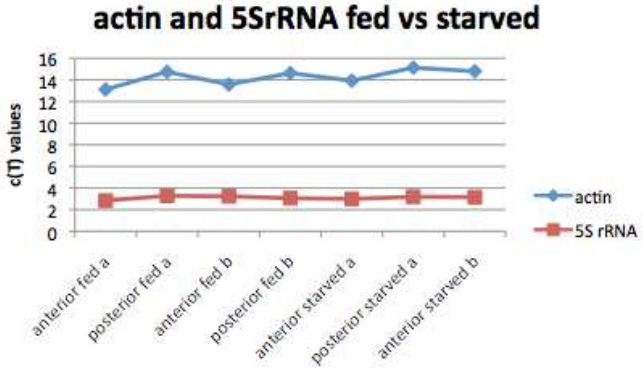

While 5S rRNA stayed fairly constant, the actin c(T) values for the starved samples were slightly higher, suggesting that actin was less abundant in starved larvae, (and also less abundant in the posterior midgut than in the anterior). Maybe 5S rRNA c(T) values were more stable because it is more abundant: due to statistical distribution there is more c(T) value variation during amplification of less abundant transcripts, therefore there is less precision in the c(T) values of less abundant RNAs, and so, less ability to detect low-fold changes [180].

5S rRNA is a component of the large ribosomal subunit, and frequently used as a reference gene for miRNA qPCR, as it is very small, only 119 nt long. It is ubiquitous and was abundantly expressed in these assays. The forward primer starts at the first nucleotide.

Reverse transcription

In the reverse transcription reaction, 1µg of RNA was used for each sample to ensure that samples were uniform. But during starvation, the amount of total RNA production probably decreased, so equivalent concentrations of RNA used in the reverse transcription reaction don't represent equal numbers of midguts, or equal numbers of larvae sampled. Here, 20 midguts were used for each sample:

FIGURE 3.31 Total amount of RNA recovered from starved vs fed larval midguts

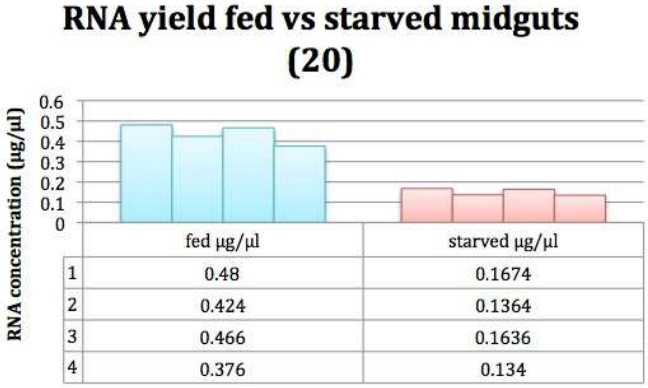

	fed µg/µl	starved µg/µl
1	0.48	0.1674
2	0.424	0.1364
3	0.466	0.1636
4	0.376	0.134

This chart shows the RNA yield from 20 larval midguts from fed (blue) or starved (pink) larvae. Starvation affected the expression of actin slightly more than ribosomal protein S7 (RPS7) (not shown) so I switched to RPS7 as the reference gene for the more recent RH2485 and restricted nutrient analyses.

Analysis of standard error for wing sizes and technical PCR replicates: Standard error = standard deviation of samples/√number of samples

Discrepancies between reported gene expression levels: sources of experimental variation

Some of the analyses of gene expression in mosquito midguts presented in Chapters One, Two, and Three showed variable results. Inter-assay variability was larger than it ought to have been. Experiments should have been planned more carefully initially, to consider what kind of

statistical analysis would be needed to support the validity of any conclusions to be drawn from the results.

There is inherent biological variability in a developing system, and many factors might affect analysis of gene expression in the midgut over developmental time in a developing mosquito population. Three reasons for variability in experimental results:

1. The principal variable might be differences in the ratio of males to females in a sample, and also differences in the photoperiod (time of dissection, day or night), the ambient temperature (controlled for at 25ºC but maybe varied due to weather) and season that the analysis was done. These factors all may affect gene expression in the developing mosquito midgut.

2. Another variable might be the number and composition of the midgut tissues sampled. The midgut is a diverse composite of many kinds of cells and tissues: the gastric cecae, the proventriculus, the malphigian tubules, the hindgut, entroendocrine cells, enterocytes, neuronal axons, tracheal branches, and the visceral muscles. Midguts are very small, and even with careful dissection there may not always be identical populations of cell types and tissues in each sample.

3. Finally, there is variability in preparation and the processing of total RNA samples, especially in the reverse transcription of RNA into cDNA.

Dietary constituents of normal diet included: **Brewers yeast flakes** (supplies all amino acids plus trace minerals including calcium, chromium, iron, magnesium, manganese, molybdenum, nickel, potassium, selenium, silicon, sodium, and zinc, also various vitamins and carbohydrates and **Tetramin fishfood** (> 40 ingredients).

REFERENCES

1. Jindra M., S.R. Palli, and L.M. Riddiford, *The juvenile hormone signaling pathway in insect development.* Annu Rev Entomol, 2013. **58**: p. 181-204.
2. Erezyilmaz D., et al., *The role of the pupal determinant broad during embryonic development of a direct-developing insect.* Dev Genes Evol, 2009. **219**(11-12): p. 535-44.
3. Ashburner M, et al., *Temporal control of puffing activity in polytene chromosomes.* Cold Spring Harb Symp Quant Biol, 1974: p. 655–662.
4. Baehrecke, E.H., *Ecdysone Signaling Cascade and Regulation of Drosophila Metamorphosis.* Archives of Insect Biochemistry and Physiology, 1996. **33**(3-4): p. 231-244.
5. Beckstead R., Lam G., and C.S. Thummel, *Specific transcriptional responses to juvenile hormone and ecdysone in Drosophila.* Insect Biochem Mol Biol, 2007. **37**(6): p. 570-8.
6. Riddiford, L.M., *Hormone receptors and the regulation of insect metamorphosis.* Receptor, 1993. **3**(3): p. 203-9.
7. Riddiford, L.M., et al., *Insights into the molecular basis of the hormonal control of molting and metamorphosis from Manduca sexta and Drosophila melanogaster.* Insect Biochemistry and Molecular Biology, 2003. **33**(12): p. 1327-1338.
8. Kiss I., et al., *Prepupal larval mosaics in Drosophila melanogaster.* Nature 1976. **262**(5564): p. 136-8.
9. Telang A., et al., *Analysis of molecular markers for metamorphic competency and their response to starvation or feeding in the mosquito, Aedes aegypti (Diptera: Culicidae).* J Insect Physiol., 2010. **56**(12): p. 1925-34.
10. Zhou X . and L.M. Riddiford, *Broad specifies pupal development and mediates the 'status quo' action of juvenile hormone on the pupal-adult transformation in Drosophila and Manduca.* Development, 2002. **129**(9): p. 2259-69.
11. Alonso, C.R., *A complex 'mRNA degradation code' controls gene expression during animal development.* Trends Genet., 2012. **28**(2): p. 78-88.
12. Mazumder, B., V. Seshadri, and P.L. Fox, *Translational control by the 3′-UTR: the ends specify the means.* Trends in Biochemical Sciences, 2003. **28**(2): p. 91-98.
13. Gingras, A., Raught B., and N. Sonenberg, *Regulation of translation initiation by FRAP/mTOR.* Genes Dev., 2001. **15**(7): p. 807-26.
14. Ambros, V., *Control of developmental timing in Caenorhabditis elegans.* Curr Opin Genet Dev, 2000. **10**(4): p. 428-33.
15. Ambros, V., *MicroRNAs and developmental timing.* Curr Opin Genet Dev, 2011. **21**(4): p. 511-7.
16. Bartel, D.P., *MicroRNAs: Genomics, Biogenesis, Mechanism, and Function.* Cell, 2004. **116**(2): p. 281-297.
17. Lee R., R.L. Feinbaum, and V. Ambros, *The C. elegans heterochronic gene lin-4 encodes small RNAs with antisense complementarity to lin-14.* Cell, 1993. **75**(5): p. 843-54.
18. Fabian Mr., S., Nahum, Filipowicz, Witold, *Regulation of mRNA translation and stability by microRNAs.* Annu Rev Biochem, 2010. **79**: p. 351-79.

19. Reinhart, B., et al., *The 21-nucleotide let-7 RNA regulates developmental timing in Caenorhabditis elegans.* Nature 2000. **403**(6772): p. 901-6.
20. Moss, E.G., *Heterochronic genes and the nature of developmental time.* Curr Biol, 2007. **17**(11): p. R425-34.
21. Thummel, C.S., *Molecular Mechanisms of Developmental Timing in C. elegans and Drosophila.* Developmental Cell, 2001. **1**(4): p. 453-465.
22. Bashirullah, A., et al., *Coordinate regulation of small temporal RNAs at the onset of Drosophila metamorphosis.* Developmental Biology, 2003. **259**(1): p. 1-8.
23. Chawla, G. and S.N. S., *Hormonal activation of let-7-C microRNAs via EcR is required for adult Drosophila melanogaster morphology and function.* Development, 2012. **139**(10): p. 1788-97.
24. Sempere, L.F., et al., *The expression of the let-7 small regulatory RNA is controlled by ecdysone during metamorphosis in Drosophila melanogaster.* Developmental Biology, 2002. **244**(1): p. 170-179.
25. Sempere, L.F., et al., *Temporal regulation of microRNA expression in Drosophila melanogaster mediated by hormonal signals and Broad-Complex gene activity.* Developmental Biology, 2003. **259**(1): p. 9-18.
26. Hurban, P. and C.S. Thummel, *Isolation and characterization of fifteen ecdysone-inducible Drosophila genes reveal unexpected complexities in ecdysone regulation.* Mol cell Biol, 1993. **13**(11): p. 7101-11.
27. Riddiford, L.M., *Juvenile hormone: the status of its "status quo" action.* Arch Insect Biochem Physiol, 1996. **32**(3-4): p. 271-86.
28. Johnson, S., S.Y. Lin, and F.J. Slack, *The time of appearance of the C. elegans let-7 microRNA is transcriptionally controlled utilizing a temporal regulatory element in its promoter.* Dev Biol, 2003. **259**(2): p. 364-79.
29. Martinez N. and W.A. J., *The interplay between transcription factors and microRNAs in genome-scale regulatory networks.* Bioessays, 2009. **31**(4): p. 435-45.
30. Andreassi C and A. Riccio, *To localize or not to localize: mRNA fate is in 3'UTR ends.* Trends Cell Biol, 2009. **19**(9): p. 465-74.
31. Moore, M.J., *From birth to death: the complex lives of eukaryotic mRNAs.* Science, 2005. **309**(5740): p. 1514-8.
32. de Moor, C., H. Meijer, and S. Lissenden, *Mechanisms of translational control by the 3' UTR in development and differentiation.* Semin Cell Dev Biol, 2005. **16**(1): p. 49-58.
33. Eulalio A., Huntzinger E., and E. Izaurralde, *GW182 interaction with Argonaute is essential for miRNA-mediated translational repression and mRNA decay.* Nat Struc Mol Biol, 2008. **15**(4): p. 346-53.
34. Bartel, D.P., *MicroRNAs: Target Recognition and Regulatory Functions.* Cell, 2009. **136**(2): p. 215-233.
35. Lim L, et al., *Microarray analysis shows that some microRNAs downregulate large numbers of target mRNAs.* Nature, 2005. **433**(7027): p. 769-73.
36. Hafner, M., M.J. Ascano, and T. Tuschl, *New insights in the mechanism of microRNA-mediated target repression.* Nat Struct Mol Biol, 2011. **18**(11): p. 1181-2.
37. Bonchuk, A., et al., *Drosophila BTB/POZ domains of "ttk group" can form multimers and selectively interact with each other.* J Mol Biol., 2011. **412**(3): p. 423-36.

38. Nolte R., et al., *Differing roles for zinc fingers in DNA recognition: structure of a six-finger transcription factor IIIA complex.* Proc Natl Acad Sci USA, 1998. **95**(6): p. 2938-43.
39. Zuker, M., *Mfold web server for nucleic acid folding and hybridization prediction.* Nucleic Acids Res., 2003. **31**(13): p. 3406-15.
40. Li, X., et al., *Predicting in vivo binding sites of RNA-binding proteins using mRNA secondary structure.* RNA, 2010. **16**(6): p. 1096-107.
41. Long, D., et al., *Potent effect of target structure on microRNA function.* Nat Struct Mol Biol, 2007. **14**(4): p. 287-94.
42. Rusinov, V., et al., *MicroInspector: a web tool for detection of miRNA binding sites in an RNA sequence.* Nucleic Acids Res., 2005. **1**(33): p. 696-700.
43. Grimson, A., et al., *MicroRNA targeting specificity in mammals: determinants beyond seed pairing.* Mol Cell Biol, 2007. **27**(1): p. 91-105.
44. Kruger J. and M. Rehmsmeier, *RNAhybrid: microRNA target prediction easy, fast and flexible.* Nucleic Acids Res., 2006. **34**(web server issue): p. 451-4.
45. Rusinov, V., et al., *MicroInspector: a web tool for detection of miRNA binding sites in an RNA sequence.* Nucleic Acids Res., 2005. **33**: p. 696-700.
46. Kertesz, M., et al., *The role of site accessibility in microRNA target recognition.* Nat Genet., 2007. **39**(10): p. 1278-84.
47. Lewis, B., C. Burge, and D.P. Bartel, *Conserved seed pairing, often flanked by adenosines, indicates that thousands of human genes are microRNA targets.* Cell, 2005. **120**(1): p. 15-20.
48. Long, D., C. Chan, and Y. Ding, *Analysis of microRNA-target interactions by a target structure based hybridization model.* Pac Symp Biocomput., 2008.
49. Kozomara, A. and S. Griffiths-Jones, *miRBase: integrating microRNA annotation and deep-sequencing data.* Nucleic Acids Res., 2010. **39**(Database issue): p. 152-7.
50. Audsley, N. and R.J. Weaver, *Neuropeptides associated with the regulation of feeding in insects.* Gen Comp Endocrinol 2009. **162**(1): p. 93-104.
51. Christophers, S.R., *Aedes aegypti (L.) The Yellow Fever Mosquito - life history, bionomics and structure*. 1960, New York: Cambridge University Press. 739.
52. Hartenstein, V., *Development of the insect stomatogastric nervous system.* Trends in Neurosciences, 1997. **20**(9): p. 421-427.
53. Hecker, H. and W. Rudin, *Morphometric parameters of the midgut cells of Aedes aegypti L. (Insecta, Diptera) under various conditions.* Cell Tissue Res., 1981. **219**(3): p. 619-27.
54. Ohlstein, B. and A. Spradling, *Multipotent Drosophila intestinal stem cells specify daughter cell fates by differential notch signaling.* Science, 2007. **315**(5814): p. 988-92.
55. Micchelli, C.A., et al., *Identification of adult midgut precursors in Drosophila.* Gene Expr Patterns, 2011. **11**(1-2): p. 12-21.
56. Micchelli, C. and N. Perrimon, *Evidence that stem cells reside in the adult Drosophila midgut epithelium.* Nature 2006. **439**(7075): p. 475-9.
57. Ohlstein, B. and A. Spradling, *The adult Drosophila posterior midgut is maintained by pluripotent stem cells.* Nature, 2006. **439**(7075): p. 470-4.
58. Mathur D, B.A., Driver I, Ohlstein, B., *A transient niche regulates the specification of Drosophila intestinal stem cells.* Science, 2010. **327**(5962): p. 210-3.

59. Jiang, H. and B.A. Edgar, *EGFR signaling regulates the proliferation of Drosophila adult midgut progenitors.* Development, 2009. **136**(3): p. 483-93.
60. Zeng X. and S.X. Hou, *Broad relays hormone signals to regulate stem cell differentiation in Drosophila midgut during metamorphosis.* Development, 2012. **139**(21): p. 3917-25.
61. Moffett, S. and D.F. Moffett, *Comparison of immunoreactivity to serotonin, FMRFamide and SCPb in the gut and visceral nervous system of larvae, pupae and adults of the yellow fever mosquito Aedes aegypti.* J Insect Sci, 2005. **5**(20).
62. Ray, K., et al., *Growth and differentiation of the larval mosquito midgut.* J Insect Sci, 2009. **9**: p. 1-13.
63. Wu, Y., et al., *Mechanisms of midgut remodeling: juvenile hormone analog methoprene blocks midgut metamorphosis by modulating ecdysone action.* Mech Dev, 2006. **123**(7): p. 530-47.
64. Gusmao D., et al., *First isolation of microorganisms from the gut diverticulum of Aedes aegypti (Diptera: Culicidae): new perspectives for an insect-bacteria association.* Mem inst Oswaldo Cruz, 2007. **102**(8): p. 919-24.
65. Clifton M. and F.G. Noriega, *Nutrient limitation results in juvenile hormone-mediated resorption of previtellogenic ovarian follicles in mosquitoes.* J Insect Physiol., 2011. **57**(9): p. 1274-81.
66. Zhu, J., L. Chen, and A.S. Raikhel, *Posttranscriptional control of the competence factor betaFTZ-F1 by juvenile hormone in the mosquito Aedes aegypti.* Proc Natl Acad Sci U S A, 2003. **100**(23): p. 13338-43.
67. Noriega, F.G., *Nutritional regulation of JH synthesis: a mechanism to control reproductive maturation in mosquitoes?* Insect Biochem Mol Biol., 2004. **34**(7): p. 687-93.
68. DiBello P., et al., *The Drosophila Broad-Complex encodes a family of related proteins containing zinc fingers.* Genetics, 1991. **129**(2): p. 385-97.
69. Margam V., Gelman D., and S.R. Palli, *Ecdysteroid titers and developmental expression of ecdysteroid-regulated genes during metamorphosis of the yellow fever mosquito, Aedes aegypti (Diptera: Culicidae).* J Insect Physiol, 2006. **52**(6): p. 558-68.
70. Takane, K., et al., *Computational prediction and experimental validation of evolutionarily conserved microRNA target genes in bilaterian animals.* BMC Genomics, 2010. **11**(101).
71. Sperling E., et al., *MicroRNAs resolve an apparent conflict between annelid systematics and their fossil record.* Proc Biol Sci., 2009. **276**(1677): p. 4315-22.
72. Qian, J., et al., *MicroRNA-277 modulates the neurodegeneration caused by Fragile X premutation rCGG.* Genomics, 2011. **97**(5): p. 294-303.
73. Pasquinelli, A.E., et al., *Conservation of the sequence and temporal expression of let-7 heterochronic regulatory RNA.* Nature, 2000. **408**(6808): p. 86-89.
74. Varghese, J. and S.M. Cohen, *microRNA miR-14 acts to modulate a positive autoregulatory loop controlling steroid hormone signaling in Drosophila.* Genes and Development, 2007. **21**(18): p. 2277-2282.
75. Xu, P., et al., *The Drosophila microRNA Mir-14 suppresses cell death and is required for normal fat metabolism.* Curr Biol, 2003. **13**(9): p. 790-5.
76. Aboobaker, A., et al., *Drosophila microRNAs exhibit diverse spatial expression patterns during embryonic development.* Proc Natl Acad Sci USA 2005. **102**(50): p. 18012-22.

77. Chang, C., et al., *The heterogeneous nuclear ribonucleoprotein K (hnRNP K) interacts with dengue virus core protein.* DNA Cell Biol, 2001. **20**(9): p. 569-77.
78. Schmidt, T., et al., *The heterogeneous nuclear ribonucleoprotein K is important for Herpes simplex virus-1 propagation.* DNA Cell Biol, 2010. **20**(9): p. 569-77.
79. Li, X., et al., *A microRNA imparts robustness against environmental fluctuation during development.* Cell, 2009. **137**(2): p. 273-82.
80. Neumuller, R., et al., *Mei-P26 regulates microRNAs and cell growth in the Drosophila ovarian stem cell lineage.* Nature, 2008. **454**(7201): p. 241-5.
81. Hafner, M., et al., *Transcriptome-wide identification of RNA-binding protein and microRNA target sites by PAR-CLIP.* Cell, 2010. **141**(1): p. 129-41.
82. Temme, C., et al., *Subunits of the Drosophila CCR4-NOT complex and their roles in mRNA deadenylation.* RNA, 2010. **16**(7): p. 1356-70.
83. Moss, E., R. Lee, and V. Ambros, *The cold shock domain protein LIN-28 controls developmental timing in C. elegans and is regulated by the lin-4 RNA.* Cell, 1997. **88**(5): p. 637-46.
84. Moss E. and L. Tang, *Conservation of the heterochronic regulator Lin-28, its developmental expression and microRNA complementary sites.* Cell, 2003. **88**(5): p. 637-46.
85. Viswanathan, S., G. Daley, and R.I. Gregory, *Selective blockade of microRNA processing by Lin28.* Science, 2008. **320**(5872): p. 97-100.
86. Melton, C., R. Judson, and R. Blelloch, *Opposing microRNA families regulate self-renewal in mouse embryonic stem cells.* Nature, 2010. **463**(7281): p. 621-6.
87. Vadla, B., et al., *lin-28 controls the succession of cell fate choices via two distinct activities.* PLoS Genet., 2012. **8**(3).
88. Huang, Y., et al., *The microRNA miR-7 regulates Tramtrack69 in a developmental switch in Drosophila follicle cells.* Development, 2013. **140**(4): p. 897-905.
89. Li, X. and R.W. Carthew, *A microRNA mediates EGF receptor signaling and promotes photoreceptor differentiation in the Drosophila eye.* Cell, 2005. **123**(7): p. 1267-77.
90. Webster R., et al., *Regulation of epidermal growth factor receptor signaling in human cancer cells by microRNA-7.* J Biol Chem, 2009. **284**(9): p. 5731-41.
91. Jiang, H., et al., *EGFR/Ras/MAPK signaling mediates adult midgut epithelial homeostasis and regeneration in Drosophila.* Cell Stem Cell, 2011. **8**(1): p. 84-95.
92. Jin, P., R. Alisch, and S.T. Warren, *RNA and microRNAs in fragile X mental retardation.* Nat Cell Biol, 2004. **6**(11): p. 1048-53.
93. Gates, J. and C.S. Thummel, *An enhancer trap screen for ecdysone-inducible genes required for Drosophila adult leg morphogenesis.* Genetics, 2000. **156**(4): p. 1765-76.
94. Charroux, B., et al., *The levels of the bancal product, a Drosophila homologue of vertebrate hnRNP K protein, affect cell proliferation and apoptosis in imaginal disc cells.* Mol Cell Biol, 1999. **19**(11): p. 7846-56.
95. Krecic, A. and M.S. Swanson, *hnRNP complexes: composition, structure, and function.* Curr Opin Cell Biol, 1999. **11**(3): p. 363-71.
96. Bourai, M., et al., *Mapping of Chikungunya virus interactions with host proteins identified nsP2 as a highly connected viral component.* J Virol, 2012. **86**(6): p. 3121-34.

97. Hayes, G. and G. Ruvkun, *Misexpression of the Caenorhabditis elegans miRNA let-7 is sufficient to drive developmental programs.* Cold Spring Harb Symp Quant Biol, 2006. **71**: p. 21-7.
98. Harris, R., et al., *Brat promotes stem cell differentiation via control of a bistable switch that restricts BMP signaling.* Dev Cell, 2011. **20**(1): p. 72-83.
99. Schwamborn, J., E. Berezikov, and J.A. Knoblich, *The TRIM-NHL protein TRIM32 activates microRNAs and prevents self-renewal in mouse neural progenitors.* Cell, 2009. **136**(5): p. 913-25.
100. Marco A., et al., *Functional shifts in insect microRNA evolution.* BGenome Biol Evol, 2010. **2**: p. 686-96.
101. Kheradpour, P., et al., *Reliable prediction of regulator targets using 12 Drosophila genomes.* Genome Res, 2007. **12**: p. 1919-31.
102. Esslinger Sm, et al., *Drosophila miR-277 controls branched-chain amino acid catabolism and affects lifespan.* RNA biol, 2013. **10**(6).
103. Esslinger, S., et al., *Drosophila miR-277 controls branched-chain amino acid catabolism and affects lifespan.* RNA Biol, 2013. **10**(6).
104. Konopova, B., V. Smykal, and M. Jindra, *Common and distinct roles of juvenile hormone signaling genes in metamorphosis of holometabolous and hemimetabolous insects.* PLoS One, 2011. **6**(12).
105. Li Y., et al., *Activity of the corpora allata of adult female Aedes aegypti: effects of mating and feeding.* insect Biochm Mol Biol., 2003. **33**(12): p. 1307-15.
106. Shapiro J. and H.H. Hagedorn, *Juvenile hormone and the development of ovarian responsiveness to a brain hormone in the mosquito, Aedes aegypti.* Gen comp Endocrinol., 1982. **46**(2): p. 176-83.
107. Telang A., et al., *Effects of larval nutrition on the endocrinology of mosquito egg development.* J Exp Biol., 2006. **209**(Pt. 4): p. 645-55.
108. Bai, H., P. Ramaseshadri, and S.R. Palli, *Identification and characterization of juvenile hormone esterase gene from the yellow fever mosquito, Aedes aegypti.* Insect Biochem Mol Biol, 2007. **37**(8): p. 829-37.
109. Nishiura, J.T., Ho P., and K. Ray, *Methoprene interferes with mosquito midgut remodeling during metamorphosis.* J Med Entomol., 2003. **40**(4): p. 498-507.
110. Miura, K., et al., *Characterization of the Drosophila Methoprene -tolerant gene product. Juvenile hormone binding and ligand-dependent gene regulation.* FEBS J., 2005. **272**(5): p. 1169-78.
111. Wozniak, M., et al., *Alternative farnesoid structures induce different conformational outcomes upon the Drosophila ortholog of the retinoid X receptor, ultraspiracle.* Insect biochem Mol Biol., 2004. **34**(11): p. 1147-62.
112. Ashok, M., C. Turner, and T.G. Wilson, *Insect juvenile hormone resistance gene homology with the bHLH-PAS family of transcriptional regulators.* Proc Natl Acad Sci USA, 1998. **95**(6): p. 2761-6.
113. Charles, J.P., et al., *Ligand-binding properties of a juvenile hormone receptor, Methoprene-tolerant.* Proc Natl Acad Sci U S A, 2011. **108**(52): p. 21128-33.
114. Restifo, L. and T.G. Wilson, *A juvenile hormone agonist reveals distinct developmental pathways mediated by ecdysone-inducible broad complex transcription factors.* Dev Genet., 1998. **22**(2): p. 141-59.

115. Li, M., E. Mead, and J. Zhu, *Heterodimer of two bHLH-PAS proteins mediates juvenile hormone-induced gene expression.* Proc Natl Acad Sci U S A, 2011. **108**(2): p. 683-43.
116. Shin, S.W., Zou Z., Saha T., Raikhel, A. S., *bHLH-PAS heterodimer of methoprene-tolerant and Cycle mediates circadian expression of juvenile hormone-induced mosquito genes.* Proc Natl Acad Sci U S A, 2012. **109**(41): p. 16576-81.
117. Abdou, M., et al., *Drosophila Met and Gce are partially redundant in transducing juvenile hormone action.* Insect Biochem Mol Biol, 2011. **41**(12): p. 938-45.
118. A., A., et al., *Molecular analysis of the initiation of insect metamorphosis: a comparative study of Drosophila ecdysteroid-regulated transcription.* Dev. Biol, 1993 **160**(2): p. 388-404.
119. Truman, J.W. and L.M. Riddiford, *Endocrine insights into the evolution of metamorphosis in insects.* Annual Review of Entomology, 2002. **47**: p. 467-500.
120. Spokony, R.F. and L.L. Restifo, *Anciently duplicated Broad Complex exons have distinct temporal functions during tissue morphogenesis.* Dev Genes Evol, 2007. **217**(7): p. 499-513.
121. Wigglesworth, V.B., *The Physiology of Metamorphosis*. 1974, Cambridge: Cambridge University Press.
122. Nijhout, H.F., *Insect Hormones*. 1994, Princeton, New Jersey: Princeton University Press.
123. Gilbert, L., R. Rybczynski, and J.T. Warren, *Control and biochemical nature of the ecdysteroidogenic pathway.* Annu Rev Entomol., 2002. **47**: p. 883-916.
124. Henrich, V.C., R. Rybczynski, and L.I. Gilbert, *Peptide Hormones, Steroid Hormones, and Puffs: Mechanisms and Models in Insect Development*, 1998. p. 73-125.
125. Telang A, F.L., Brown M. R., *Larval feeding duration affects ecdysteroid levels and nutritional reserves regulating pupal commitment in the yellow fever mosquito Aedes aegypti (Diptera: Culicidae).* J Exp Biol., 2007. **210**(Pt 5): p. 854-64.
126. Jenkins, S.P., M.R. Brown, and A.O. Lea, *Inactive prothoracic glands in larvae and pupae of Aedes aegypti: Ecdysteroid release by tissues in the thorax and abdomen.* Insect Biochemistry and Molecular Biology, 1992. **22**(6): p. 553-559.
127. Hagedorn, H.H., et al., *The ovary as a source of alpha-ecdysone in an adult mosquito.* Proc Natl Acad Sci U S A, 1975. **72**(8): p. 3255-9.
128. Mirth, C.K., J.W. Truman, and L.M. Riddiford, *The ecdysone receptor controls the post-critical weight switch to nutrition-independent differentiation in Drosophila wing imaginal discs.* Development, 2009. **136**(14): p. 2345-53.
129. Caldwell, P., M. Walkiewicz, and M. Stern, *Ras activity in the Drosophila prothoracic gland regulates body size and developmental rate via ecdysone release.* Curr Biol, 2005. **15**(20): p. 1785-95.
130. Colombani, J., et al., *Antagonistic actions of ecdysone and insulins determine final size in Drosophila.* Science, 2005. **310**(5748): p. 667-70.
131. Riehle, M.A. and M.R. Brown, *Insulin stimulates ecdysteroid production through a conserved signaling cascade in the mosquito Aedes aegypti.* Insect Biochemistry and Molecular Biology, 1999. **29**(10): p. 855-860.
132. Nieto M., et al., *Antisense miR-7 impairs insulin expression in developing pancreas and in cultured pancreatic buds.* Cell Transplant, 2012. **21**(8): p. 1761-74.
133. Rehmsmeier, M., et al., *Fast and effective prediction of microRNA/target duplexes.* RNA, 2004. **10**(10): p. 1507-17.

134. Ashburner, M., *Patterns of puffing activity in the salivary gland chromosomes of Drosophila.* Chromosoma, 1967. **21**(4): p. 398-428.
135. Ashburner, M., *Puffing patterns in Drosophila melanogaster and related species.* Results Probl Cell Differ, 1973. **4**: p. 101-51.
136. Becker, H., *Die Puffs der Speicheldrüsenchromosomen von Drosophila Melanogastee.* Chromosoma, 1959. **10**(1-6): p. 654-678.
137. Segraves, W.A. and D.S. Hogness, *The E75 ecdysone-inducible gene responsible for the 75B early puff in Drosophila encodes two new members of the steroid receptor superfamily.* Genes and Development, 1990. **4**(2): p. 204-219.
138. Burtis, K., et al., *The Drosophila 74EF early puff contains E74, a complex ecdysone-inducible gene that encodes two ets-related proteins.* Cell, 1990. **61**(1): p. 85-99.
139. Koelle, M., et al., *The Drosophila EcR gene encodes an ecdysone receptor, a new member of the steroid receptor superfamily.* Cell, 1991. **67**(1): p. 59-77.
140. Thomas, H., H. Stunnenberg, and A.F. Stewart, *Heterodimerization of the Drosophila ecdysone receptor with retinoid X receptor and ultraspiracle.* Nature, 1993. **362**(6419): p. 471-5.
141. Oro, A., M. McKeown, and R.M. Evans, *Relationship between the product of the Drosophila ultraspiracle locus and the vertebrate retinoid X receptor.* Nature, 1990. **347**(6290): p. 298-301.
142. Yao, T., et al., *Drosophila ultraspiracle modulates ecdysone receptor function via heterodimer formation.* Cell, 1992. **71**(1): p. 63-72.
143. Laudet, V., *Evolution of the nuclear receptor superfamily: early diversification from an ancestral orphan receptor.* J Mol Endocrinol, 1997. **19**(3): p. 207-26.
144. Evans, R.M., *The steroid and thyroid hormone receptor superfamily.* Science, 1988. **240**(4854): p. 889-95.
145. Kumar, R., B. Johnson, and E.B. Thompson, *Overview of the structural basis for transcription regulation by nuclear hormone receptors.* Essays Biochem, 2004. **40**: p. 27-39.
146. Hall, B. and C.S. Thummel, *The RXR homolog ultraspiracle is an essential component of the Drosophila ecdysone receptor.* Development, 1998. **125**(23): p. 4709-17.
147. Cho, W., M. Kapitskaya, and A.S. Raikhel, *Mosquito ecdysteroid receptor: analysis of the cDNA and expression during vitellogenesis.* Insect Biochem Mol Biol, 1995. **25**(1): p. 19-27.
148. Wang, S.F., et al., *Differential expression and regulation by 20-hydroxyecdysone of mosquito ecdysteroid receptor isoforms A and B.* Mol Cell Endocrinol, 2002. **196**(1-2): p. 29-42.
149. Segraves, W.A., *Steroid receptors and other transcription factors in ecdysone response.* Recent Prog Horm Res., 1994. **49**: p. 167-95.
150. Nishiura, J.T., K. Ray, and J. Murray, *Expression of nuclear receptor-transcription factor genes during Aedes aegypti midgut metamorphosis and the effect of methoprene on expression.* Insect Biochem Mol Biol, 2005. **35**(6): p. 561-73.
151. Tsai, M. and B.W. O'Malley, *Molecular Mechanisms of Action of Steroid/Thyroid Receptor Superfamily Members.* Annual Review of Biochemistry, 1994. **63**(1): p. 451-486.

152. Perissi, V., et al., *A corepressor/coactivator exchange complex required for transcriptional activation by nuclear receptors and other regulated transcription factors.* Cell, 2004. **116**(4): p. 511-26.
153. Bitra, K. and S.R. Palli, *Interaction of proteins involved in ecdysone and juvenile hormone signal transduction.* Arch Insect Biochem Physiol, 2009. **70**(2): p. 90-105.
154. Zhu, J., et al., *The competence factor beta Ftz-F1 potentiates ecdysone receptor activity via recruiting a p160/SRC coactivator.* Mol Cell Biol, 2006. **26**(24): p. 9402-12.
155. Parthasarathy, R. and S.R. Palli, *Stage- and cell-specific expression of ecdysone receptors and ecdysone-induced transcription factors during midgut remodeling in the yellow fever mosquito, Aedes aegypti.* J Insect Physiol, 2007. **53**(3): p. 216-29.
156. Konopova, B. and M. Jindra, *Broad-Complex acts downstream of Met in juvenile hormone signaling to coordinate primitive holometabolan metamorphosis.* Development, 2008. **135**(3): p. 559-568.
157. Minakuchi, C., T. Namiki, and T. Shinoda, *Kruppel homolog 1, an early juvenile hormone-response gene downstream of Methoprene-tolerant, mediates its anti-metamorphic action in the red flour beetle Tribolium castaneum.* Dev Biol, 2009. **325**(2): p. 341-50.
158. Castaneda, L. and R.F. Nespolo, *Phenotypic and genetic effects of contrasting ethanol environments on physiological and developmental traits in Drosophila melanogaster.* PLoS One, 2013. **8**(3).
159. Billas, I., et al., *Structural adaptability in the ligand-binding pocket of the ecdysone hormone receptor.* Nature, 2003. **426**(6962): p. 91-6.
160. Carlson, G., et al., *The chemical and biological properties of methoxyfenozide, a new insecticidal ecdysteroid agonist.* Pest Manag Sci, 2001. **57**(2): p. 115-9.
161. Guittard, E., et al., *CYP18A1, a key enzyme of Drosophila steroid hormone inactivation, is essential for metamorphosis.* Dev Biol, 2011. **349**(1): p. 35-45.
162. Nishiura, J.T., et al., *Modulation of larval nutrition affects midgut neutral lipid storage and temporal pattern of transcription factor expression during mosquito metamorphosis.* J Insect Physiol., 2007. **53**(1): p. 47-58.
163. Davidowitz, G., L.J. D'Amico, and F.H. Nijhout, *Critical weight in the development of insect body size.* 2003. **5**(2): p. 197.
164. Beadle, G.W., E.L. Tatum, and C.W. Clancy, *Food Level in Relation to Rate of Development and Eye Pigmentation in Drosophila Melanogaster.* Biological Bulletin, 1938. **75**(3): p. 447-462.
165. Layalle, S., N. Arquier, and P. Leopold, *The TOR pathway couples nutrition and developmental timing in Drosophila.* Dev Cell, 2008. **15**(4): p. 568-77.
166. Edgar, B.A., *How flies get their size: genetics meets physiology.* Nat Rev Genet, 2006. **7**(12): p. 907-16.
167. Fielenbach, N. and A. Antebi, *C. elegans dauer formation and the molecular basis of plasticity.* Genes Dev, 2008. **22**(16): p. 2149-65.
168. Karp, X. and V. Ambros, *Dauer larva quiescence alters the circuitry of microRNA pathways regulating cell fate progression in C. elegans.* Development, 2012. **139**(12): p. 2177-86.
169. Zhang, X., et al., *microRNAs play critical roles in the survival and recovery of Caenorhabditis elegans from starvation-induced L1 diapause.* Proc Natl Acad Sci U S A, 2011. **108**(44): p. 17997-8002.

170. Christodoulou, F., et al., *Ancient animal microRNAs and the evolution of tissue identity.* Nature, 2010. **463**(7284): p. 1084-8.
171. Hahn, D. and D.L. Denlinger, *Meeting the energetic demands of insect diapause: nutrient storage and utilization.* J Insect Physiol, 2007. **53**(8): p. 760-73.
172. Nijhout, H.F., *Size matters (but so does time), and it's OK to be different.* Dev Cell, 2008. **15**(4): p. 491-2.
173. Arrese, E. and J.L. Soulages, *Insect fat body: energy, metabolism, and regulation.* Annu Rev Entomol., 2010. **55**: p. 207-25.
174. Scott, R., O. Schuldiner, and T.P. Neufeld, *Role and regulation of starvation-induced autophagy in the Drosophila fat body.* Dev Cell, 2004. **7**(2): p. 167-78.
175. Singh, R., et al., *Autophagy regulates adipose mass and differentiation in mice.* J Clin Invest 2009. **119**(11): p. 3329-39.
176. Heaton, N., et al., *Dengue virus nonstructural protein 3 redistributes fatty acid synthase to sites of viral replication and increases cellular fatty acid synthesis.* Proc Natl Acad Sci U S A, 2010. **107**(40): p. 17345-50.
177. Lovis P Fau - Roggli, E., et al., *Alterations in microRNA expression contribute to fatty acid-induced pancreatic beta-cell dysfunction.* 2008(1939-327X (Electronic)).
178. Lee, J. and J.K. Kemper, *Controlling SIRT1 expression by microRNAs in health and metabolic disease.* Aging, 2010. **2**(8): p. 527-34.
179. Noriega, F., et al., *Aedes aegypti midgut early trypsin is post-transcriptionally regulated by blood feeding.* Insect Mol Biol, 1996. **5**(1): p. 25-9.
180. Bustin, S., et al., *The MIQE guidelines: minimum information for publication of quantitative real-time PCR experiments.* Clin Chem, 2009. **55**(4): p. 611-22.